THERMOREGULATORY EFFECTS OF PSYCHOSTIMULANTS AND EXERCISE: DATA-DRIVEN MODELING AND ANALYSIS

by

Abolhassan Behrouzvaziri

A Dissertation

Submitted to the Faculty of Purdue University

In Partial Fulfillment of the Requirements for the degree of

Doctor of Philosophy

Department of Mathematics

Indianapolis, Indiana

May 2018

THE PURDUE UNIVERSITY GRADUATE SCHOOL
STATEMENT OF COMMITTEE APPROVAL

Dr. Yaroslav Molkov, Chair
Department of Mathematical Sciences
Dr. Alexey S. Kuznetsov
Department of Mathematical Sciences
Dr. Julia Concetta Arciero
Department of Mathematical Sciences
Dr. Leonid L. Rubchinsky
Department of Mathematical Sciences

Approved by:
Dr. Evgeny Mukhin
Head of the Graduate Program

ACKNOWLEDGMENTS

First of all, I would like to sincerely thank my advisor Dr. Molkov for his genuine support and encouragement during my Ph.D. program. He was always there when I needed him and patiently answering my questions and listening to my concerns. He was not only an academic advisor who mentored me academically but also a friend who I feel comfortable to talk. His support and dedication to my program didn't stop when he moved into another state. He is a real definition of an advisor and a friend, someone who walks with you and shows you the path and pushing you even when you want to give up.

I would like to mention my biology mentor and teacher, Dr. Zaretsky. He patiently describes all the details of our projects and shares his insight to my level of understanding. In my life so far, I've never met any other biologist who can remember or even explains those topics in such details. Also, I like to thank my peers Yeon Joo Yoo, Morozova Ekaterina, and Michelle LaPradd for their support and collaboration during the works that are used as parts of this thesis.

Also, I would like to thank Dr. Evgeny Mukhin, Graduate Programs Director. He always helped me to find the best solution whenever I needed to make some decisions for my program. He is a patient advisor and genuine human and a person who truly loves mathematics. Also, I'd like to express my sincere gratitude to Dr. Zhongmin Shen for all his help and support since the very first day that I came to IUPUI.

I am so thankful for all the help and support from my friends and family, to my father who never stopped believing in me, to my brother who was standing by me and listening to me, to my friends who made the best days of my life and finally to my wife. She is not only my wife but my best friend who stays up with me and studying through years of my program.

TABLE OF CONTENTS

LIST OF TABLES

LIST OF FIGURES

LIST OF ABBREVIATIONS

M-H algorithm	Metropolis-Hastings algorithm
MCMC method	Markov Chain Monte Carlo method
Meth	Methamphetamine
Exc	Excitatory
Inh	Inhibitory
HD	High Dose
Med	Medullary node
SPN	Sympathetic preganglionic node

ABSTRACT

Author: Behrouzvaziri, Abolhassan. PhD
Institution: Purdue University
Degree Received: May 2018
Title: Thermoregulatory Effects Of Psychostimulants And Exercise: Data-Driven Modeling And Analysis
Major Professor: Yaroslav I. Molkov

Thermoregulation system in mammal keeps their body temperature in a vital and yet narrow range of temperature by adjusting two main activities, heat generation, and heat loss. Also, these activities get triggered by other causes such as exercise or certain drugs. As a result, thermoregulation system will respond and try to bring back the body temperature to the normal range. Although these responses are very well experimentally explored, they often can be unpredictable and clinically deadly. Therefore, this thesis aims to analytically characterize the neural circuitry components of the system that control the heat generation and heat loss. This modeling approach can help us to analyze the relationship between different components of the thermoregulation system without directly measuring them and explain its complex responses in mathematical form. The first chapter of the thesis is dedicated to introducing a mathematical modeling approach of the circuitry components of the thermoregulation system in response to Methamphetamine which was first published in [1]. Later, in other chapters, we will expand this mathematical framework to study the other components of this system under different conditions such as different circadian phases, various pharmacological interventions, and exercise.

This thesis is composed by materials from the following papers. CHAPTER 1 uses the main idea, model, and figures from References [1]. Meanwhile, CHAPTER 2 is based on [2] coauthored with me and is reformatted according to Purdue University Thesis guidelines. Also, CHAPTER 3 interpolates materials from reference [3] coauthored and is reformatted to comply with Purdue University Thesis guidelines. CHAPTER 4 is inserted from the reference [4] and is reformatted according to Purdue University Thesis guidelines. Finally, CHAPTER 5 is based on Reference [5] and is reformatted according to Purdue University Thesis guidelines. Some materials from each of these references have been used in the introduction Chapter.

CHAPTER 1. MOTIVATION AND BACKGROUND

1.1 Motivation

Thermoregulation systems in mammal keep their body temperature in a vital and yet narrow range of temperature by adjusting two main activities, heat generation, and heat loss. For example, as a response to the cold environment, the system signals the body to increase the heat production through non-shivering thermogenesis which is not related to the shivering induced locomotion activities. Also, the system may try to increase the body temperature via decreasing the heat dissipation from blood through cutaneous vasoconstriction [6]. On the other hand, to lower the body temperature, non-shivering thermogenesis would be shut off and excess heat is dissipated by increasing blood flow near the skin via cutaneous vasodilation, or through evaporative heat loss using the skin sweat.

Physical activities or drugs can perturb the thermoregulation system activity in animals and change the body temperature to the outside of the equilibrium range. Consequently, the thermoregulation system signals the associated body organs for a series of heat generation or dissipation actions to maintain the vital range of temperature. However, sometimes the reaction of thermoregulation system to these perturbations is not trivial or predictable. Therefore, to learn more about the mechanism of these reactions, we need to observe the thermoregulation system outside of its equilibrium state. This allows us, for example, to measure how quickly it returns to the equilibrium or the pattern that the system follows back to its equilibrium. Also, we observe the responses of the system to other physical or chemical factors outside of the equilibrium. When we compare these responses to those in an equilibrium state, we can quantify certain properties of the thermoregulatory system.

As mentioned, we would like to perturb the thermoregulation system and then observe its behavior. For example, we can achieve it by impacting the balance of certain neurotransmitters in the system e.g. by administrating a substance that is known to cause thermoregulation system's reaction. We can also make the perturbation by physical activity or changing the environmental properties such as ambient temperature. In this thesis, for the first case we chose to inject Orexin antagonist and for the second perturbation type, we selected physical exercise, changing ambient temperature, and different circadian phases.

Dose-related temperature response to Methamphetamine (Meth) is very complicated and not linear. Relatively low doses of Meth (≤1 mg/kg) cause a temporary but rapid increase in body temperature [7]. However, as the dose of Meth increases, the dose-response curve changes in a non-trivial fashion. At doses between 1 and 5 mg/kg the peak temperatures do not increase but the temperature peak time progressively shifts to the later times: for example, the peak temperature for a 1 mg/kg dose (38˚C) occurs at 60 min while the peak for a 5 mg/kg dose (38˚C) occurs at ~180 minutes. After doses of Meth of 10 mg/kg temperature once again rapidly rises, peaking between 60 and 90 min, followed by a small decrease and then secondarily rises again remaining elevated for 5 hours after injection [7].

In exercise, the administration of amphetamine slows down the temperature rise (thus decreasing core body temperature) at the beginning of the run without affecting oxygen consumption. In contrast, a lower dose of amphetamine (1 mg/kg) does not change measured parameters.

Due to non-trivial responses of thermoregulation system in mammals to exercise and amphetamines, it is difficult to analyze it via experiments since it is required to quantify the metabolism, and heat exchange between different body compartments in conscious animals.

Therefore, in a series of publications, a set of mathematical models were constructed to characterize the thermoregulation system. The experimental data used to calibrate these models were collected from the body temperature of rats in different ambient temperatures, different exercise intensities, different doses of amphetamines and circadian conditions. The main components of these models are heat production (controlled the movement and metabolism) and heat dissipation (controlled by cutaneous vasoconstriction or vasodilation).

Later in this chapter, we will describe the general model that was used to study the body temperature responses to Methamphetamine and how we calculate the parameters of this model. This model was created and developed by Molkov et al. [1]. Next, in chapter 2 we will expand this model to study temperature responses to methamphetamine and stress in relation to orexinergic neurotransmission. In chapter 3 we modify their model to unmask the impact of circadian variability in body temperature responses to methamphetamine. In chapter 4 we introduced the heat dissipation component into their model. We tried to mathematically model the heat exchange between core body and muscles and characterize their temperature change

during exercise. This development in their model helps us in chapter 5 where we aim to find how amphetamine impacts the mechanism of exhaustion during running.

1.2 Background and Initial Models

Fatal hyperthermia caused by administration of amphetamines is a typical clinical condition, yet for a long time we didn't have a mathematical model explaining the etiology and pathogenesis of this condition. Dose dependence of temperature responses to methamphetamine is not linear and demonstrates a complicated and delayed pattern. Molkov et al. (2014) used mathematical modeling to study this phenomenon and suggested that a balanced combination of excitatory and inhibitory mechanisms may explain this complexity.

Temperature responses caused by amphetamines have several phases including both hypothermic and hyperthermic reactions. Also, it's seen to be dependent on ambient temperature, dose, and previous injections of the drug in an animal. Amphetamines evoke responses of many neuromediator systems. On the other hand, body temperature is controlled by multiple and complex neuronal circuitry mechanisms. Unfortunately, to make data interpretation more accessible, the majority of the researchers in this field have focused on simplified experiments, and therefore they often don't have much of real-life prognostic potential. To explore and explain the complexity of this phenomenon we needed a mathematical or theoretical framework accounting for an extensive set of reported experimental facts. For this purpose, the authors in [1] developed a mathematical model that characterizes and explains this complex dose dependence of temperature responses to methamphetamine. Here I aimed to introduce their effort and findings. This model and some of the results will be the basis of the chapters 2 through 5.

At room temperature (24C) Meth causes 1 to 2 C temperature increase which can take up to several hours depending on the injected dose. More specifically, low doses of Meth (≤ 1 mg/kg) evoke a rapid increase in body temperature up to approximately 38C, which can continue for about 2 hours (Figure 1.3). At higher doses, the temperature response becomes a much more complicated phenomenon. In fact, between doses of 1 and 5 mg/kg the temperature rises to a similar level but the time that the peak occurs progressively shifts. After injection of 1 mg/kg, the temperature rises to a maximum at between 60 to 100 minutes while after the administration of 5 mg/kg the peak happens around 180 minutes. Surprisingly, after higher doses of Meth (≥ 10

mg/kg and above) temperature rapidly increases without delay and almost right after injection with a maximum between 60 and 90 minutes at about 39C. The peak is followed by a persisting high temperature up to 5 h after the injection.

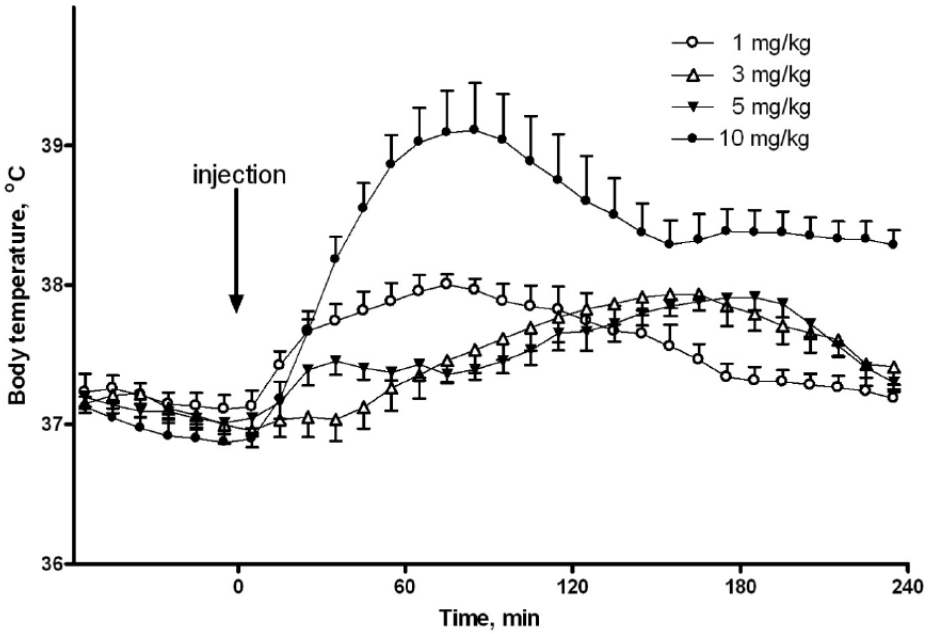

Figure 1.1 Experimental Data for dose-dependence temperature responses to Meth. All temperatures were measured 1 hour before the injections at t=0. [1]

The neuronal circuitry mechanisms responsible for these responses are well explored. Recently, Dorsomedial hypothalamus was characterized to be a key and significant region whose activity is an essential factor in causing fever and stress responses [8]. Interestingly, responses to Methamphetamines are very similar to those induced by the activation of neurons in the dorsomedial hypothalamus in conscious rats. Some of these responses are such as mild hypertension, tachycardia, hyperthermia, and observable locomotion activity [9]. On the other hand, inhibition of dorsomedial hypothalamus with the administration of muscimol noticeably reduces responses to ecstasy which is a commonly abused derivative of amphetamine [10].

Also, the pathways controlling such activities as thermoregulation and locomotion mediated by dorsomedial hypothalamus commonly include the raphe pallidus in the brainstem.

Additionally, during the first hours after the injection of moderate doses of Meth, the temperature responses are weaker than the ones to the low doses of Meth. This response suggests that an

inhibitory component is involved in temperature response. Furthermore, if we block the inhibitory synaptic transmission in dorsomedial hypothalamus and raphe pallidus, we can cause thermogenic reactions which indicate that both regions receive inhibitory inputs [11].

Also, inhibition provoked by Methamphetamine might be mediated by serotonergic receptors or inhibitory subtypes of dopaminergic receptors [12]. By introducing the model (Figure 1.1), authors translate the aggregate excitatory node (Excitation) to the dorsomedial hypothalamus (and other supramedullary excitatory inputs). The output of this node to the medullary node (Medulla) will be combined with the already explained accumulated inhibitory drive (Inhibition). The weighted sum of these inputs to Medulla will define its activity level. To account for the responses to the high doses of Meth, the high-dose node is identified as the secondary excitatory part of this model which doesn't get aggregated with the inhibitory component directly. In fact, this node projects on the thermogenic pathway at the inframedullary sympathetic preganglionic (Spinal Cord) node which controls activation of thermogenesis. This activity is determined by the interaction between excitatory and inhibitory components whose activation depends on blood concentrations of Meth. Accordingly, in Figure 1.3 the authors described how temperature responses to Meth are related to the various doses. The least dose (1 mg/kg) is not large enough to fully activate either of Inhibitory or Excitatory nodes.

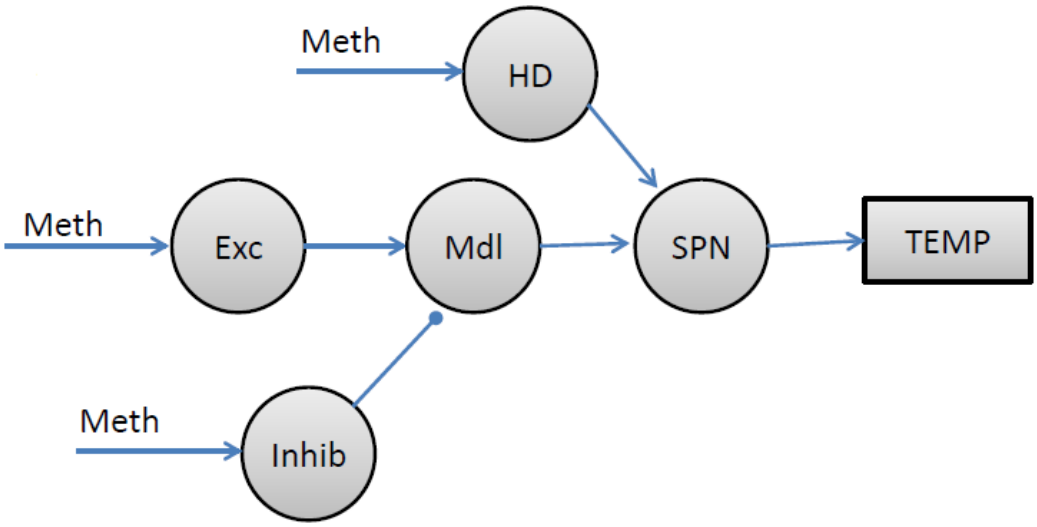

Figure 1.2 Each circle in Model corresponds to a neural component which is Meth dose dependentt. The activity of each node is characterized by sigmoid function. [1]

Hence, temperature response at this dose is mostly evoked by a single excitatory multisynaptic pathway to Spinal Cord. At the higher dose, 3 mg/kg, Meth concentration is still not enough to activate the High-Dose (HD) Excitatory node; however, it is sufficient to activate the Inhibition. As mentioned earlier, the activity of Medulla is defined by a weighted sum of the excitatory and inhibitory components (Figure 1.3), which in this case is slightly larger than the indicator line for 3 mg/kg.

At 3 mg/kg, temperature doesn't increase quickly, hence in their model the inhibitory component competes with the excitatory node. The balance between excitatory and inhibitory nodes, whose sensitivity to Meth is incrementally different, yields to a delayed respond immediately after the injection. However after sometimes, the blood concentration of Meth decreases at which the Inhibitory node keeps being active, but it is also enough to activate the excitatory component. At the highest dose, the High-Dose node gets activated which increases the total excitation. This node creates a much more significant excitatory activation in compare with supramedullary. Although the Excitatory node provides a similar amount of output (Figure 1.3), its impact on Spinal Cord is much more balanced off by the (negative) inhibitory component. This amount of excitatory outputs results in a much stronger increase in temperature at the beginning of the highest dose compared to what we see in lower doses.

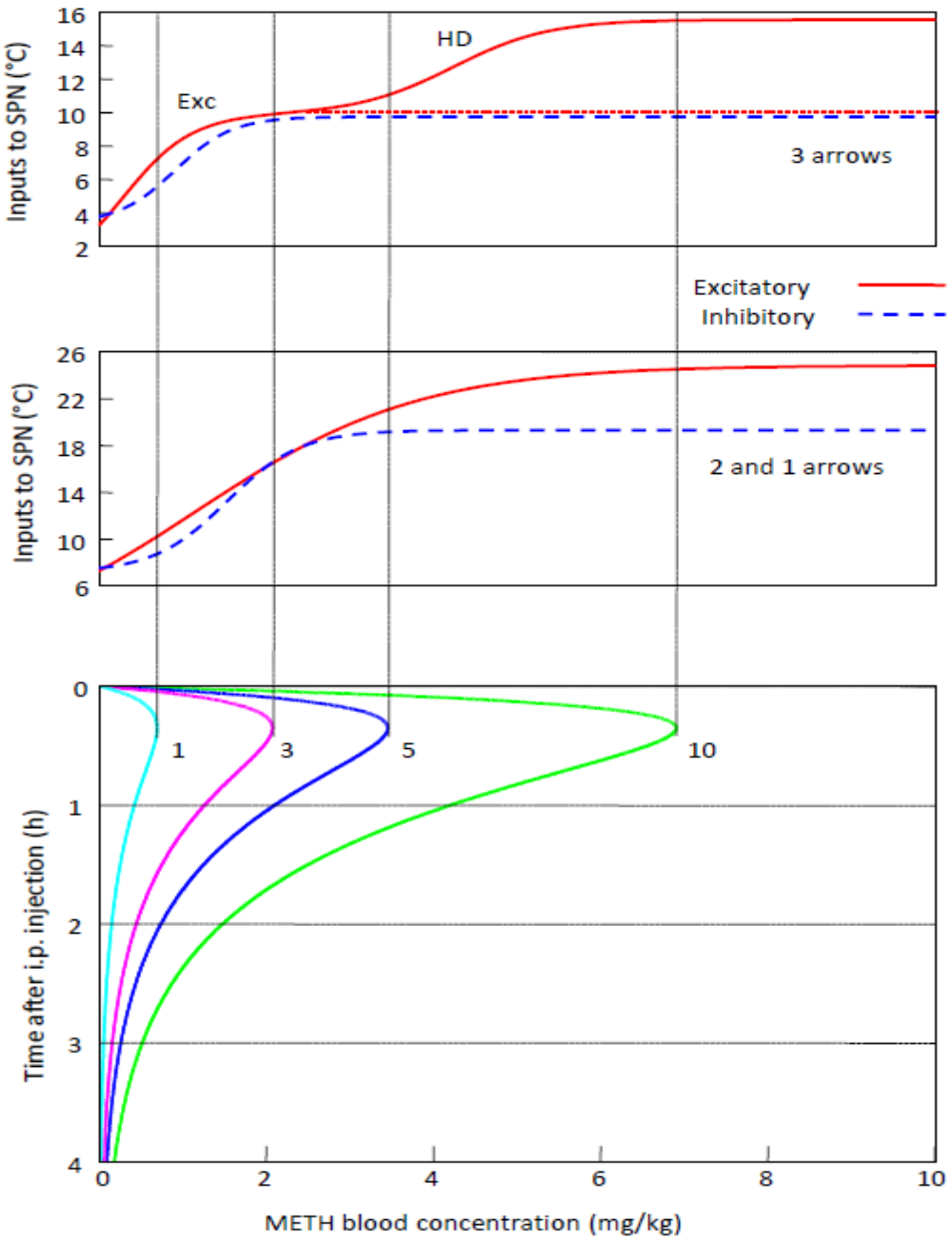

Figure 1.3 The top plot is the Meth dose dependence activity functions of the excitatory and inhibitory and HD nodes in the network model. The middle plot is the activity for the reduced model where we only have 2 nodes (Exc and Inh). Lowest plot is the function of Meth concentration in blood for 4 doses of Meth including 1, 3, 5 and 10 mg/kg. [1]

1.3 Model construction

The authors in [1] used the following components in the model design:

1) The pharmacokinetics of Meth concentrations in blood after injection;

2) A network model based on neural network whose components' activities depend on Meth concentration in the blood;

3) Finally a body temperature dynamics which is based on the output signal from each node.

1.3.1 Pharmacokinetics Model

Methamphetamine is absorbed very quickly from the peritoneum, and almost exponentially eliminated from the blood [13, 14]. Since the authors didn't collect the data about the volume of the Meth distribution in blood, they used the following equations to describe the drug concentrations in units of mg/kg in their model:

$$\frac{dx}{dt} = -\frac{x}{\tau_a}$$
$$\frac{dy}{dt} = \frac{x}{\tau_a} - \frac{y}{\tau_e} \qquad (1.1)$$

where t is time in minutes, $x(t)$ is the intraperitoneal Meth concentration and $y(t)$ is the Meth concentrations in blood. This means that x/τ_a is for drug absorption with a time constant τ_a, and also y/τ_e is used for the drug elimination from the blood with a time constant of τ_d. Also, the initial conditions are assumed to be $x(0) = D, y(0) = 0$ because the administration of a dose D is done at time $t = 0$ without any prior injection for the animal. If one solves the ODE's in (1.1) with those initial conditions, one easily finds the analytical solution explicitly as follows:

$$y(t) = D(\tau_a/\tau_e - 1)^{-1}\left(e^{-t/\tau_a} - e^{-t/\tau_e}\right) \qquad (1.2)$$

This model is used to describe the time dependence of Meth concentration in the blood at time t minutes after the injection of the particular dose.

1.3.2 Neural Network Model

Per the introduction in section 1.2, the Neural network is used in the model construction to show the connectivity and interrelations of the neural circuitry components in the three major brain regions. These components are known to control the regular thermoregulatory activities in the rodent. First, the excitatory part which is coming through dorsomedial hypothalamus to premotor sympathetic neurons in ventromedial medulla which is noted here as Medullary node. This excitatory node is connected to the sympathetic preganglionic region in the spinal cord which is shown as SPN node. In the end, the output of the SPN node defines the body temperature.

As seen in [1] and other studies, the dose dependence of temperature responses to amphetamines is not analytically trivial which means there is no linear or simple relation that can explain it. [7, 15-19].

This behavior is reported on Figure 1.1 where after the injection of a low dose of Meth an immediate increase in body temperature is observed. This response is more significant in magnitude than the two higher doses but smaller than the highest experimented dose. This response means that the activity of the inhibitory node should reduce the excitation drive in the system. It's been reported that at high doses of amphetamines, they seem to be active below the level of the medulla [16]. Accordingly, this model assumes a second and stronger excitatory component that can be activated only by higher doses of Meth and hence is called HD node.

This neural network used to create the model circuitry is shown in Figure 1.2 which is a simple feed-forward neural network. The Meth dependent activity of supramedullary excitatory node (*Exc*), Inhibitory node (*Inhib*) and the high-dose node *HD* is defined by activation (sigmoid) function in neural populations, P_i ($i = Exc,\ Inhib,\ HD$), and is calculated using the following equation:

$$P_i(t) = \sigma(w_i \cdot y(t) + \gamma_i) \qquad (1.3)$$

Here $\sigma(x) = \dfrac{1 + \tanh x}{2}$ is a logistic function, and w_i is a used for the Meth sensitivity of each node for which $y(t)$ calculates the Meth concentration in blood at each given time according to equation (1.2). Finally γ_i defines baseline for the activity of each node P_i. This means that the

units of sensitivity parameters ($w_{\mathrm{Exc}}, w_{\mathrm{Inhib}}$,and w_{HD}) are $(\mathrm{mg/kg})^{-1}$ and they have the dimensionless parameters $\gamma_{\mathrm{Exc}}, \gamma_{\mathrm{Inhib}}$ and γ_{HD}.

Using the projection weights of Exc and Inh nodes into Mdl, a weighted sum defines the activity of the *Mdl* as follows:

$$P_{\mathrm{Mdl}}(t) = w_{\mathrm{Exc}\rightarrow\mathrm{Mdl}} \cdot P_{\mathrm{Exc}}(t) - w_{\mathrm{Inhib}\rightarrow\mathrm{Mdl}} \cdot P_{\mathrm{Inhib}}(t) \qquad (1.4)$$

The SPN component uses the output of *Mdl* and combines it with the additional excitatory input from *HD* node as the follows:

$$P_{\mathrm{SPN}}(t) = P_{\mathrm{Mdl}}(t) + w_{\mathrm{HD}\rightarrow\mathrm{SPN}} \cdot P_{\mathrm{HD}}(t) + \gamma_{\mathrm{SPN}} \qquad (1.5)$$

1.3.3 Temperature Model

Finally, the activity of SPN is used to describe the change in temperature by a first-order linear ordinary differential equation as follows:

$$\tau_T \frac{dT}{dt} = P_{\mathrm{SPN}}(t) - (T - T_0) \qquad (1.6)$$

Where T_0 is assumed to be the baseline body temperature of rodent, and *T* is defined as the body temperature in degrees Celsius, and finally time constant for the temperature response τ_T. Consequently, the outputs of *Mdl* and *SPN* are assumed to be in degree Celsius.

Temperature response described in (1.6) has two components. These are the two main parts that we use later in this thesis when we construct other temperature models. These components are called heat production and heat dissipation of the system. Heat dissipation happens due to the difference between the body and an ambient temperature. According to Newton's cooling law, the dissipation is proportional to the difference of the body and environment temperatures. Also, the heat dissipates through skin proportionally to its thermal conductivity. This term in (1.6) is inversely related to the temperature time constant τ_T. This conductivity correlates with the cutaneous blood flow. When body temperature increases, cutaneous vasodilation may increase thermal conductivity of the skin. At room temperature, the cutaneous vessels are known to be fully constricted, and Meth also has vasoconstrictive effect [10, 20, 21] thus counteracting potential feedback evoked by hyperthermia. Therefore, Molkov et al. assumed that the τ_T stays

constant throughout all experiments. Another important assumption was about the basal temperature which is defined by the basal metabolism. This baseline temperature cannot be decreased by any feedback mechanisms due to hyperthermia. This is a valid assumption because the system was studied at room temperature for which no additional heat production or dissipations activities are impacting the baseline metabolism.

1.4 Conclusions

In [1] the authors explored the complex mechanism of temperature responses to Meth based on a model defined by a balance of dose-dependent excitatory and inhibitory components. Some of the significant results are:

1) Lethal hyperthermia can be caused by even moderate doses of Meth if the natural balance of these excitatory and inhibitory components is changed.

2) This model can help explore the changes in the circuitry caused by different perturbation of system including repeated administrations of Meth (Meth addiction studies) and changes in the state of the system by administration of other pharmacological agents. Due to the complexity of the system, differences in responses may prevent us from unequivocal discoveries about underlying mechanisms. Instead, we can use some statistical inference applied to the changes of model parameters. For instance, after injection of an antagonist for some receptors, using this model we can expect a noticeable reduction in interconnectivity of some components of the neural network. In this case, we can conclude that the impacted neurotransmitter mediates this connection. Finally, in repeated drug consumption, the perturbations of related model parameters can help us understand the drug tolerance and addiction better.

CHAPTER 2. OREXINERGIC NEUROTRANSMISSION IN TEMPERATURE RESPONSES TO METHAMPHETAMINE AND STRESS

2.1 Introduction

Amphetamine and its derivatives are among the most prevalent abused drugs in the world [22]. Amphetamines can cause various medical complications including myocardial infarctions, ischemic and hemorrhagic strokes, rhabdomyolysis, renal failure, and fatal hyperthermia [23-29]. Despite this, there is little understanding of neural mechanisms underlying hyperthermia produced by amphetamines. For instance a similar dose of amphetamine may cause a mild effect in some patients but be fatal to others; this can occur even though the blood levels of the drug appear low [30, 31].

In rats, amphetamines cause the central release of monoamines and the subsequent activation of the sympathetic nervous system causing in heat generation by brown adipose tissue (BAT) [32, 33] and skeletal muscle [34]. In addition, amphetamines decrease heat dissipation through cutaneous vasoconstriction [35, 36]. The brain areas mediating these effects are not known but it has previously shown that sympathetic and behavioral responses mediated, by the substituted amphetamine MDMA, can be prevented by suppressing neuronal activity in the dorsomedial hypothalamus [10], the area which is now well-established to participate in the control of heat production in the BAT and heat dissipation through the skin [8]. This is one of the few brain regions containing neurons that project trans-synaptically to both the adrenal gland and skeletal muscle [37] and these dual-projecting neurons contain the peptide orexin [38]. It has also been further shown that Meth and d-amphetamine activate orexin-containing neurons [39, 40].

Central activation of orexin receptors increases body temperature, BAT sympathetic nerve activity and thermogenesis, plasma epinephrine, and heart rate [41-45]. The systemic administration of SB-334867 (SB), an OX_1R antagonist, hereinafter referred as SB, prevents increases in heart rate and mean arterial pressure in models of stress and panic [46, 47], and suppresses hyperthermia caused by stress of injection [48]. Pretreatment with SB has also been shown to significantly attenuate hyperthermia evoked by a moderate but not a low or high dose of Meth [48]. Unfortunately, in the cited study temperature fluctuations resulting from the stress

of two intraperitoneal injections (SB and Meth) made it impossible to quantify the effect of SB on low doses of Meth using a traditional data analysis.

The differential effects of SB on the temperature responses to different doses of Meth do not allow for a straight-forward interpretation. Recently, Molkov et al. developed a mathematical model [1] that reproduced dose-dependent temperature responses to methamphetamine. The model described interactions of putative brain nuclei that participate in thermoregulation. We use this model to provide mechanistic explanation of how the orexin antagonist SB-334867 affects complex Meth-induced dynamics of the body temperature.

2.2 Methods and Data preparations

To study the effect of SB-334867 on methamphetamine-evoked temperature responses two separate experimental series were performed. In the first series SB was administered in the dose of 10 mg/kg. In second series, SB was administered in the dose 30 mg/kg. In each study we have used the corresponding vehicles.

In each series rats were randomly assigned to one of eight groups (n=6-8 per group): one of two pretreatments (SB vs vehicle), followed by one of four treatments (saline or one of three doses of Meth). Each rat received only one treatment. Experiments were performed in a temperature controlled room at T=25^{o}C and relative humidity 30-70%. Air temperature and humidity were monitored by independent sensors. For all experiments deviations of the temperature from 25ºC did not exceed 0.8ºC. After baseline physiological parameters were recorded for at least 30 min, animals received an intraperitoneal injection of either vehicle or SB-334867. Thirty min later, rats received an intraperitoneal injection of either saline or one of three doses of methamphetamine (1 mg/kg, 5 mg/kg, or 10 mg/kg). Although there is a wide range of methamphetamine doses that humans abuse, the doses we chose include ones that are commonly used recreationally (1 mg/kg) as well as larger doses that may be reached by binge users (5 and 10 mg/kg) [49]. For convenience we refer to these doses as “low”, “moderate”, and “high” respectively. Each rat was used for only one injection of Meth or saline.

2.3 Model Construction

2.3.1 General Approach

In their studies [1] Molkov et al. were able to fit experimental data on dose-dependence of temperature responses to Meth with appropriate precision using a mathematical model which was constructed using known anatomy of circuitry involved into responses to amphetamines. The core of the model is a feed-forward sequence of connected excitatory nodes: Excitatory (*Exc*, putatively hypothalamic), Medullary (*Med*) and sympathetic premotor node (*SPN*), out of which *SPN* directly defines a heat generation output (Figure 2.1). We assume that the signal from SPN is transmitted "as is" to the effector organs controlling thermogenesis. This allows combining the whole downstream chain into a single output. Excitatory node is sensitive to Meth as well as there are two more Meth-sensitive nodes – Inhibitory (*Inhib*) and "high dose" (*HD)*. The Inhibitory drive competes with the Excitatory input to affect the Medullary node, while the *HD* node requires high dose of Meth to be activated, hence the name. Complex dose-dependence of temperature responses to Meth is formed by the competition of two excitatory inputs and one inhibitory input, all of which have different sensitivities to Meth.

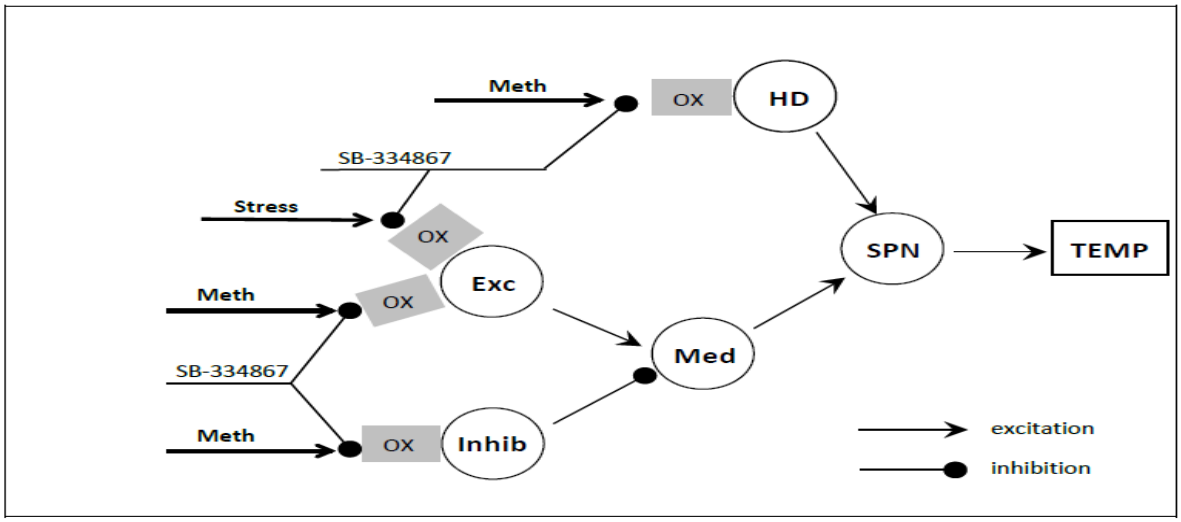

Figure 2.1 Schematic of the model neuronal circuitry involved in responses to methamphetamine. Stress input and the orexin receptors (shown by gray rectangles labeled "OX") are added to extend the circuitry used in [1]. Effect of Stress and/or Meth can be affected by the orexin receptor antagonist SB-334867. Each circle represents a neural population. Abbreviations: Exc – excitatory node, Inhib – inhibitory node, HD – high-dose activated node, Med – medullary node, SPN – sympathetic preganglionic node, TEMP – temperature.

Low doses of Meth (1 mg/kg i.p. and below) activate the Excitatory node almost exclusively, and administration of those doses evokes a monophasic mild hyperthermia. Higher doses (3-5 mg/kg i.p.) are able to activate the inhibitory node, which completely masks the activity of the Excitatory node. As a result, immediately after injection of Meth there is no temperature response, but after partial elimination of the drug, the excitatory drive is disinhibited, and temperature increases display a delayed monophasic response. Finally, high doses (10 mg/kg i.p.) activate the *HD* node, and cause immediate powerful hyperthermia followed by a secondary temperature increase due to transient activation of the Excitatory node.

To analyze the orexin data we first modified the existing model to accommodate stress. Since inhibition of the dorsomedial hypothalamus, a putative excitatory node, suppresses sympathetic activation from both stress [50] and amphetamines [10], we hypothesized that stress and Meth both provide direct inputs to the Excitatory node. Each stress stimulus was modeled as a spike of activity of short duration.

Next, we assumed that SB affects Meth and stress inputs at the relevant nodes. Excitatory node exhibits some tonic activity without Meth [1]. If the projections from Excitatory and/or Inhibitory node to Medullary node are orexinergic, the antagonist would cause dramatic (up to 3^{o}C) hypothermia by itself. However, as it will be shown in the Results, the administration of the antagonist alone did not result in any hypothermia whatsoever. Therefore, we were restricted to placing orexin receptors on the Meth-sensitive populations to mediate effects of Meth, but not to cause any perturbations by the receptor blockade alone.

By fitting the temperature responses to Meth after different doses of SB we calculated values of the model parameters.

2.3.2 Implementation of the Model

The model consisted of three components: pharmacokinetics describing concentration of Meth in the blood after injection; a neural network whose activity was dependent on Meth and SB; and a temperature control system driven by a signal from the neural network.

We assumed that after the injection the drug is being absorbed in the blood from the peritoneum and is also being eliminated from the blood. Accordingly, drug concentrations are described by the following equations:

$$\frac{d[M_p]}{dt} = -\frac{[M_p]}{\tau_u}$$
$$\frac{d[M]}{dt} = \frac{[M_p]}{\tau_u} - \frac{[M]}{\tau_d} \quad (2.1)$$

where *t* is time in minutes, M_p is the intra-peritoneal drug concentration, and M is the blood drug concentration (both in mg/kg). $[M_p]/\tau_u$ represents drug absorption with time constant τ_u, and $[M]/\tau_d$ represents drug elimination with time constant τ_d. Initial conditions are $[M_p](0) = D$, $[M](0) = 0$ for injections made at time *0* where *D* is the initial dose of the drug being modeled. System (2.1) can be solved explicitly as:

$$[M](t) = D\left(\frac{\tau_u}{\tau_d} - 1\right)^{-1}(e^{-t/\tau_u} - e^{-t/\tau_d}) \quad (2.2)$$

for $t > 0$, and $[M](t) = 0$ if $t < 0$. Stress input from the injection made at $t = t_0$ was modeled as a single exponential function

$$S(t, t_0) = \begin{cases} e^{-(t-t_0)/\tau_s}, \text{if } t > t_0 \\ 0, \text{if } t \le t_0 \end{cases} \quad (2.3)$$

In their study, the neural circuitry is modeled as a feed-forward artificial neural network. The excitatory node *Exc* receives two stress inputs at $t = -30$ min and $t = 0$ min from injections of SB (or vehicle) and Meth (or saline) respectively. The outputs of Meth-sensitive neural populations are calculated as follows:

$$P_{Exc}(t) = \sigma(w_S S(t, -30) + w_S S(t, 0) + w_{Exc}[M](t) + \gamma_{Exc})$$
$$P_{Inh}(t) = \sigma(w_{Inh}[M](t) + \gamma_{Inh})$$
$$P_{HD}(t) = \sigma(w_{HD}[M](t) + \gamma_{HD}) \quad (2.4)$$

where $\sigma(x) = (1 + \tanh x)/2$ is a sigmoid activation function, $w_i(t)$ is the sensitivity of $P_i(t)$ to Meth, and γ_i is the basal excitability of P_i, $i \in (Exc, Inh, HD)$. To account for the effect of the SB, we used different values of $(w_S, w_{Exc}, w_{Inh}, w_{HD})$ for different doses of SB.

The activity of medullary population *Med* is described as follows:

$$P_{Med}(t) = w_{Exc\to Med}P_{Exc}(t) - w_{Inh\to Med}P_{Inh}(t) \quad (2.5)$$

where $w_{Exc\to Med}$ and $w_{Inh\to Med}$ are the weights of the excitatory and inhibitory projections from *Exc* to *Med* and *Inhib* to *Med*, respectively. Inframedullary population *SPN* transmits the activity of *Med* but is additionally excited by the Meth-sensitive *HD* population as follows:

$$P_{SPN}(t) = P_{Med}(t) + w_{HD\to SPN}P_{HD}(t) + \gamma_{SPN} \quad (2.6)$$

where $w_{HD\to SPN}$ is the weight of the excitatory projection from *HD* to *SPN*, and γ_{SPN} is the basal excitability of *SPN*.

The temperature response is modeled by a first-order linear ODE driven by the *SPN* signal as follows:

$$\tau_T \frac{dT}{dt} = P_{SPN}(t) - (T - T_0) \quad (2.7)$$

where T is the body temperature in degrees Celsius, τ_T is the time constant of the temperature response, and T_0 is the baseline body temperature.

2.3.3 Estimation of the Model's parameters

We used the Bayesian approach for inferring the model parameters. Then, statistical analysis is used to estimate statistical significance of changes in $(w_S,\ w_{Exc},\ w_{Inh},\ w_{HD})$ individually when 30, 10, and 0 mg/kg of SB are injected, respectively. To do this, we constructed a corresponding posterior probability density function (PDF) of the parameter vector $= (w_S,\ w_{Exc},\ w_{Inh},\ w_{HD})$ considering other parameters fixed at values shown in the Table 2.1. According to Bayes' rule, this probability distribution is proportional to the probability that an observed temperature time series $\{T_i\}$ is produced by their model with the given $\boldsymbol{W}$, usually referred to as a likelihood. Assuming that the residuals are normally distributed, the posterior PDF $p(\boldsymbol{W} \mid \{T_i\})$ is given by the following formula:

$$p(\boldsymbol{W} \mid \{T_i\}) = \exp\left\{-\sum_{i=-50}^{180} \frac{[T_i - T(\boldsymbol{W}, i)]^2}{2\sigma_i^2}\right\} \quad (2.8)$$

where $T(\boldsymbol{W}, i)$ is the temperature calculated by their model at time i with the given $\boldsymbol{W}$. T_i and σ_i are respectively a mean and a standard deviation of the body temperature over a corresponding group of animals at time i by increments of 2 minutes.

We used the Markov Chain Monte Carlo (MCMC) approach, in particular the modified Metropolis-Hastings algorithm [51-54], to create an ensemble of points distributed according to the PDF (2.8). Once we had the ensembles, we calculated mean values of the parameters and their standard errors for each group: vehicle, SB10, and SB30, and used two-sample z-test to estimate statistical significance of the differences in parameter values between the groups. We assumed that p-value < 0.05 means that SB has a statistically-significant effect on the corresponding parameter of the model.

Parameter	**Value**	**Parameter**	**Value**
$\boldsymbol{\tau_u(Meth)}$**, min**	8.25	τ_T, min	89.2
$\boldsymbol{\tau_d(Meth)}$**, min**	57.5	T_0, $°C$	37
$\boldsymbol{\tau(Stress)}$**, min**	10	γ_{Exc} , mg/kg	-0.357
$\boldsymbol{w_{Exc\to Mdl}}$ **,** $\boldsymbol{°C}$	9.89	γ_{Inh} , mg/kg	-1.335
$\boldsymbol{w_{Inh\to Mdl}}$ **,** $\boldsymbol{°C}$	6.38	γ_{HD} , mg/kg	-3.69
$\boldsymbol{w_{HD\to SPN}}$ **,** $\boldsymbol{°C}$	5.66	γ_{SPN} , $°C$	-3.35

Table 2.1 Values of parameters that were considered not affected by SB (adapted from [1])

2.4 Results

2.4.1 SB suppresses stress-induced hyperthermia

The first intraperitoneal injections evoked increases in the body temperature, which tended to return to baseline before the second injection in some groups. We have pooled the responses to the first injection in all groups before administration of Meth according to pretreatment to make four groups (two doses of SB and two vehicles for each dose of SB). However, there was no difference between responses to different vehicles, so data for both vehicles were pooled together as a single group. This reduced the number of groups to three. The increase of body temperature in response to the first injection was statistically significantly attenuated by both doses of SB (Figure 2.2), whereas there was no statistically significant difference between the two doses of SB ($p>0.05$).

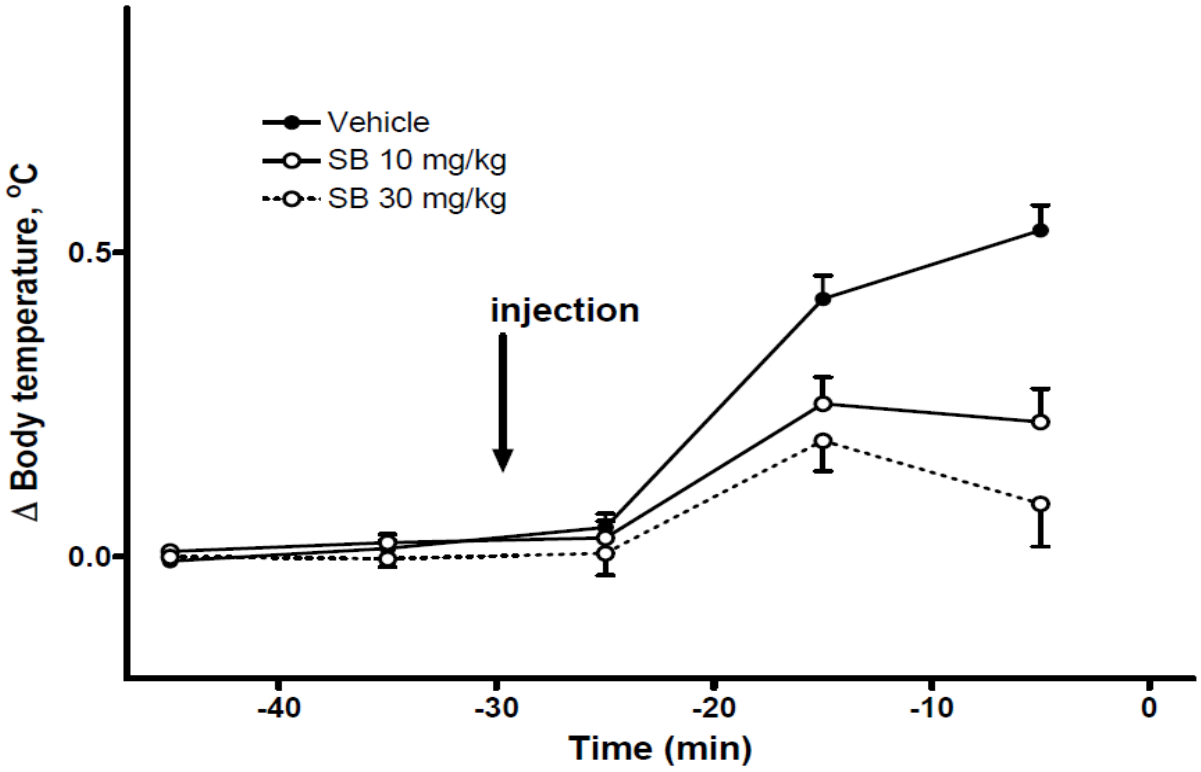

Figure 2.2 Effect of SB on stress-induced body temperature increase associated with injections (n=24-26 per group). Black circles, solid line – pooled vehicle data; open circles, solid line – SB 10 mg/kg; open circles, dashed line – SB 30 mg/kg. Injection was performed at t = –30 min.

2.4.2 Effects of SB-334867 on temperature responses to Meth

The effects of Meth on body temperature were not different between the two vehicles used for the different doses of SB. These effects had complex dose-dependence, which has previously been described [1, 17, 48, 55]. In short, low (1 mg/kg) and high doses of Meth (10 mg/kg) evoked virtually immediate response while response to intermediate dose (5 mg/kg) was delayed. Peak hyperthermia after low and intermediate doses was similar (38.2 $\pm$ 0.1 ^{o}C vs 38.2$\pm$0.1 ^{o}C) but occurred at different moments (76$\pm$11 min vs 226$\pm$15 min after injection). The highest dose of Meth evoked a robust hyperthermia with temperatures reaching 39.5$\pm$0.2 °C within 90 min of administration with the temperature subsequently declining from 90 to 150 min, followed by a plateau until the end of the recording period (up to 200 min). Injections of saline evoked slight

increases of body temperature, which were short-lived: temperature returned to baseline within 60 min.

The responses to the same doses of Meth after SB are shown in Figure 2.3, after the low dose of Meth (1 mg/kg), rats treated with SB had lower body temperature than rats treated with vehicle during 3 h after administration of Meth (Figure 2.3 B, F). However, this difference did not at any time reach statistical significance in the experiment with the lower dose of SB (10 mg/kg, Figure 2.3 B). However, the suppression of the response to the low dose of Meth became statistically significant after the injection of higher dose of the antagonist (30 mg/kg, Figure 2.3 F).

Next, after an intermediate dose of Meth (5 mg/kg) temperature transiently increased but remained lower than temperatures in the vehicle group. Furthermore, this dose of SB significantly attenuated thermogenic response after 70-90 min. In contrast, after the higher dose of SB (30 mg/kg) intermediate dose of Meth evoked a rapid hyperthermic response (Figure 2.3 G) such that core temperature rose statistically significantly above the vehicle group. Qualitatively this response resembles a temperature response to a high dose of Meth in the vehicle group (Figure 2.3 D).

Finally, the response to a high dose of Meth (10 mg/kg) was not modified by the lower dose of SB (Figure 2.3 D) whereas the higher dose of SB significantly increased and prolonged the response to the high dose of Meth with the difference progressively increasing for over 120 min after the administration of Meth.

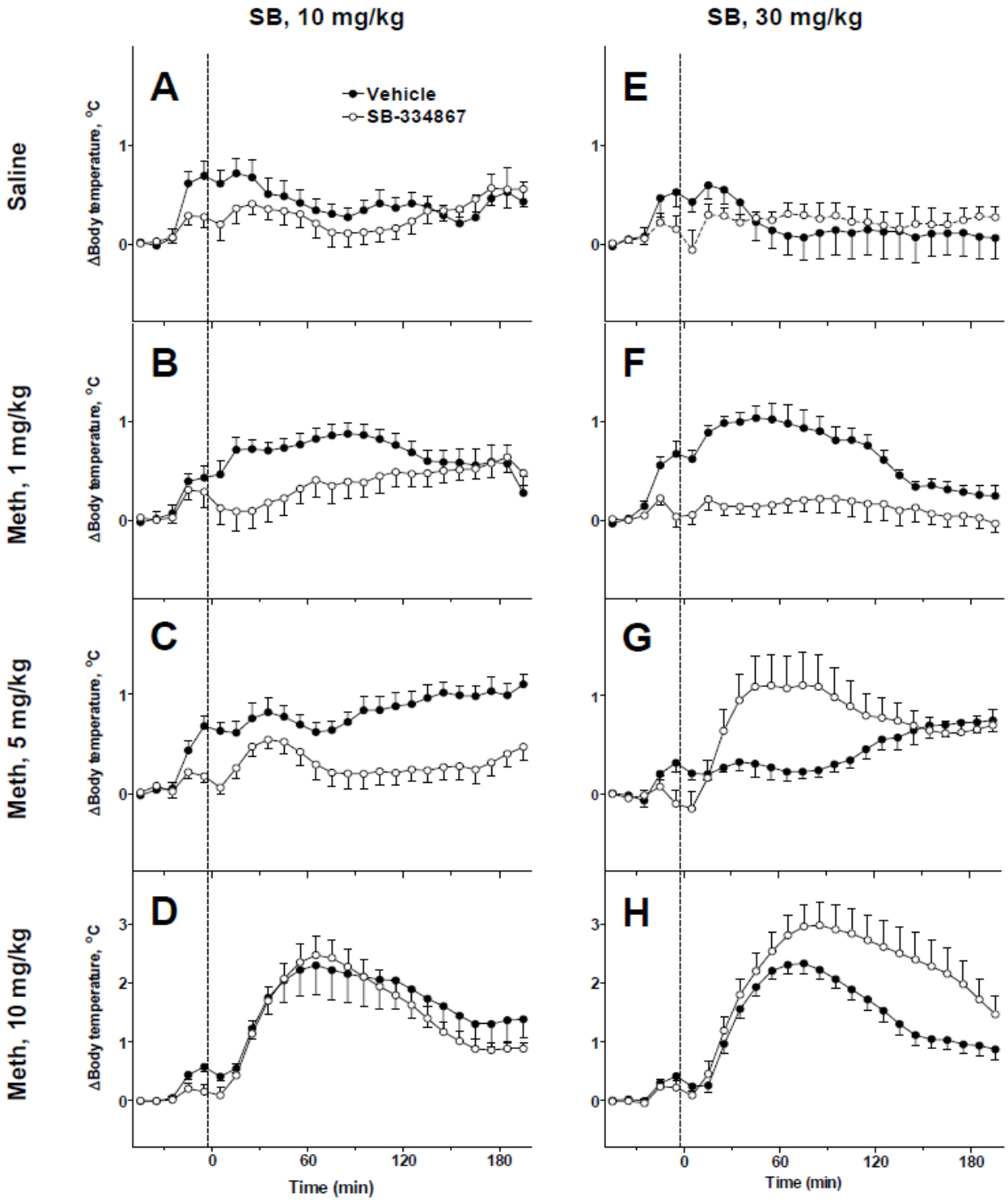

Figure 2.3 Changes in the body temperature evoked by Meth after two doses of SB-334867, Meth is injected at t = 0 min (dashed lines). SB is injected 30 min prior to Meth. A-D: SB 10 mg/kg; E-H: SB 30 mg/kg. Each plot contains responses to the dose of Meth shown on the left: 0 (Saline), 1, 5 or 10 mg/kg after injection of either vehicle (black circles) or SB (open circles).

2.5 Effects of SB on estimates of the model parameters

In this study we used the Metropolis algorithm to implement a Markov Chain Monte Carlo approach to estimate the posterior distribution of model parameters. Specifically, this algorithm generates a multidimensional cloud of points in the parameter space distributed according to the PDF (formula 8 in Methods) for a given experimental series $\{T_i\}$. Four parameters (w_S , w_{Exc}, w_{Inh}, w_{HD}) have been sampled for three different doses of SB. We demonstrate the corresponding clouds in projections onto (w_{Exc}, w_{Inh}) and onto (w_S, w_{HD})-planes shown in Figure 2.4 A and Figure 2.4 B respectively. Each panel contains three clouds labeled "Vehicle", "SB, 10 mg/kg" and "SB, 30 mg/kg". These clouds are well separated implying that the differences in parameter values are statistically significant.

Statistical analysis confirms that antagonism of orexin receptors leads to statistically significant changes in estimates of the model parameters. Particularly, the stress amplitude w_S is reduced by administration of the orexin antagonist (Figure 2.4 C), although, there was no significant difference in w_S estimates between 10 and 30 mg/kg of the antagonist. Also, parameters of sensitivity to Meth of both excitatory and inhibitory drives, w_{Exc}, w_{Inh}, were decreased by administration of SB (Figure 2.4 D,E). The suppression was dose-dependent. The lower dose of the antagonist significantly decreased w_{Exc} , but the effect was virtually absent for w_{Inh}. However, the higher dose of SB was much more efficient in suppressing the Meth sensitivity of both the inhibitory and excitatory drives. Finally, the Meth sensitivity of HD node was progressively increased with increasing dose of SB (Figure 2.4 F) implying an ability of this population to be activated by progressively lower doses of Meth.

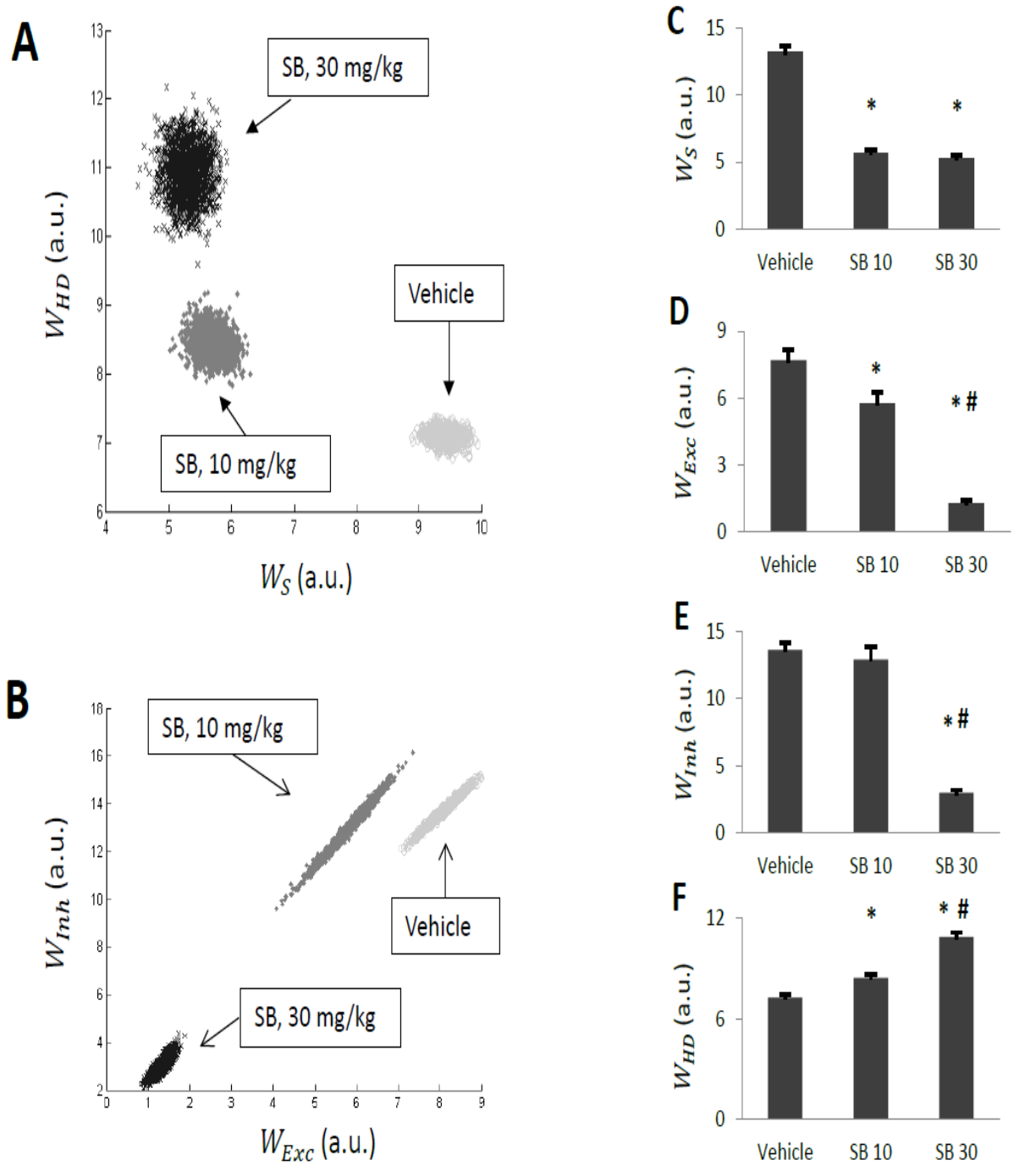

Figure 2.4 Parameter estimates generated by Monte-Carlo simulations, A-B: Statistical ensembles of parameters (amplitude of stress, and Meth-sensitivities of three Meth-dependent populations) projected onto (w_S, w_{HD})-plane (A) and (w_{Exc}, w_{Inh})-plane (B) for each of the three doses of SB (vehicle, 10 and 30 mg/kg). C-F: Individual parameters for each dose of SB. * denotes statistically significant difference from vehicle (SB 0, $p<0.05$) between SB 10 and SB 30 ($p<0.05$).

2.6 Effects of SB on the network components

Of particular interest is how SB-evoked changes in the parameters of the model affect activation profiles of Meth-sensitive network components. Activities of *Exc*, *Inhib* and *HD* as functions of the blood concentration of Meth are shown at Figure 2.5 A, B and C. SB downgrades the slope of the dose-dependence curve in case of *Exc* and *Inhib*, which signifies desensitization of these nodes (more Meth is required to evoke same response). The effect of SB on *Exc* is significant for both doses of antagonist and increases with dose. In contrast, an effect of the lower dose of SB on *Inhib* is subtle. Unlike two other Meth sensitive populations, *HD* gains higher sensitivity to Meth when SB is present as its dose-dependence curve shifts to the left. Therefore, lower concentrations of Meth are able to activate this neuronal population.

Superposition of inputs from these populations results in complex modification of *SPN* activity which ultimately controls the thermal response. The dose-dependence of *SPN* activity is shown in the Figure 2.5 D, which is aligned with simulated pharmacokinetic profile of Meth after various doses of Meth used in this study (Figure 2.5 E). The low dose of Meth (1 mg/kg, Meth-1 in Figure 2.5 E) does not evoke any significant response when either of SB doses is present.

The intermediate Meth dose (5 mg/kg, Meth-5 in Figure 2.5 E) is sufficient to elicit strong thermogenesis after the higher dose of SB (30 mg/kg, SB30 in Figure 2.5 D) but not after the lower dose of the antagonist (10 mg/kg, SB10 in Figure 2.5 D). 10 mg/kg of SB desensitizes *Exc*, barely affects *Inhib*, and sensitizes *HD*. Together these changes leave the activity of *SPN* at the peak Meth concentration caused by the injection of 5 mg/kg of Meth almost unaltered (Figure 2.5 D, E). In contrast, 30 mg/kg of SB sensitize HD a little more (Figure 2.5 C), but more importantly this dose substantially desensitizes the *Inhib* population (Fig. 5B) leading to disinhibition of *SPN* activity (compare SB10 and SB30 in Figure 2.5 D).

As mentioned SB induces sensitization of *HD* population to Meth (Figure 2.4 F, Figure 2.5 C) which results in longer activation of the *HD* component by the same Meth concentration profile (Meth-10 in Figure 2.5 E) due to progressively lower *HD* activation threshold (compare Veh, SB10 and SB30 in Figure 2.5 D).

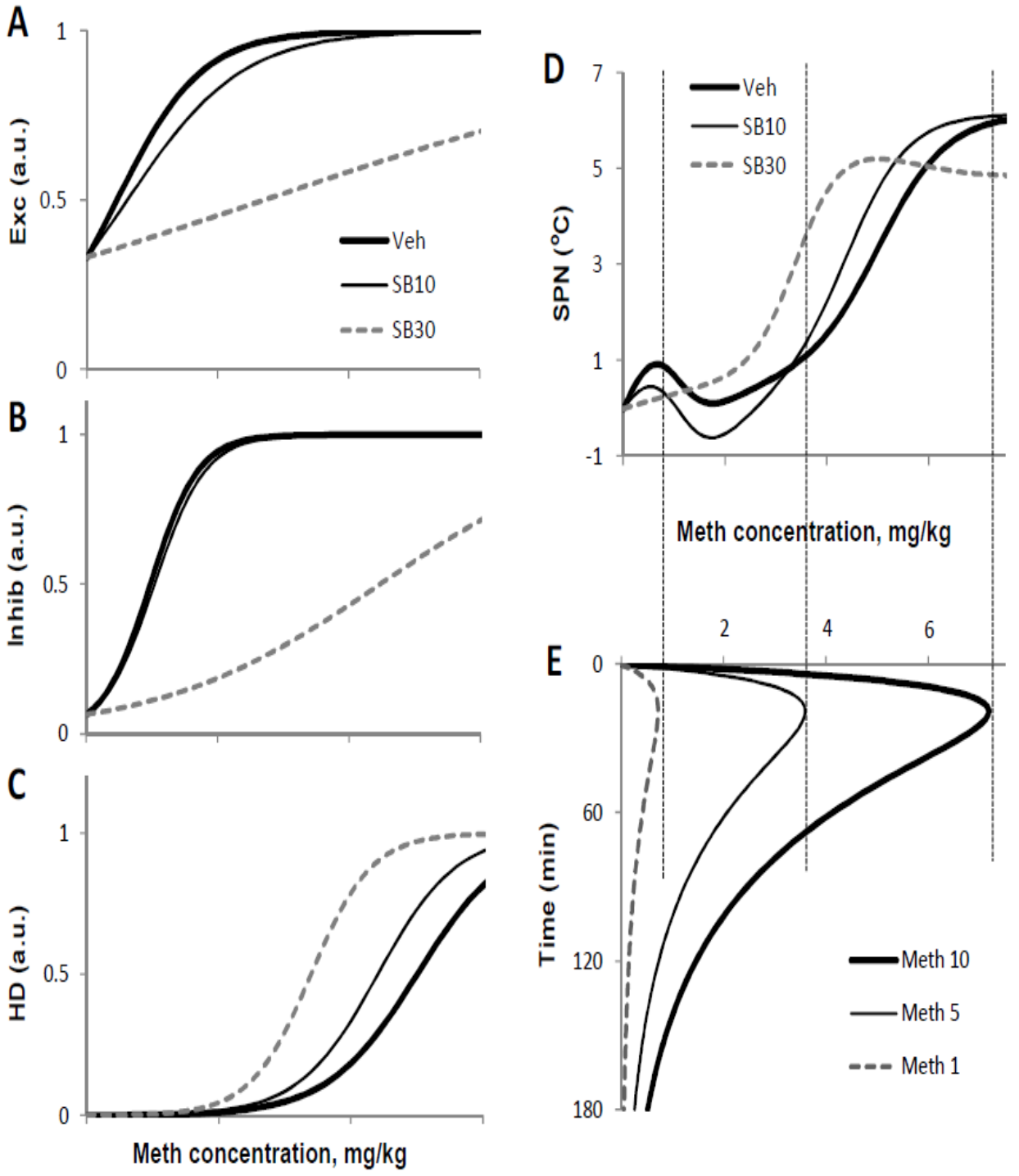

Figure 2.5 Activation curves of nodes of the model compared with pharmacokinetics of Meth. A-D: Activity of the network nodes as functions of Meth concentration in the blood after three doses of SB-334867: 0 (Veh), 10 and 30 mg/kg using best fit parameters. E: Time courses of the Meth concentration after different doses of Meth (1, 5 and 10 mg/kg) as generated by the model.

2.7 Effects of SB on the temperature responses to Meth

2.7.1 Control responses to Meth

Without SB and Meth, injections of the vehicle and saline cause stress which activates *Exc* (see Fig. 1). This activation results in two early "peaks" of temperature in the beginning due to two injections separated by 30 min, followed by a decline to baseline (Fig. 6A).

For 1 mg/kg of Meth, stress and Meth together activate *Exc* far greater than *Inhib* resulting in higher and longer maximum temperature after 1 mg/kg than after saline, however, the gradual decline afterwards was similar (Fig. 6B).

Following the vehicle, the intermediate dose of Meth (5 mg/kg) activates both *Exc* and *Inhib* to their full extent effectively cancelling each other, and the second "stress bump" almost completely disappears. Accordingly, the body temperature does not react until after 60 min when the Meth concentration falls below the activation threshold of *Inhib*. This explains the plateau and gradual increase in temperature in the late phase (Fig. 6C).

Finally, after 10 mg/kg of Meth at the early stage the activation levels of *Exc* and *Inhib* are saturated and negating each other. *HD* component is activated which results in an immediate robust temperature increase (Fig. 6D). After approximately 70 min the Meth concentration falls below *HD*'s activation threshold, and the temperature starts declining. Later on, in about 120 min, Meth decreases enough to deactivate *Inhib* and, thus, to disinhibit *Exc* which temporarily slows the temperature drop or even initiates a secondary peak (not seen in Fig 6D).

For more details about temperature responses to Meth alone see [1].

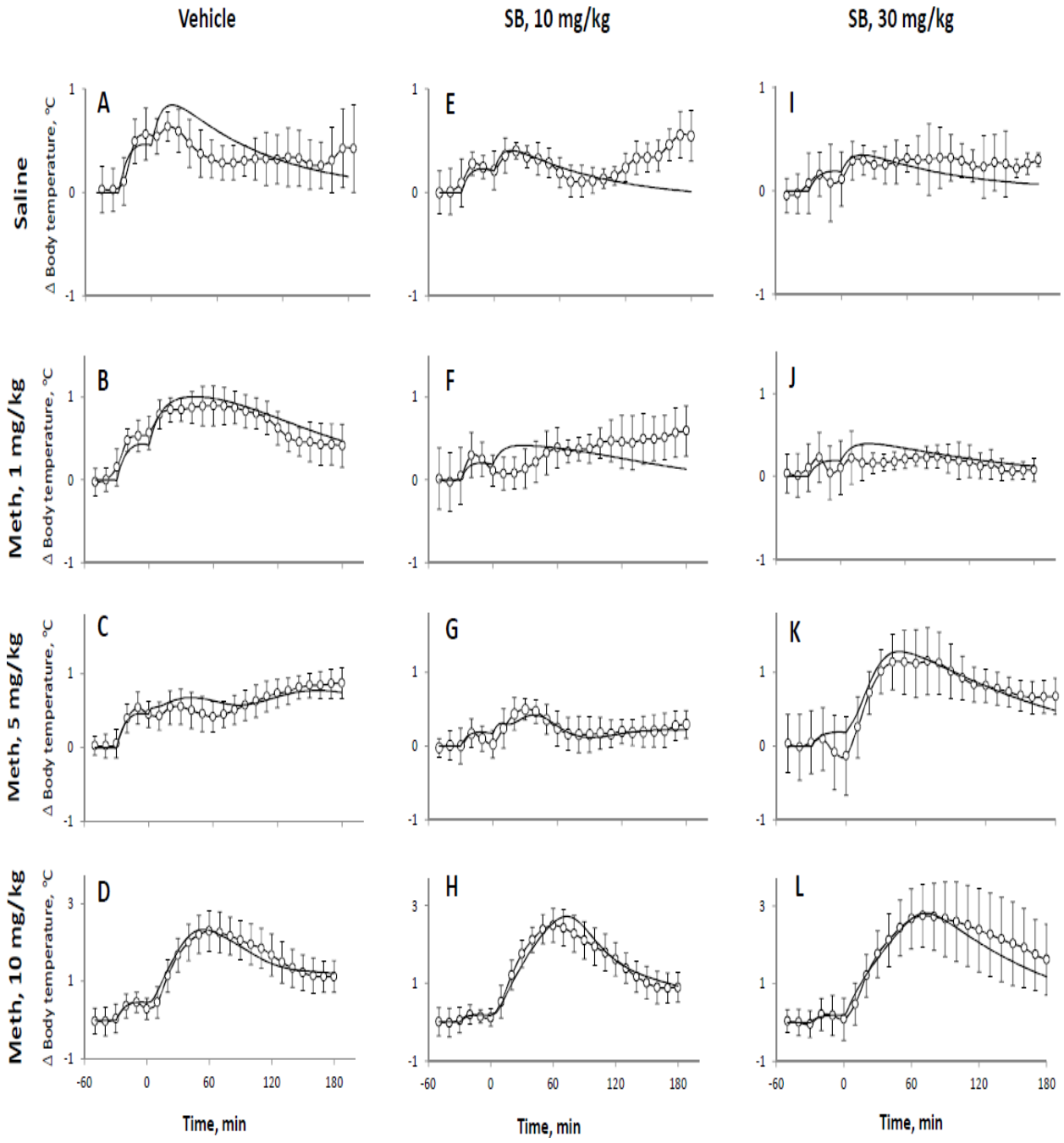

Figure 2.6 Comparison of experimental data and model responses, Experimental data shown by open circles (average temperature); error bars represent standard deviations over a group of rats. Model responses using best fit parameters are shown as thick lines. SB vehicles for both doses were pooled into a single group. Columns of graphs correspond to different doses of the antagonist (A-D: Vehicle, E-H: 10 mg/kg and I-K: 30 mg/kg as marked at the top), rows of graphs correspond to different doses of Meth (Saline, 1, 5 and 10 mg/kg, as marked at the left).

2.7.2 Responses to Meth after SB

Administration of SB itself results in a spike in temperature due to stress caused by the injection which is partially suppressed by the drug (Figure 2.2). The second bump on the temperature curve in Fig. 6E corresponds to the injection of saline. The suppression of the responses to stress does not increase significantly with increasing dose of the orexin antagonist (compare Figure 2.6 E and I).

After administration of SB the temperature response to the low dose of Meth does not exceed that of animals injected with saline (compare Figure 2.6 F, J and E, I) suggesting that the temperature responses to the low dose of Meth are eliminated (see Figure 2.5 D).

At the intermediate dose of Meth (5 mg/kg) the temperature responses are noticeably and differentially altered by 10 and 30 mg/kg of SB (Figure 2.6 C, G, K). After 10 mg/kg of SB the temperature curve loses the late ascending phase present in Figure 2.5 C. This modification is concerned with SB-evoked desensitization of *Exc* to Meth (see Figure 2.4 D, Figure 2.5 A, D). After the higher dose of SB (30 mg/kg) there appears strong immediate hyperthermia (Figure 2.6 K) explained by sensitization of *HD* and desensitization of *Inhib* (Figure 2.5 B, C, D).

Finally, after 10 mg/kg of Meth, both *Exc* and *Inhib* are activated to some extent by overcoming the blockade, but activation of *HD* overshadows the activity of the two, producing progressively larger temperature increase with increasing dose of SB (Figure 2.6 D, H, L). This augmented hyperthermia as well as its longer duration is also mediated by SB-induced sensitization of the *HD* node and desensitization of *Inhib* to Meth (see Figure 2.5).

2.7.3 Mechanism of HD sensitization

Orexin is an excitatory neurotransmitter [56]. Accordingly, a blockade of orexin receptors is expected to reduce the activity of the postsynaptic neurons in presence of orexinergic synaptic inputs. From this perspective, the desensitization of *Exc* and *Inhib* populations by the orexin antagonist allows for a straightforward interpretation. Specifically, we can assume that these two nodes receive orexinergic projections from Meth-activated neurons, and, hence, these inputs are suppressed by the orexin receptor antagonism (see Figure 2.2).

In the model presented in Figure 2.1 we assumed that SB affects the parameters of sensitivity of Meth-dependent populations w_{Exc}, w_{Inh}. This worked out very well to reproduce the data and is consistent with orexin excitatory action. In contrast, the *HD* population gets sensitized by the

antagonist, which contradicts to the excitatory influence of orexin. Therefore, we assume that Meth-activated excitatory input, which this node receives, is not mediated by orexin. Instead, *HD* node may receive strong inhibition from another neural population whose activity is controlled by orexin receptors. In the presence of the orexin antagonist the activity of this inhibitory population gets reduced which in turn disinhibits *HD* (Figure 2.7 A).Therefore, progressive sensitization of *HD* (Figure 2.4 F), which was described above by an increase in w_{HD}, is more likely a result of *HD* disinhibition as illustrated in Figure 2.7 A.

The orexinergic drive in Figure 2.7 A can be Meth-dependent or Meth-independent. In the former case the net Meth-dependent input to HD will be defined by the difference of Meth-induced excitation and inhibition. In presence of SB, the inhibition is reduced which results in the increased HD sensitivity to Meth characterized by the parameter w_{HD}. In the latter case, the orexin antagonist does not affect the Meth-dependent input directly. It rather alters the basal excitability of the HD population defined by the orexin-dependent tonic inhibition it receives. Accordingly, a more biologically correct way to describe this is to alter γ_{HD} for different doses of SB, rather than w_{HD}.

γ_{HD} estimates obtained by Monte Carlo simulations using $(w_S, w_{Exc}, w_{Inh}, \gamma_{HD})$ as a set of SB-affected parameters are shown in Figure 2.7 B. As expected, this parameter progressively declines with increasing SB dose which leads to changes in *HD* activation curve almost indistinguishable from shown in Figure 2.5 C. Obviously, the likelihood for these two models is almost the same, and hence they are equally probable from Bayesian standpoint.

To summarize, the sensitization of *HD* component of the network is concerned with its disinhibition. Their experimental data does not allow for a conclusion if this inhibition is Meth-activated or not.

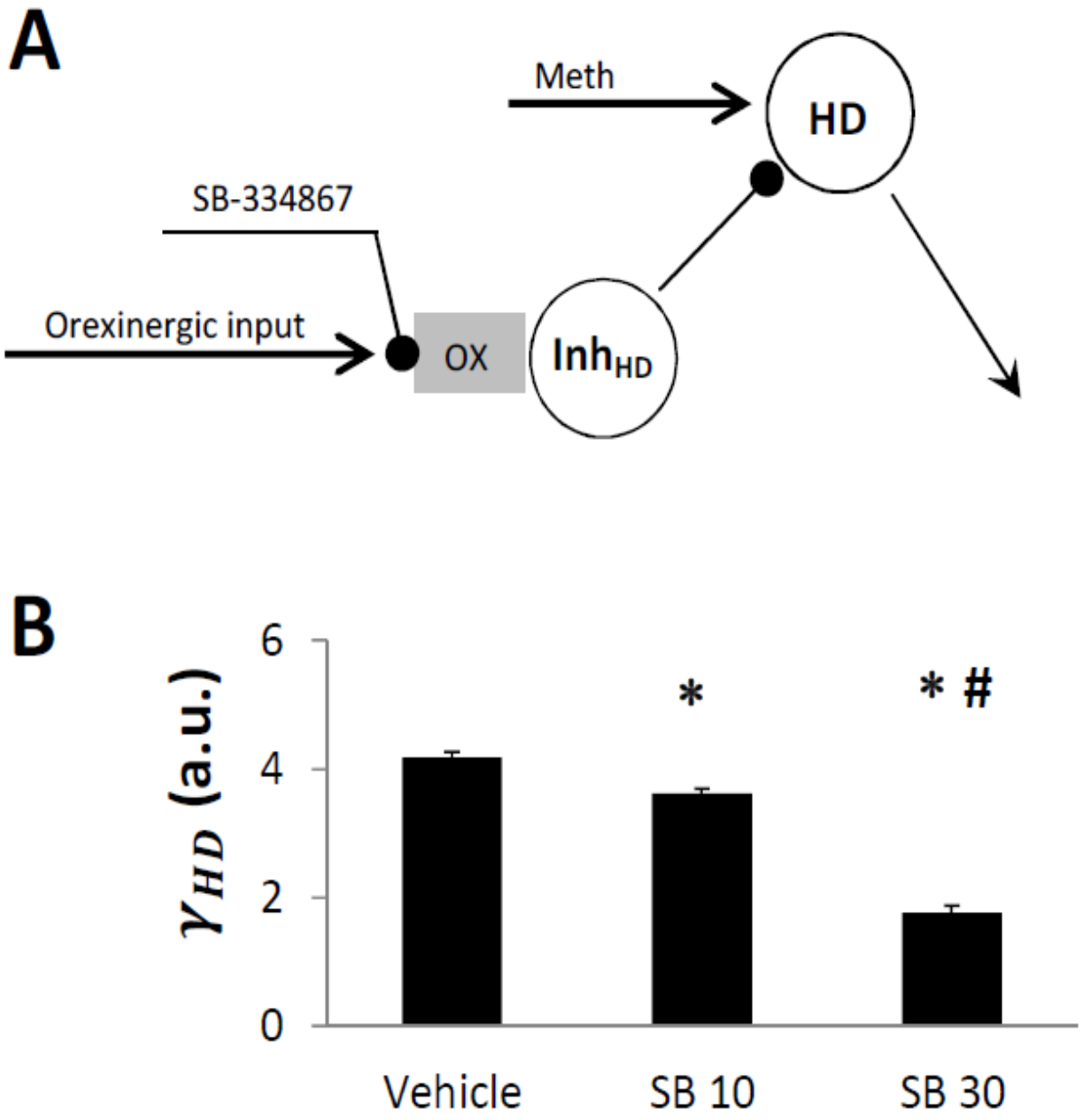

Figure 2.7 Interpretation of HD sensitization as a change of inhibitory tone to the HD: A: The mechanism of HD sensitization by the orexin receptor antagonist. SB suppresses activation of the inhibitory population Inh_{HD} by orexinergic input which disinhibits HD and thus lowers its activation threshold. B: Effect of SB on the basal inhibitory tone to HD population γ_{HD} when it is used as an SB-affected parameter instead of w_{HD}. * - the estimate is statistically significantly different from the one for Vehicle (SB-0, $p<0.05$); # - the estimates are statistically significantly different between SB 10 and SB 30 ($p<0.05$). See Results for more details.

2.7.4 Effect of inhibition failure

The inhibitory control of *HD* population described above may originate from the *Inhib* node of the circuitry (see Figure 2.1). In this case we can synthesize the network architecture by combining the schematics from Figure 2.1 A and Figure 2.7 A as shown in Figure 2.8 A. We implemented a corresponding mathematical model and found that it fitted our experimental data with comparable precision (not shown) and hence had similar likelihood.

This model has a very important implication for the role of inhibition in this system. Indeed, both excitatory components, *Exc* and *HD*, appear to be controlled by the inhibitory drive whose failure may have dramatic consequences. Our simulations demonstrate the consequences of such failure. Figure 2.8 B demonstrates how temperature responses to Meth change if the maximal activity of *Inhib* population is bounded. In our simulations we used a relatively low dose (3 mg/kg) which does not produce major response under baseline conditions (see unmodified 100% inhibition in Figure 2.8 B). If the maximal activity of the *Inhib* population was decreased by two times (50% inhibition), the body temperature rose by almost 2 degrees. When *Inhib* was completely silenced, the body temperature reached life-threatening levels at almost 40^{o} C (0% inhibition in Figure 2.8 B).

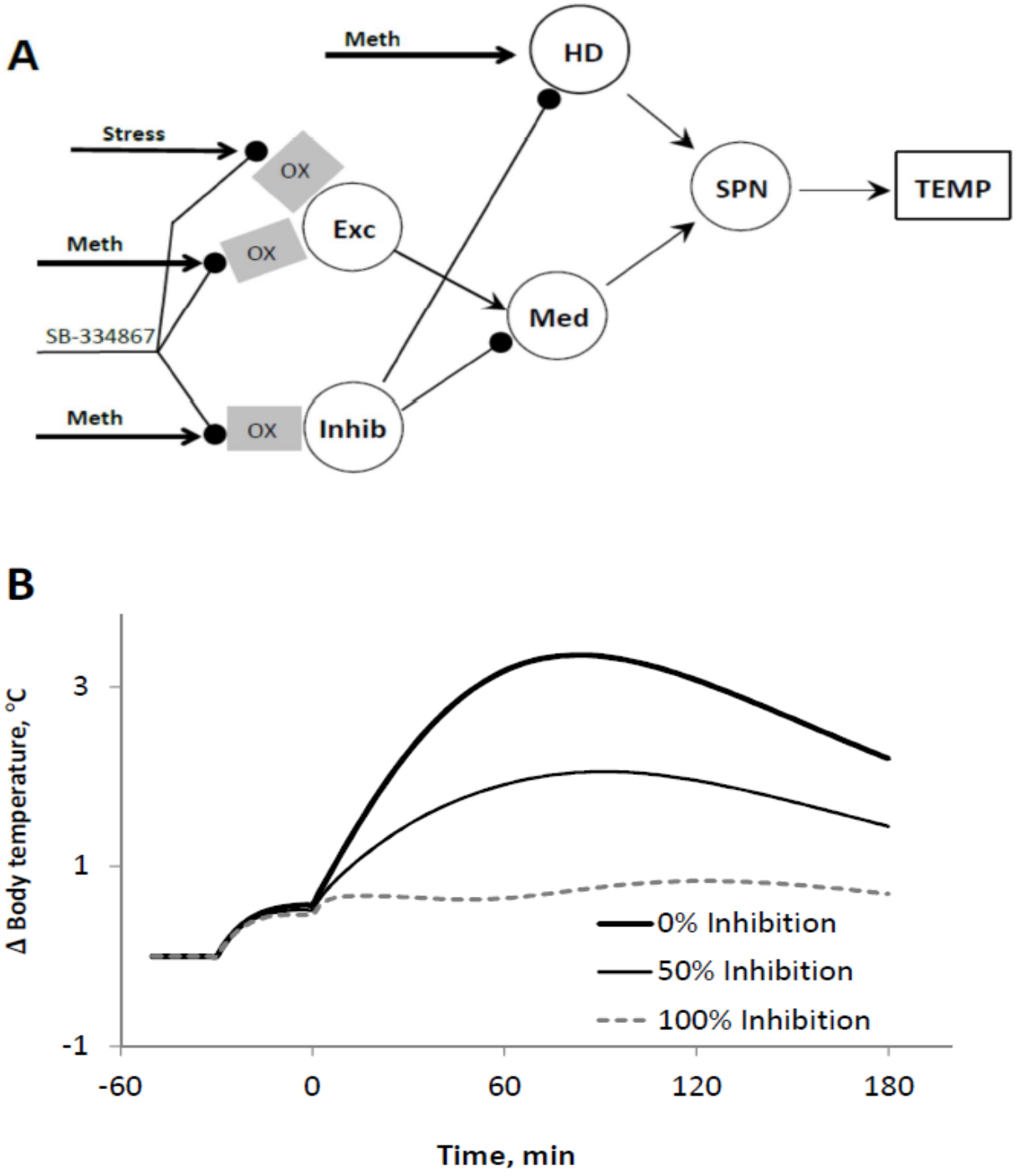

Figure 2.8 Reduced model and effect of inhibitory failure on the response: A. The extended model schematic in which the inhibitory tone to HD originates from Inhib population (see explanations in the Results). B: Effect of inhibitory failure in the modified model on the response to 3 mg/kg of Meth (see details in the Results).

2.8 Discussion

2.8.1 Biological Implication

This study builds upon previously published mathematical models [1], which were based on the premise that body temperature response to Meth is dependent upon the interaction between two neural components: excitatory and inhibitory drives. The difference in strength between these two signals ultimately determines the dynamics of body temperature.

The injections of SB (0 mg/kg, 10 mg/kg, and 30 mg/kg) differentially modify temperature responses to low, intermediate and high doses of Meth (0 mg/kg, 1 mg/kg, 5 mg/kg, and 10 mg/kg). Previously it was reported that 10 mg/kg of SB suppressed the temperature response to stress of injection and also late hyperthermia induced by the intermediate (5 mg/kg) dose of Meth [48]. The limited conclusiveness of that study was concerned with the fact that SB-related effects on the temperature response in the early phase ($t < 60$ min) were impossible to separate from stress-induced temperature fluctuations resulting from two intraperitoneal injections.

In this study using mathematical modeling we were able to reliably decompose the effect of SB into stress- and Meth-related components, and thus provide a straight-forward mechanistic explanation for the intricate alterations of the temperature responses to different doses of Meth induced by orexin receptor antagonism.

2.8.2 Two excitatory components in temperature responses to Meth

In publication [1], where the authors suggested the circuitry shown in Figure 2.1 to explain the complexity of the temperature responses to Meth, they also considered an alternative model where the excitatory populations, *Exc* and *HD*, were combined into a single excitatory node. The data used in that study failed to emphasize the plausibility of either architecture.

In the present study we have shown that two distinct excitatory populations are necessary to explain differential effects of the orexin receptor antagonist on the responses to low and high doses of Meth. Specifically, activation of the first excitatory population (*Exc* in Figure 2.8 A) by low doses of Meth is mediated by orexinergic neurotransmission, while the direct Meth-dependent input to the second population (*HD*) does not rely on orexin receptor activation.

The details of the network architecture shown in Figure 2.7 A and Figure 2.8 A clarify the nature of high activation threshold of the *HD* component which is yet another distinctive feature of the

second excitatory population in the network. The lack of response of this population to low doses of Meth is not concerned with its lower sensitivity, but rather defined by a tight inhibitory control originated either from *Inhib* or some other inhibitory neuronal population(s). High doses of Meth are needed to overcome this inhibition. In either case the source of this inhibition is dependent upon orexinergic input. Orexin receptor antagonism suppresses the inhibition and thus lowers *HD* activation threshold which underlies SB-induced exaggeration of responses to high doses of Meth.

2.8.3 Biological implications

The results of this work have several important implications to consider.

Amphetamines are known to activate orexin-containing neurons in the perifornical area [39, 40]. From the phenomena observed in our experiments we conclude that this activation of orexinergic cells is required for temperature responses to Meth. The entire hypothalamus including dorsomedial hypothalamus contains orexin-containing fibers [57], which can mediate the above effects of Meth. However, this activation can be mono- or polysynaptic (for example, perifornical area – ventral tegmental area – hypothalamus, or have even more connections).

The *Inhib* population in the network plays an extremely important role in counteracting hyperthermia. Previously, Molkov et al. have demonstrated that an imbalance of excitatory and inhibitory components can result in significant amplification of the response to relatively low doses of Meth [1]. The details of the circuitry proposed in this study emphasize the importance of the inhibitory component(s) even more. Simulations shown in Figure 2.8 B demonstrate that a relatively low dose (3 mg/kg), which does not induce virtually any response in intact animals (see 100% inhibition in Figure 2.8 B), can evoke profound hyperthermia typical for much higher doses (compare 0% inhibition in Figure 2.8 B with Figure 2.6 D). The impairment of the inhibitory control can not only allow excitation to pass through *Med*, but also lower the *HD* activation threshold so that this population gets activated by relatively low Meth doses.

Another implication of our results is that using orexin receptor blockade as a treatment for other ailments could cause life-threatening side effects. In particular, orexin antagonists were proposed to prevent or treat addictions to various drugs [58, 59]. An increase in excitability of the *HD* population in presence of SB highlights a potential danger of its use to treat drug abuse if the person uses the drug during treatment. Indeed, suppression of acute effects of amphetamines by

the orexin antagonist may force an abuser to increase the dose which may cause life-threatening hyperthermia due to a dysfunction of the inhibitory population(s). Similarly, our model predicts that narcoleptic patients, whose condition is putatively caused by a lack of orexin [60], may be at higher risk of life-threatening overdose of amphetamine-like stimulants, which are usually prescribed to treat such patients [61].

[45] reported that administration of orexin into raphe pallidus evoked activation of thermogenesis in the BAT and increased body temperature in anesthetized rats. Surprisingly, local microinjection of SB into the same area also induced thermogenesis and hyperthermia [45]. Our analysis provides possible interpretation of this data as the network has both excitatory and inhibitory populations activated by orexin. Namely, activation of the excitatory drive by orexin can evoke thermogenic response, whereas a blockade of orexin receptors in the inhibitory population will remove the inhibitory tone which may result in a similar effect.

2.9 Conclusions

In this study, using mathematical modeling, we mechanistically explained non-trivial alterations of temperature response to various doses of Meth at presence of the orexin receptor antagonist. Our model can be used to generate experimentally-testable predictions on the thermogenic effects of Meth when activity of orexin receptors is modified. The model has several essential features regarding the mechanisms of Meth-evoked hyperthermia and stress response.

- Both low dose of Meth and stress activate the excitatory component which is mediated by orexin receptors and hence can be suppressed by SB.
- The inhibitory component of the response to Meth is also mediated by orexin.
- Orexin antagonism disinhibits, and thus increases the sensitivity of the component normally activated by the high dose of Meth.
- Insufficient inhibitory drive can cause fatal hyperthermia after relatively low doses of Meth. This insufficiency can be provoked by a decreased orexinergic tone either due to deficiency of orexinergic transmission (narcolepsy) or after administration of orexin receptor antagonists (e.g. used for drug abuse treatments).

CHAPTER 3. CIRCADIAN VARIABILITY OF BODY TEMPERATURE RESPONSES TO METHAMPHETAMINE

3.1 Introduction

Vital parameters of living organisms exhibit circadian rhythmicity. Daily variations of body temperature in rats may exceed 1^{o}C, with body temperature at night being higher than during daytime. Accordingly, temperature fluctuations in response to low doses of amphetamines appear comparable to daily variations of body temperature: i.p. injection of 1 mg/kg of methamphetamine (Meth) increases body temperature by approximately same 1^{o}C [1, 17]. Intermediate doses of Meth (5 mg/kg, i.p.) evoke a response of similar magnitude, but delayed in time [1, 62]. Therefore, it is reasonable to hypothesize that the temperature responses to psychostimulants may differ depending on the time of the day. However, despite rats are nocturnal animals, most of the studies of drugs of abuse in rodents are performed during the day. To the best of our knowledge, this is the first study to describe circadian variability of responses to methamphetamine (Meth).

There is a clear interaction between circadian rhythmicity and effects of amphetamines. First, amphetamines induce arousal which could be due to alterations in the neuronal activity controlling circadian rhythms. Administration of Meth results in activation of orexin-containing neurons [2, 39, 40], which are critical for normal circadian rhythmicity and are activated during active phase of day cycle. Chronic use of Meth leads to disruption of normal circadian rhythmicity. If Meth is freely provided to rats in the drinking water, they establish an oscillatory pattern of activity [63]. Although the period of these oscillations is close to circadian (24-36 h), they are independent of the circuits mediating normal circadian rhythmicity, as these oscillations also emerge in rats with a lesioned suprachiasmatic nucleus (SCN) [64].

To explain the circadian variability of temperature responses to Meth, in this study, we used a mathematical model which was previously developed to explain complex, multiphasic responses of body temperature to Meth during the daytime [1, 62]. The model is based on the premise that body temperature variations after Meth administration have both an excitatory and inhibitory drive. The difference in strength between these two signals determines the dynamics of body temperature. Using this model, we assimilated the experimentally obtained nighttime temperature responses to Meth. Then, we used Bayesian inference analysis to find which

parameters of the model are significantly different between phases of the circadian cycle, and interpreted the differences we found.

3.2 Methods and Data Preparation

To determine temperature responses to Meth three groups of animals were studied in home cages at room temperature in rooms with lights on at 8 am and off at 8 pm. In the first group (Meth-1) experiments we injected Meth at 1 mg/kg i.p., in the second (Meth-5) 5 mg/kg i.p, and the third normal saline. For each group, half of animals were assigned to experiment during light phase (i.p. injection between 10 and 11 am), and others were injected at dark (between 10 and 11 pm). Each animal received only one injection of Meth. The number of animals in each group was chosen so that the amplitude of Meth-induced temperature deviation from the baseline was statistically significantly different between the day and night groups.

3.3 Model Construction

3.3.1 General Model approach

Experimental data on dose-dependence of temperature responses to Meth during daytime were described with acceptable precision by a mathematical model previously published in. [1]. In short, the model consisted of three components: pharmacokinetics describing concentration of Meth in the blood after injection; a neural network which had Meth-dependent inputs, and a temperature control system driven by a signal from the neural network (Figure 3.1).

We assumed that after the injection the drug was absorbed in the blood from the peritoneum and was also simultaneously being eliminated from the blood. Accordingly, drug concentrations were described by the following equations:

$$\frac{d[M_p]}{dt} = -\frac{[M_p]}{\tau_u}$$
$$\frac{d[M]}{dt} = \frac{[M_p]}{\tau_u} - \frac{[M]}{\tau_d} \qquad (3.1)$$

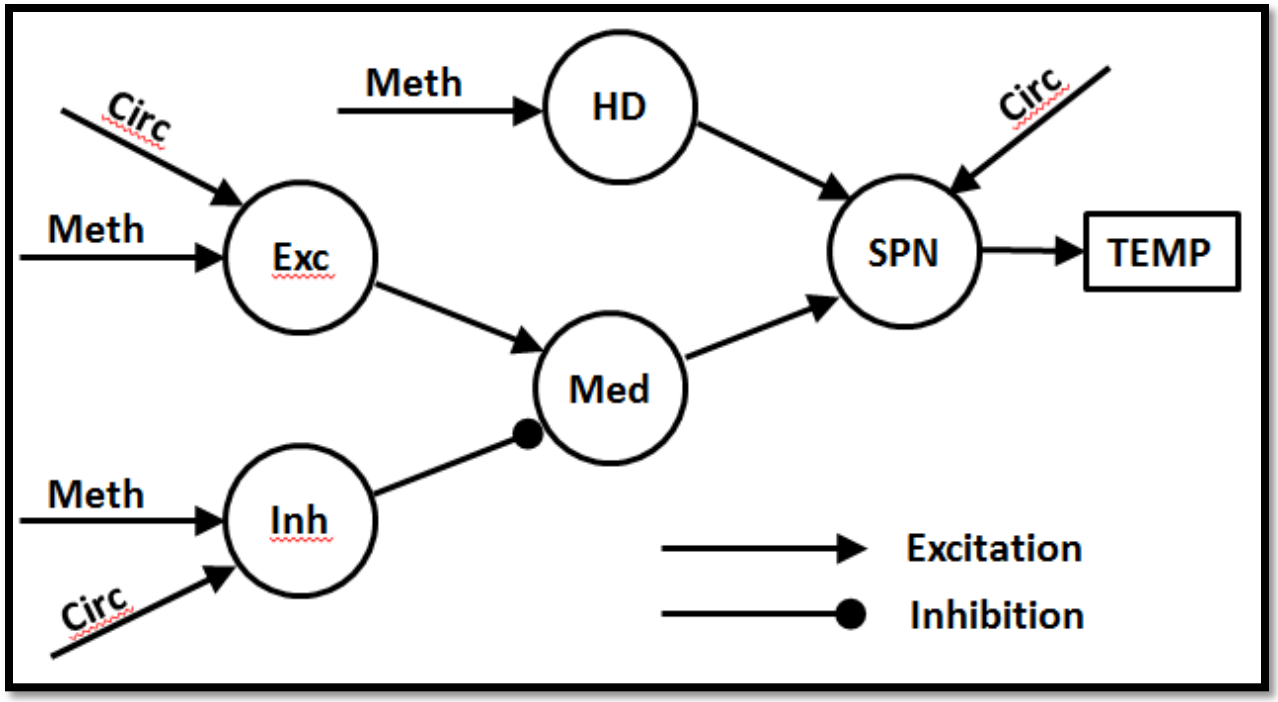

Figure 3.1 Schematic of the network mediating the temperature responses to Meth suggested by [1] incorporating circadian phase-dependent inputs. Each circle represents a neural population. Meth-sensitive populations (see "Meth"-labeled arrows) are modeled as an artificial neuron with sigmoidal activation function applied to its input (see text for a detailed description). "Circ"-labeled arrows represent circadian phase dependent inputs. Exc, excitatory; Inh, inhibitory; HD, high dose; Med, medulla; SPN, sympathetic preganglionic neuron; TEMP, temperature.

where *t* is time in minutes, M_p is the intra-peritoneal drug concentration, and M is the blood drug concentration (both in mg/kg). $[M_p]/\tau_u$ represents drug absorption with time constant τ_u, and $[M]/\tau_d$ represents drug elimination with time constant τ_d. Initial conditions are $[M_p](0) = d$, $[M](0) = 0$ for injections made at time *0* where *d* is the dose of the drug administered. System (3.1) can be solved explicitly as:

$$[M](t) = d\left(\frac{\tau_u}{\tau_d} - 1\right)^{-1}(e^{-t/\tau_u} - e^{-t/\tau_d}) \qquad (3.2)$$

for $t > 0$, and $[M](t) = 0$ if $t < 0$.

In this study, we use exactly the same formalism as in [1] to model the neural circuitry as a feed-forward artificial neural network. The outputs of Meth-sensitive neural populations are calculated as follows:

$$\begin{aligned} P_{Exc}(t) &= \sigma(w_{Exc} \cdot [M](t) + \gamma_{Exc}) \\ P_{Inh}(t) &= \sigma(w_{Inh} \cdot [M](t) + \gamma_{Inh}) \\ P_{HD}(t) &= \sigma(w_{HD} \cdot [M](t) + \gamma_{HD}) \end{aligned} \quad (3.3)$$

where $\sigma(x) = (1 + \tanh x)/2$ is a sigmoid activation function, $w_i(t)$ is the sensitivity of $P_i(t)$ to Meth, and γ_i is the parameter defining baseline activity of the population P_i, $i \in \{Exc, Inh, HD\}$. The activity of medullary population *Med* is described as follows:

$$P_{Med}(t) = w_{Exc \to Med} \cdot P_{Exc}(t) - w_{Inh \to Med} \cdot P_{Inh}(t) \quad (3.4)$$

where $w_{Exc \to Med}$ and $w_{Inh \to Med}$ are the weights of the excitatory and inhibitory projections from Exc to Med and Inh to Med, respectively. Inframedullary population SPN duplicates the activity of Med but is additionally excited by the Meth-sensitive HD population as follows:

$$P_{SPN}(t) = P_{Med}(t) + w_{HD \to SPN} \cdot P_{HD}(t) + \gamma_{SPN} \quad (3.5)$$

where $w_{HD \to SPN}$ is the weight of the excitatory projection from HD to SPN, and γ_{SPN} is the activity of *SPN* in absence of inputs from Med and HD.

The temperature dynamics is modeled by a first-order linear ODE driven by the SPN signal as follows:

$$\tau_T \frac{dT}{dt} = P_{SPN}(t) - (T - T_0) \quad (3.6)$$

where T is the body temperature in degrees Celsius, τ_T is the time constant of the temperature response, and T_0 is the baseline body temperature. See [1] for all parameter values.

The equilibrium temperature was defined as the temperature at which the right hand side of (3.6) is equal to zero after Meth is completely washed out. Accordingly, it is a function of baseline activities of the nodes which can be calculated as follows.

$$T_{eq} = w_{Exc \to Med}\sigma(\gamma_{Exc}) - w_{Inh \to Med}\sigma(\gamma_{Inh}) + \gamma_{SPN} + T_0 \quad (3.7)$$

3.3.2 Circadian variability

The major assumption of the study was that animals have different status of the Meth-response system described above during active and inactive phases of the day. Specifically, we assumed that the responses are mediated by the same network, but the baseline activity of its nodes may be different during the day and at night. Accordingly, we used the experimental datasets we obtained for the day and nighttime to estimate the parameters of the model defining baseline activities of the nodes, i.e. γ_{Exc}, γ_{Inh} and γ_{SPN}. All other parameters were assumed independent of the circadian phase, so we used their values estimated in the original Meth-response study [1]. In our model, the baseline activity levels of the nodes are supposed to be defined by synaptic and neuromodulatory inputs independent of Meth, so the day vs. night differences in the values of parameters γ_{Exc}, γ_{Inh} and γ_{SPN} can be interpreted as circadian-related (changes of) external inputs to the network.

3.3.3 Statistical Estimation for Model's Parameters

We used the Bayesian approach for inferring the model parameters. Then, we employed statistical analysis to calculate statistical significance of changes in γ_{Exc}, γ_{Inh}, γ_{SPN} between day and night. To do this, we constructed a corresponding posterior probability density function (PDF) of the parameter vector $\boldsymbol{\gamma} = (\gamma_{Exc}, \gamma_{Inh}, \gamma_{SPN})$. According to Bayes' rule [65], this probability distribution is proportional to the probability that an observed temperature time series $\{T_i\}$ is produced by our model with the given $\boldsymbol{\gamma}$, usually referred to as a likelihood. Assuming that the residuals are normally distributed and non-informative priors for the parameters, the posterior PDF, $p(\boldsymbol{\gamma} \mid \{T_{i,d}\})$, is given by the following formula:

$$p\left(\boldsymbol{\gamma} \mid \{T_{i,d}\}\right) \sim \exp\left\{-\sum\nolimits_{d=1,5} \sum_{i=30}^{300} \frac{\left[T_{i,d} - T(\boldsymbol{\gamma}, i, d)\right]^2}{2\sigma_{i,d}^2}\right\} \qquad (3.8)$$

where $T(\boldsymbol{\gamma}, i, d)$ is the temperature calculated by our model at time *i* for dose *d* with the given $\boldsymbol{\gamma}$. $T_{i,d}$ and $\sigma_{i,d}$ are respectively a mean and a standard deviation of the body temperature over a corresponding group of animals for dose *d* at time *i* by increments of 10 minutes. We used the data starting from 30 minutes after the injection when the effect of the stress becomes negligible.

We used the Markov Chain Monte Carlo (MCMC) approach, specifically the Metropolis-Hastings algorithm adapted for reconstruction of dynamical systems [5, 51-53, 66, 67], to create

a statistical ensemble of points distributed according to the PDF (3.8). Once we had the ensembles, we calculated mean values and standard errors for the three parameter estimates for each combination of time of day and dose of Meth. Then, we used a two-sample t-test to evaluate the statistical significance of differences between the groups. P-value < 0.05 was accepted as a statistically-significant effect of the daytime on the corresponding parameter of the model.

3.4 Results

3.4.1 At night rats have higher body temperature and stronger stress response

Baseline (initial) body temperature of animals before the injections was 0.8 ºC higher on average at night for all groups (Saline, Meth 1 mg/kg, and Meth 5 mg/kg, Figure 3.2). The intraperitoneal injection of saline evoked a transient increase of the body temperature (Figure 3.2 A). This increase developed faster and was almost twice as great during the nighttime. The body temperature returned to initial values approximately one hour after the injection and did not change significantly for the remaining 5 hours after that.

3.4.2 At night rats exhibit a weaker hyper-thermic response to the 1 mg/kg dose of Meth

Lower dose of Meth (1 mg/kg) induced monophasic hyperthermia both during the day and at night (Figure 3.2 B). However, the maximal increase of the temperature was approximately half at night compared with the day. The maximal hyperthermia was observed 30 minutes after the injection at night while it occurred after 90 minutes during the day.

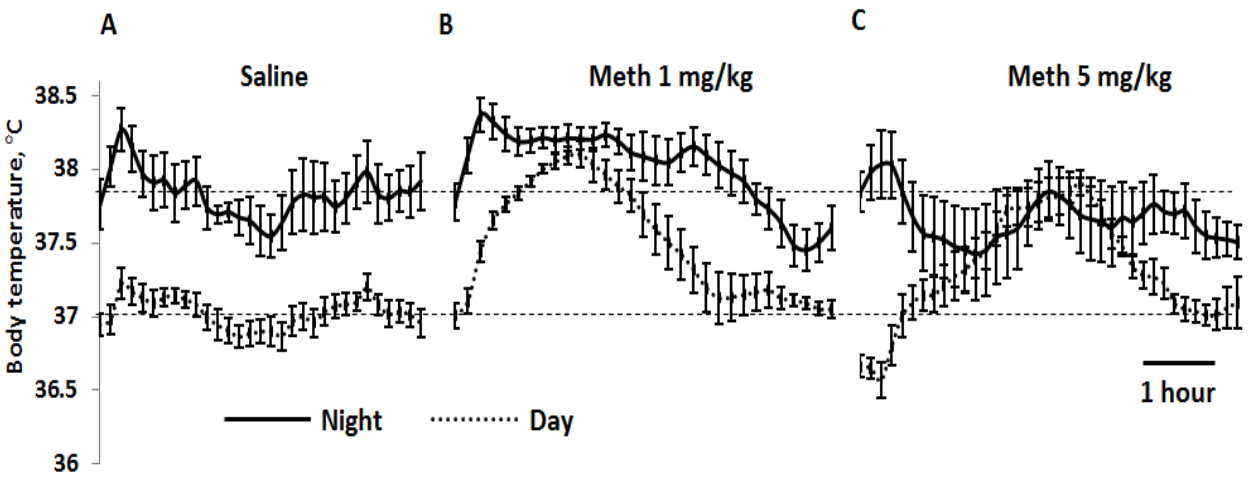

Figure 3.2 Experimental data on body temperature responses to i.p. injections of saline and two different doses of Meth at night (solid lines) and during the day (dotted lines). Data is shown as mean +/- SEM (N = 6). Dashed lines show approximate initial temperature.

3.4.3 At night, there is no hyper-thermic response to the intermediate dose of Meth

Higher dose of Meth (5 mg/kg) when administered during the daytime caused a delayed hyper-thermic response peaking at approx. 200 min since the injection (Figure 3.2 C). In contrast, at night, the same dose did not produce hyperthermia. Moreover, the temperature had a clear tendency to decrease, which was not observed during the day.

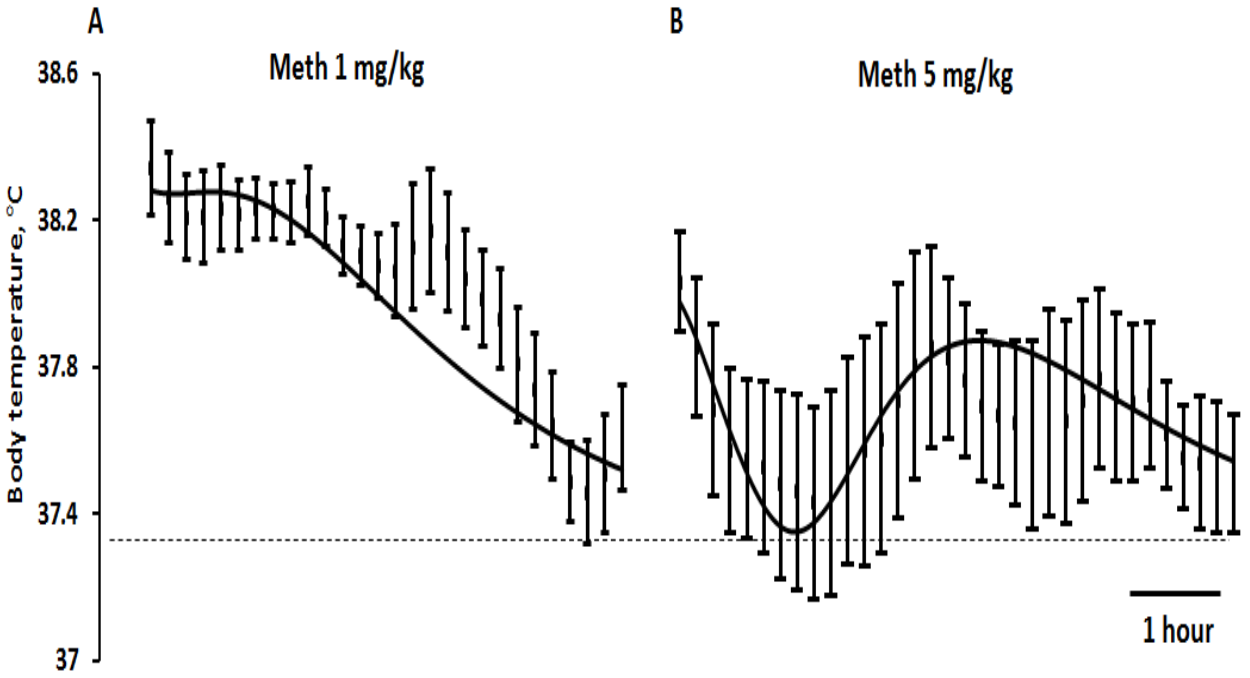

Figure 3.3 Temperature dynamics as reproduced by the model (solid curves) with parameters corresponding to the mode of PDF (8) superimposed on experimental data obtained at night (error bars) since 30 min after the injection of 1 mg/kg of Meth (**A**) and 5 mg/kg of Meth (**B**). Chi-square test [68]: sum squared standardized residual, $\chi^2 = 33.4$; number of degrees of freedom, $\nu = 51$; p-value = 97%. Coefficients of determination: $R^2 = 0.74$ for 1 mg/kg; $R^2 = 0.51$ for 5 mg/kg. Dashed line shows the equilibrium temperature estimate.

3.4.4 At night, the excitatory node has substantially higher baseline activity

We used model (3.1) to fit the above experimental data (see Figure 3.3 and its legend for the most probable model responses and conventional goodness-of-fit measures).

Then we sampled the PDF (3.8) to estimate parameters γ_{Exc}, γ_{Inh}, γ_{SPN} and their standard errors during the day and at night (Figure 3.4) as described in Methods. We found that at night the parameters defining baseline activities of Exc and Inh nodes, γ_{Exc} and γ_{Inh}, respectively, have statistically significantly higher values (Figure 3.4 A, B). Specifically, from day to night, the drive to excitatory node, γ_{Exc}, changes from about -0.35 to about 0.05 (Figure 3.4 A), which correspond to an increase in baseline activity of the Exc from approx. 30% to above 50% of maximum. The day-to-night change in the drive to the inhibitory node is relatively small from

approx. -1.3 to -1.0 (Figure 3.4 B) corresponding to the increase in its baseline activity from approx. 7% to 12%. Therefore, the baseline activity of the excitatory node is increased to a substantially greater extent than of the inhibitory node, which has a net positive effect on the baseline activity of the medullary node (see Figure 3.1). There was no statistically significant difference in γ_{SPN} values between day and night (Figure 3.4 C).

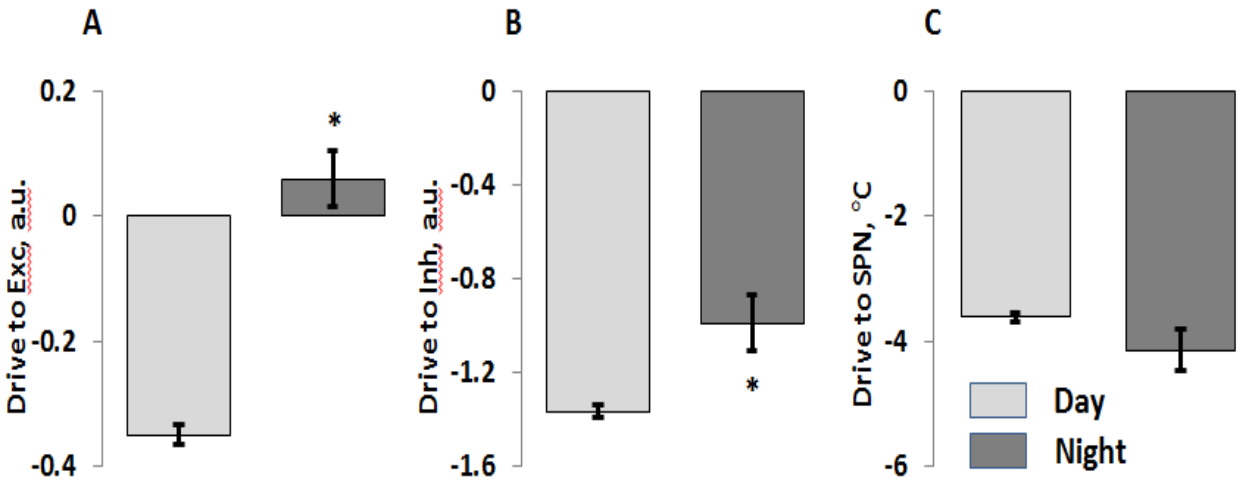

Figure 3.4 Inferences of circadian phase dependent parameters during the day (light gray) and at night (dark gray) shown as mean +/- SD of the posterior PDF (see Methods). * denotes statistically significant difference of daytime and nighttime values.

3.4.5 Meth reduces the equilibrium temperature in a dose-independent manner

As mentioned, during the day the average baseline temperature was approximately 0.8 ºC lower than at night. Specifically, the initial temperatures during the day and at night were 37.02 ± 0.04 ºC vs. 37.81 ± 0.09 ºC, respectively. In rats injected with saline the equilibrium temperature (see Eq. (3.7)) was equal to the baseline temperature. However, after Meth injections the equilibrium temperature appeared to be significantly lower. Specifically, during the day the equilibrium temperature was 36.66 ± 0.09 ºC, and at night it was 37.34 ± 0.06 ºC (Figure 3.3, Figure 3.5). Hence, on average, Meth injection caused a statistically significant decrease in the equilibrium temperature by 0.36 ºC during the day, and by 0.47 ºC at night.

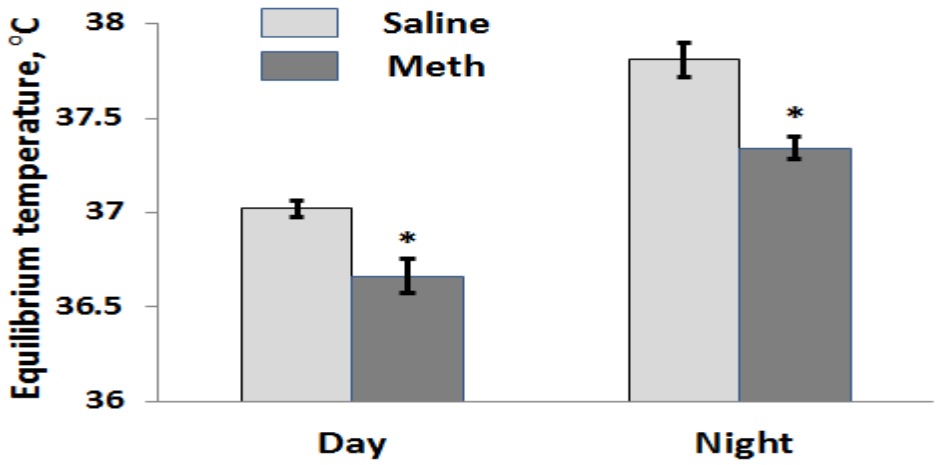

Figure 3.5 Estimates of equilibrium temperature for each combination of saline vs. Meth and day vs. night. Groups injected with either dose of Meth are pooled together.

To check whether this effect is dose dependent or not, we estimated the parameters γ_{Exc}, γ_{Inh}, γ_{SPN} separately for the groups of rats injected with 1 mg/kg and 5 mg/kg of Meth at night (Figure 3.6). We did not find statistically significant difference between the 2 doses in individual parameter values (Figure 3.6 A, B, C), as well as in the equilibrium temperatures (Figure 3.6 D).

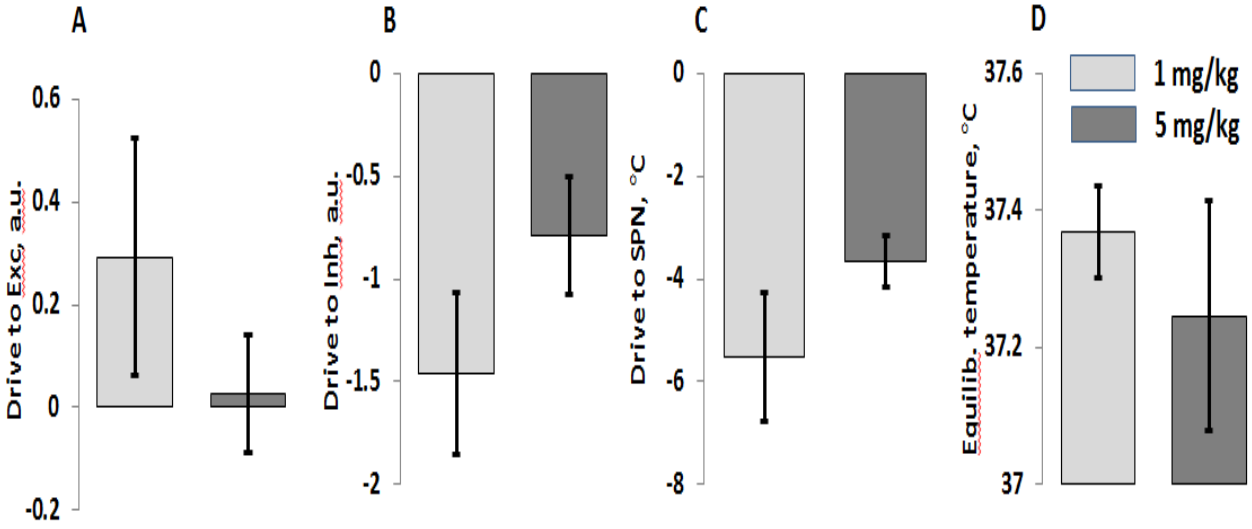

Figure 3.6 Comparison of circadian phase dependent parameter estimates at night for experimental groups injected with 1 mg/kg of Meth (light gray) and 5 mg/kg of Meth (dark gray). No statistically significant differences observed.

3.5 Discussion

3.5.1 Mechanisms of circadian variations of Meth responses

As we previously described in [1, 62], the temperature response to the administration of Meth has three distinct components putatively mediated by three distinct neuronal populations/nodes (Figure 3.1) that have different activation thresholds for Meth, and, hence, get activated at different Meth concentration levels.

The node most sensitive to Meth is labeled Exc in Figure 3.1. It is an excitatory node which can be activated by a low dose of Meth. This node mediates virtually immediate increase in the body temperature after injection of 1 mg/kg during the day (Figure 3.2, middle panel, dotted curve). By estimating the parameters of the model using the data obtained at night (Figure 3.2, two right panels) we found that at night the excitatory node has much higher baseline activity (~30% of max during the day vs. ~50% of max at night, see also Figure 3.3). We speculate that at night the corresponding population of neurons receives additional excitatory drive which may be treated as circadian rhythm related input.

Due to saturation, higher baseline activity of the excitatory node leaves less room for this population to further increase its activity after Meth injection. Specifically, during the day 70% of the maximal activity is still available, while only 50% remains available at night. Accordingly, the low dose of Meth (1 mg/kg) additionally activates this population to a lesser extent at night, which contributes to the attenuation of hyperthermia following Meth injection (Figure 3.2, middle panel).

The intermediate dose of Meth used in our study (5 mg/kg) is sufficient to activate not only the excitatory but also the inhibitory node (Figure 3.1). During the day, the excitatory and inhibitory components are almost level until the concentration of Meth falls below the threshold of the inhibitory component activation (see [1] for details). However, at night, due to saturation of the excitatory node activity as described above, the inhibitory node starts dominating during the initial phase of the response thus causing a transient reduction in temperature (Figure 3.4, right panel).

Another mechanism underlying smaller increase of the temperature after the low dose of Meth and a slightly hypothermic response to the intermediate dose at night is a reduction in the equilibrium temperature after the Meth injection. Since the initial temperature at night appears

almost a half degree higher than the equilibrium temperature (37.81 ºC vs. 37.34 ºC, respectively), the already weakened effect of the excitatory node activation occurs on the top of the declining trend towards the lowered equilibrium temperature.

3.5.2 Mechanisms of higher baseline temperature at night

In this study, we found that the excitatory node (Exc) of the neuronal network responsible for temperature fluctuations after Meth injections (Figure 3.1) has higher baseline activity. Specifically, Exc increases its baseline activity from ~30% of max during the day to ~50% at night. Such an increase, according to Eq. (3.7), would result in ~2ºC increase in temperature. At night, the baseline temperature was elevated by 0.8ºC only, so some compensatory mechanisms should be involved. In Figure 3.3 B one can see that parameter γ_{Inh}, which defines the baseline activity of the inhibitory node (see Inh in Figure 3.1), is also increased at night. This has a negative effect on the equilibrium temperature of about 0.5ºC. The remaining compensation (approx. 0.7ºC) must have been provided by other, e.g. thermoregulatory, mechanisms.

3.5.3 Mechanisms of lower equilibrium temperature after injection of Meth

We found that after either dose of Meth the equilibrium temperature reduces relative to the baseline temperature by 0.36ºC and 0.47ºC during the day and at night, respectively (Figure 3.5). The equilibrium temperature (as described by Eq. 7) depends on baseline activities of three nodes in the network, $\sigma(\gamma_{Exc})$, $\sigma(\gamma_{Inh})$ and γ_{SPN}. Accordingly, the reduction in the equilibrium temperature can result from either lower $\sigma(\gamma_{Exc})$ and/or γ_{SPN}, or higher $\sigma(\gamma_{Inh})$. Unfortunately, for obvious reasons it is impossible to infer these quantities in our experimental paradigm without injecting Meth. However, we can speculate that by design of the model, the dependence of Exc and Inhib nodes on Meth concentration is already explicitly described by Eq. (3.3), and the reduction in equilibrium temperature occurs due to long lasting alterations in the thermoregulatory system manifesting themselves by a reduction in γ_{SPN}.

3.5.4 Putative neuronal structures and neurotransmission

The original model was based on existing but rather limited experimental identification of structures responsible for temperature variations after Meth injections [1]. We speculated that the excitatory component (Exc node in Figure 3.1) of the response is mediated by dorsomedial hypothalamus (DMH) which projects to the pre-sympathetic neurons in the ventromedial

medullary region (raphe pallidus, Med node) relaying the signal further down to sympathetic preganglionic neurons in the spinal cord (SPN node). The inhibitory drive (Inh) putatively originates from supramedullary (preoptic nucleus or ventrolateral PAG) and/or intramedullary (rostro-ventral lateral medulla) structures.

Previously we demonstrated that temperature responses to Meth are mediated by orexinergic neurotransmission [2]. Moreover, using the mathematical model [1] we inferred that both the excitatory and inhibitory components are likely to be activated by orexinergic signals induced by Meth administration. In the present study, we show that at night the excitatory and inhibitory nodes receive additional drive. Importantly, the night is an active time for rats when orexinergic neurons are firing. Therefore, it is reasonable to suggest that additional drive to the excitatory and inhibitory nodes emerging at night is orexinergic. This suggestion leads to an interesting prediction. We previously reported that blockade of orexinergic neurotransmission during the day did not evoke any thermal responses by itself [2]. However, at night, when the status of the thermoregulatory network is modulated by orexinergic inputs, the same manipulation should lead to significant body temperature variations.

3.6 Conclusions

In this study, we were the first to measure and compare the body temperature responses in rats to injections of Meth during daytime and at night. We found that at night, which is their active time of the day, rats exhibit much weaker temperature fluctuations after Meth administration as compared to their time of rest.

Using mathematical modeling, we inferred that at night the neuronal circuitry mediating thermal responses to Meth receives additional excitatory inputs primarily converging at the excitatory node which has the lowest activation threshold to Meth. These inputs substantially increase the baseline activity of this node. Therefore, its additional activation after Meth administration at night turns out to be much weaker compared to the daytime because of saturation.

Furthermore, we observed that in the long run the temperature tends to stabilize at lower levels after Meth washes out. This reduction in the equilibrium temperature was similar for both doses of Meth used in this study, and was substantially stronger at night, which further reduced hyperthermia and exaggerated hypothermic components of the response.

CHAPTER 4. EXERCISE ACTIVATES COMPENSATORY THERMOREGULATORY REACTION IN RATS: A MODELING STUDY

4.1 Introduction

To compensate for overall life style-induced decrease of exercise [69], millions of people around the world participate in various sports. Many of these people choose to exercise and compete outdoors. Since outdoor running occurs most frequently in the warmer months of the year, the participants are at risk for developing heat-related illnesses.

The most devastating heat-related illness is exertional heat stroke. Occurring in otherwise healthy people, heat stroke affects people at the most productive times of their lives. Between 1990 and 2010 an average of 2 high school and college football players died each year due to heat stroke [70]. The US Centers for Disease Control estimate that each year 660 heat related deaths occur [71]. Along with the risk for death, those suffering heat stroke lose the ability to work or perform normal activities and may suffer life-long medical complications even after recovery. As the number of marathoners in USA exceeds a half a million [72], the ability to predict who is prone to heat stroke could benefit thousands of people. The dynamics of the body temperature is a major determinant of a heat stroke [73], so the ability to predict a heat stroke is largely an ability to predict changes in body temperature.

Mammals have developed multiple thermoregulatory mechanisms to maintain their core body temperature within a relatively narrow range. In cold environments, the body produces heat through non-shivering thermogenesis and decreases heat dissipation through cutaneous vasoconstriction [6]. Correspondingly, in warm environments, non-shivering thermogenesis is shut off and excess heat is dissipated by increasing blood flow near the skin and, in humans, through evaporative heat loss through sweat.

During exercise an additional heat is produced by contractions of the skeletal muscles. Unlike “classical” heat stroke where the primary cause of heat stroke is ineffective dissipation of heat in hot and/or humid environment, exertional heat stroke develops due to excessive production of heat from work/exercise. In these cases, heat stroke is produced by heat production outstripping maximal heat dissipation. It is logical to hypothesize that during exercise heat production unrelated to exercise would be suppressed (for review see [74]). However, activity-

thermoregulatory heat substitution had not been analyzed in terms of resulting body temperature dynamics. Thermoregulatory processes affecting heat production during exercise are difficult to study, as the corresponding experimental paradigms require measuring the metabolism in, and heat exchange between, different body compartments in conscious running animals. In this study, we use mathematical modeling to characterize thermoregulatory processes from easy to measure body temperature dynamics observed at different ambient temperatures and exercise intensities.

4.2 Methods and Data Preparation

Two series of experiments were performed in two separate groups of rats – running at room temperature (T_a =25^{o}C, N=6) and running at high ambient temperature (T_a =32^{o}C, N=4). Each rat was subjected to four experiments: either had run on the treadmill at one of three speeds (6, 12 and 18 m/min with zero incline) or had stayed on the idle treadmill belt (0 m/min with zero incline).

4.3 Model Construction

4.3.1 General Model Design

The time constant of telemetric probe measured by us was relatively small (0.96±0.01 min), which allowed us to neglect the inertia of measurements in the model.

In a model containing only one compartment any additional heat production due to running will result in immediate increase of body temperature. This contradicts the dynamics of body temperature in first minutes after an initiation of running, when body temperature does not change or can even slightly decrease. Therefore, we excluded one compartment models from further consideration.

Our working mathematical model contained two compartments which generate heat aptly named core body and muscles. We considered that muscles perform the physical work, and are producing heat during exercise. Muscles are insulated from environment, and as such can dissipate heat only to the core. Biologically we expect the heat generated by the muscles to be transferred to the core proportionately to the difference of temperature between the two compartments. In turn changes of heat production in the core are not a direct result of performing the physical work, and are of regulatory origin. The core can also dissipate heat to the

environment with heat loss proportionate to the difference between core body and ambient temperatures.

In rats, the bones and muscles together constitute 45-50% of body weight [75], while skeleton comprises only approximately 3% [76]. Therefore, we explicitly assumed that two compartments of the model (core body and muscles) have equal heat capacities. We introduced net heat accumulation in the core P_0 as the difference between overall heat production in the core and dissipation to the environment. We assumed that at rest all heat to be generated in the core. Based on the experimental data [77] the temperature of the muscles was considered equal to the temperature of the core without exercise as an initial condition. P_m was defined as the additional heat produced by the muscles due to exertion. Both P_0 and P_m were considered constant throughout exercise. Initial model fitting was performed by varying the parameters P_0 and P_m in order to check the basic validity and the ability to reproduce experimental data.

Differential equations describing the change in temperature for each compartment were written as follows. The rate of change in the temperature of the core over time $(dT_c/dt, °C/min)$ is affected by the net heat accumulation in the body and the heat transfer from muscles.

$$\frac{dT_c}{dt} = P_0 + \eta(T_m - T_c) \tag{4.1}$$

where η is a heat transfer coefficient, which indicates the percent of temperature differential transferred from the muscles to the core per minute and measured in min^{-1}. We found that $\eta = 0.125\ min^{-1}$ provided an average value of the rate of heat transfer, which best reproduced the data.

Correspondingly, the rate of change in temperature of the muscles $(dT_m/dt, °C/min)$ was affected by heat produced due to running and heat exchange with the core.

$$\frac{dT_m}{dt} = P_m - \eta(T_m - T_c) \tag{4.2}$$

At equilibrium we know that the temperature is not changing indicating that

$$dT_c/dt = dT_m/dt = 0 \tag{4.3}$$

At initial resting conditions, there is no additional heat generated by exercise, $P_m = 0$, and the net heat accumulation in the core $P_0 = 0$. To satisfy condition (4.3) and considering resting

conditions we set the initial temperature of the muscles equal to the initial temperature of the core $T_m(0) = T_c(0) = T_0$. This temperature is higher than ambient temperature due to baseline heat production by the organism. Any baseline heat production in muscles before the exercise is considered as a part of the P_0, while the P_m reflects only the heat produced from exercise.
The explicit solution of the system of equations can be found for any given time t as:

$$T_c = T_0 + P_0\left(\frac{t}{2} + \frac{1 - e^{-2\eta t}}{4\eta}\right) + P_m\left(\frac{t}{2} - \frac{1 - e^{-2\eta t}}{4\eta}\right) \tag{4.4}$$

$$T_m = T_0 + P_0\left(\frac{t}{2} - \frac{1 - e^{-2\eta t}}{4\eta}\right) + P_m\left(\frac{t}{2} + \frac{1 - e^{-2\eta t}}{4\eta}\right) \tag{4.5}$$

4.3.2 Model Parameter Estimation

A temperature time-series for each running speed at each ambient temperature consisted of 16 points for each rat (15 min running), which were calculated by obtaining medians for corresponding time intervals as described in Data Processing. For each ambient temperature T_a and speed j we calculated the mean temperature among rats at time t at as $\{T_t^j\}_{t=0}^{15}$. Also, we denote the predicted value of T_c from our model using [4] at time t as $T(P_0, P_m, T_0, t)$.

For a fixed speed j, we considered, T_t^j,of the time series $\{T_t^j\}_{t=0}^{15}$ as independent identically distributed normal random variables with mean $T(P_0, P_m, T_0, t)$ and variance $\sigma^2 = \sum_{t=0}^{15} s_t^2 /16$, where s_t^2 is the sample variance found for each time t=0,1…,15, i.e. $T_t^j \sim N(T(P_0, P_m, T_0, t), \sigma^2)$. Then, the likelihood function, the conditional joint probability density function, is given by the product of the conditional distributions as noted: $\prod_{t=0}^{15} f(\{T_t^j\}_{t=0}^{15} | T_0, P_0, P_m)$. The likelihood function can be calculated as recommended in [1, 52, 78]:

$$L\left(\{T_t^j\}_{t=0}^{15} | T_0, P_0, P_m\right) = \frac{1}{(2\pi)^{\frac{16}{2}}\sigma^{16}} \exp\left\{-\frac{1}{2\sigma^2}\sum_{t=0}^{15}\left(T_t^j - T(P_0, P_m, T_0, t)\right)^2\right\} \tag{4.6}$$

where $j = 0, 6, 12, 18\ (m/min)$.

4.3.3 Model Reduction and Analysis

By maximizing the likelihood (4.6) we obtained a best-fit set of parameter values (P_0, P_m, T_0) for each speed at two different ambient temperatures, $25°C$ and $32°C$. Then by assuming that the likelihood (4.6) represents a Bayesian posterior probability distribution for the model parameters, we calculated the 95% confidence regions of parameter estimates on the (P_0, P_m)-plane, which demonstrated strong negative correlation between estimates of these two parameters. This correlation results in large variability of estimate for individual parameters. This also indicated that any independent prior limitations on the value of one of the parameters could significantly improve the precision of the estimates for both of them.

To formulate the prior restrictions on the parameters, we considered two hypotheses. First, we hypothesized that the heat production in the core at high ambient temperature is at its minimum, and hence cannot be further lowered by exercise, while heat dissipation remains constant. Mathematically this means that the net heat production in the core P_0 at $T_a = 32\ °C$ remains equal to 0 for all treadmill speeds. The statistical analysis confirmed that the estimate for P_0 is not statistically significantly different from 0 for any speed. Second, we hypothesized that the heat production in the muscles P_m is independent of T_a and depends only on the intensity of the exercise (speed of the treadmill). Following these hypotheses, at $T_a = 32\ °C$, we fixed $P_0 = 0$ for all speeds, and used the likelihood function to determine the best-fit P_m values for each speed. Then, these P_m values were substituted into the model for $T_a = 25°C$, which was used to obtain the distribution of P_0 values for different speeds at $25°C$.

4.4 Results

4.4.1 Body Temperature Dynamics

All rats were kept in home cages at room temperature before being placed on the treadmill. The time during which the baseline temperature was recorded was sufficient to achieve uniform values of core body temperature in all groups within 37.3±0.2^{o}C. No statistical differences between baseline temperatures in all experiments (for various ambient temperatures and speeds) were found. The dynamics of the average temperature for each group is shown in Figure 4.1. The temperature in all groups eventually rose, including animals on the idle belt (Figure 4.1, 0 m/min). In a room temperature environment $T_a = 25°C$ the core temperature decreased slightly

before starting to rise; this decrease was observed at all running speeds (Figure 4.1 A). In the warm environment, $T_a = 32°C$, the body temperature did not decrease initially, however the temperature did not start to increase for at least 3 min (Figure 4.1 B). After 5 min body temperatures were increasing in a linear fashion in all groups until the end of the run (15 min total, Figure 4.1 A, B).

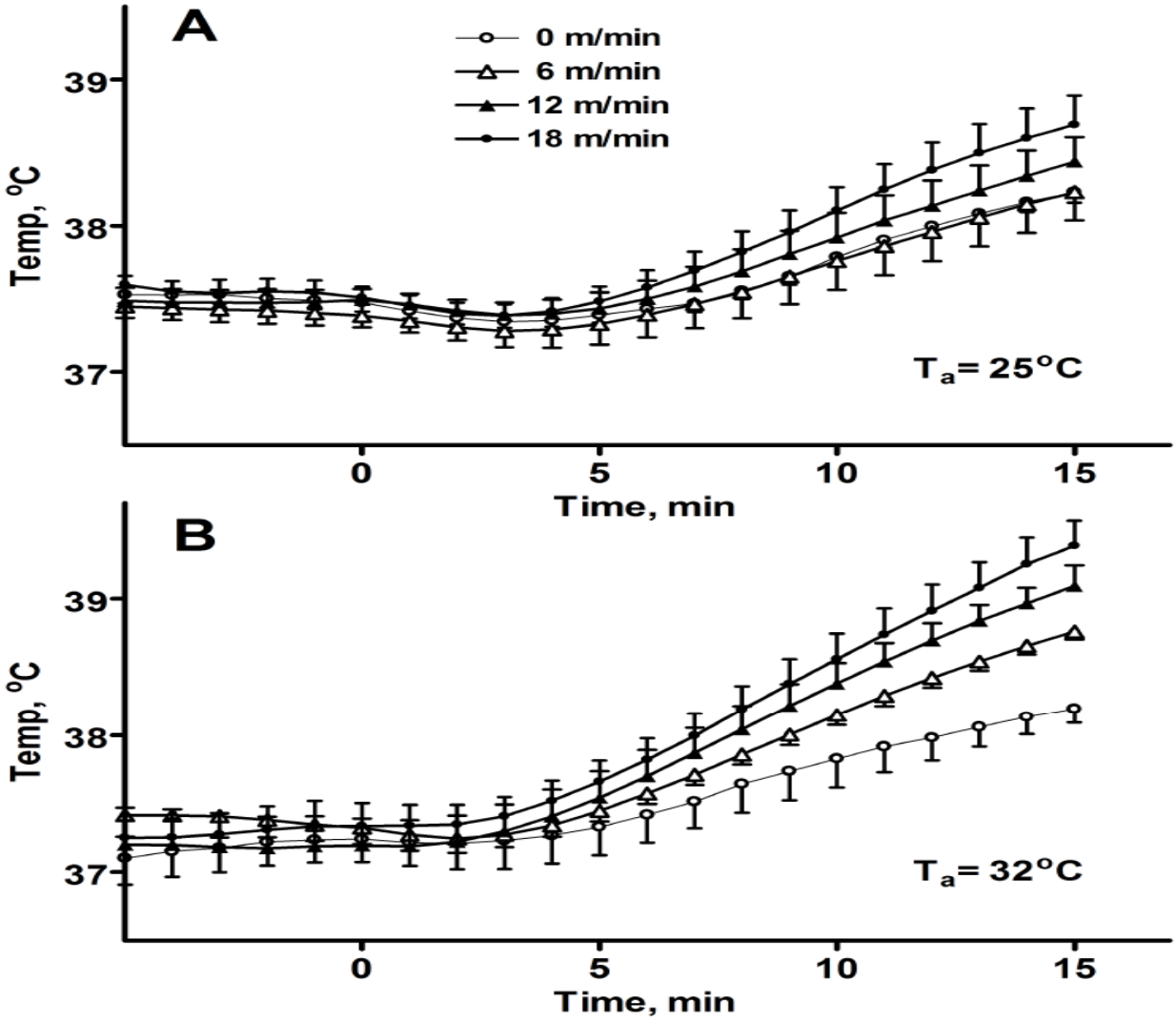

Figure 4.1 Experimental data: the average and standard deviations of the core body temperature of rats running on a treadmill for 15 min at various speeds in two environments – (**A**) at 25°C and (**B**) at 32°C. Rats were in their home cages before the run, transferred to the treadmill at t=0 min, and the belt was set to the actual speed in 30 sec.

The presence of a "hypothermic" phase is more obvious when experimental data for both ambient temperatures are plotted together (Figure 4.2A). We have used the estimate of the rate of change in the core temperature from 6 to 11 minutes to determine the rate of heat accumulation. In the control group which was placed on an idle treadmill, the rate of change of the core temperature was almost identical for both ambient temperatures (Figure 4.2B). However, at $25°C$ running at the speed of 18 m/min subtly increased the rate of heat accumulation, whereas at 32^{o} C running at 18 m/min led to almost two-fold faster increase in temperature (Figure 4.2 B).

After analysis of the experimental data we can summarize a few qualitative observations and phenomena characterizing short-term running on a treadmill as follows. First, the running at the treadmill results in increases in body temperatures which do not appear immediately, but rather after a delay. Second, increases in temperature are preceded by slight decreases at room temperature, while no initial change in temperature is observed in the warm environment. Finally, the rate of heat accumulation is not significantly different between animals running with different speeds at room temperatures. In a warm environment, however, the increase in the running speed correlates with the rate of heat accumulation.

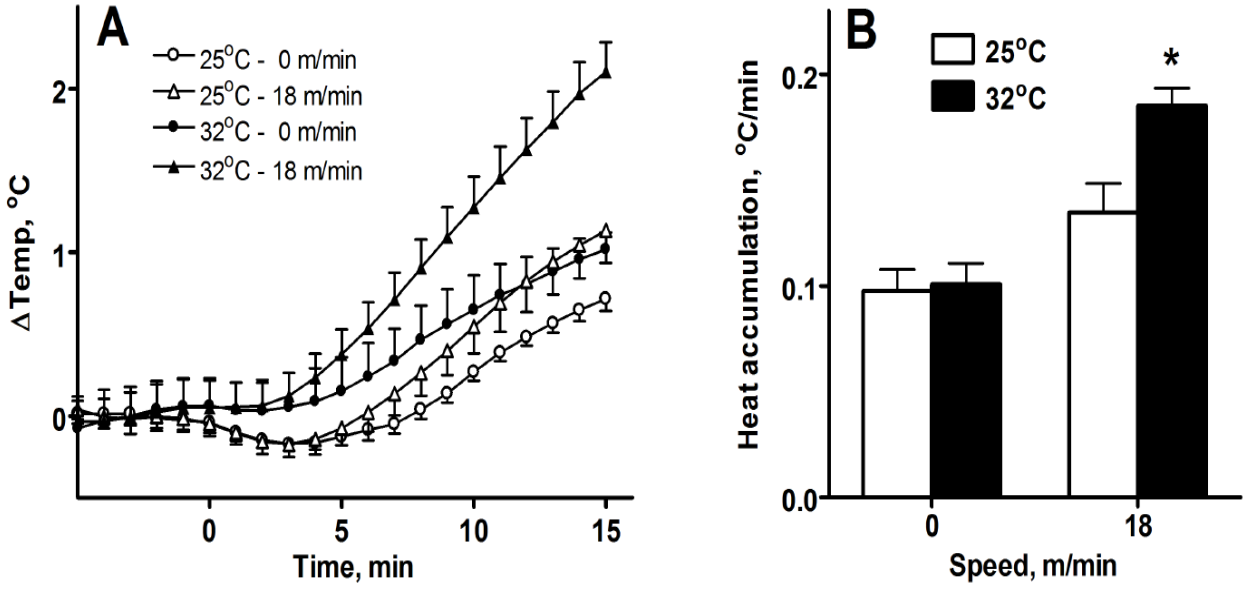

Figure 4.2 Comparison of the body temperature dynamics (**A**) and heat accumulation rate (**B**) between animals at two ambient temperatures which were either running at 18 m/min or staying on the idle belt. Heat accumulation rate was calculated as an average rate of the body temperature change between 6 and 11 min. * indicates statistically significant difference with staying on the idle belt ($p<0.05$).

4.4.2 The model with unrestricted parameter values

At first, we utilized the likelihood function [6] to find the confidence regions for all model parameters in all groups as described in Methods section. The analytically calculated (for the high ambient temperature) 95% confidence regions on the (P_m, P_0)-parameter plane have an elliptical shape and are shown on Figure 4.3 A. Figure 4.3 B and C represent the best-fit estimates and standard errors for P_0 and P_m respectively.

The P_0 and P_m estimates appear strongly correlated. This suggests that the model with unrestricted parameter values is overdetermined. Practically, it means that the model with higher heat production in the muscles and accordingly lower net heat production in the core can describe the same temperature curve equally well. Consequently, while the ellipses in Figure 4.3 A are largely separated, their projections onto P_m and P_0 axes (which represent the confidence intervals for each parameter individually) heavily overlap. Accordingly, no conclusion can be drawn about exercise intensity dependent changes in individual parameters, as those changes appear statistically insignificant due to large standard errors. The standard approach to overcome the problem of the overdetermined model is to introduce appropriate prior restrictions on its parameter values. We formulated two biologically plausible hypotheses and verified that none of them contradicted our modeling results with unrestricted parameter values.

First, Figure 4.3 B shows that at room temperature P_0 drops to negative values for all speeds, whereas this is not observed in warm environment. Such drop in P_0 represents a decrease in the core metabolism. With an increase in ambient temperature, the core metabolism is decreasing to maintain the appropriate body temperature until metabolism reaches a minimum value. Our first hypothesis is that at $T_a = 32°C$ this limit is reached, and accordingly the exercise cannot lead to any further thermoregulatory decrease in the core heat production. Mathematically, this hypothesis states that for all speeds at high ambient temperature P_0 remains equal to 0. Statistical analysis indeed shows that at $T_a = 32°C$, none of the P_0 estimates for different speeds are statistically different from 0. This fact is reflected in Figure 4.3 A as confidence regions of P_0 for each speed contained $P_0 = 0$. Our second hypothesis follows that the heat production in the muscles correlates with exercise and its intensity, and does not depend on the ambient temperature. In support of this idea no statistically significant differences were found between P_m values for different ambient temperatures, at identical treadmill speeds (Figure 4.3 C).

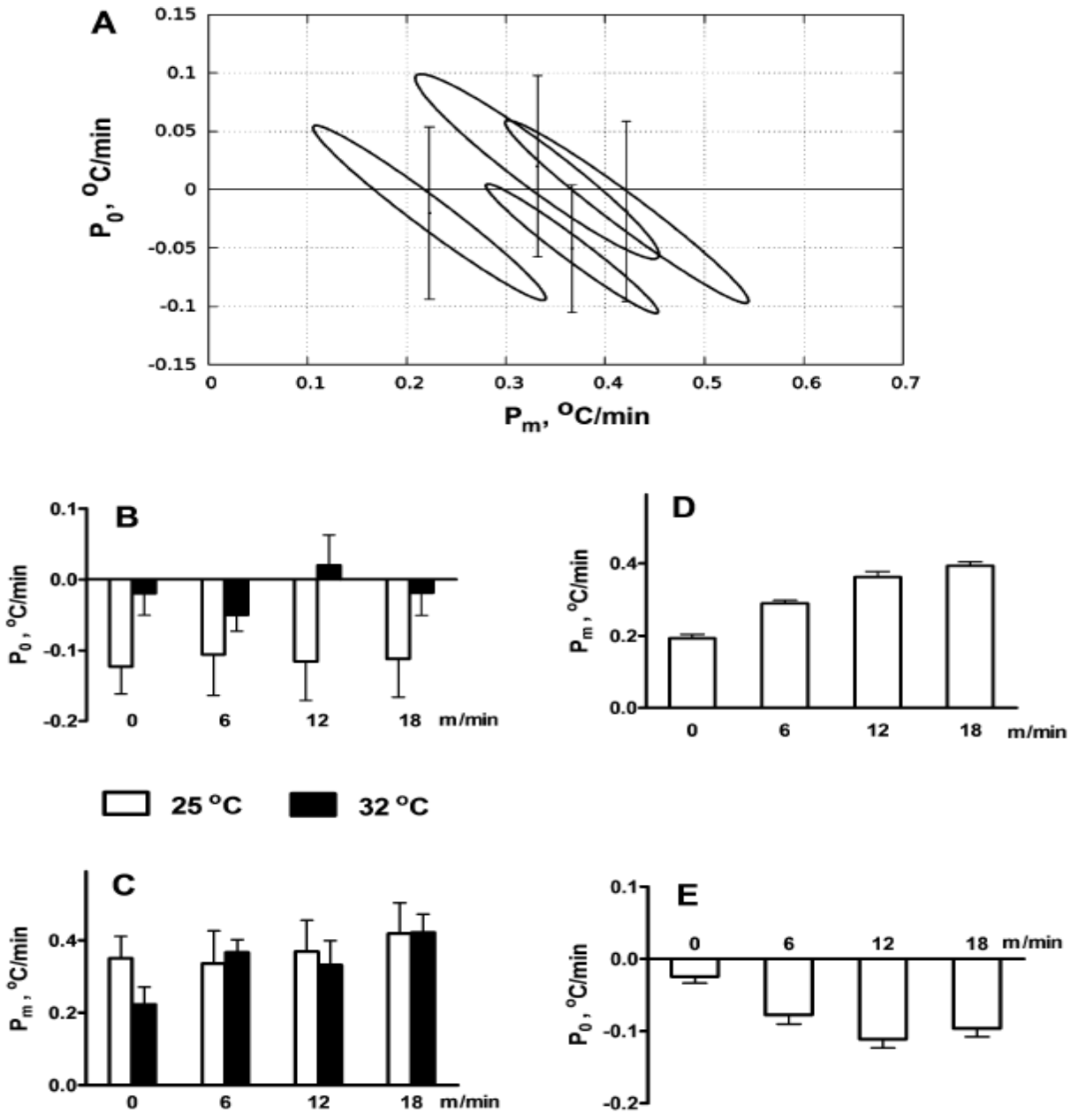

Figure 4.3 (**A**) Confidence regions on the (P_0, P_m)-plane for each of the four studied speeds (0, 6, 12, and 18 m/min) at 32 ^{o}C; **B-C**: Parameter estimates before the model reduction for two ambient temperature, 25 $℃$ and 32 $℃$: (**B**) P_0 vs speed, (**C**) P_m vs speed; **D-E**: Parameter estimates after model reduction: (**D**) P_m vs speed at T_a =32 $℃$ after P_0 is set to 0 for the experiments at 32 $℃$, (**E**) P_0 estimates at different speeds of running at 25^{o}C with P_m values from panel D under an assumption that heat generation in the muscles does not depend on the ambient temperature.

4.4.3 The restricted model

The first condition which we applied to the model was fixing $P_0 = 0$ at the high ambient temperature. As expected, this restriction allowed calculation of P_m with much better precision (Figure 4.3D). Increasing the treadmill speed resulted in progressive increases in heat production by the muscles. Interestingly, just placing an animal on the treadmill resulted in heat production in the muscles comparable to the non-zero speeds. Specifically, the heat production at zero speed is approximately one half of the heat produced at the highest running speed of 18 m/min.

Following the second hypothesis that P_m depends on speed, but not on ambient temperature, we used the P_m values shown in Figure 4.3D to define changes of P_0 for the ambient temperature $T_a = 25°C$ (Figure 4.3 E). Overall, the model reproduced experimental temperature dynamics: calculated values were within standard deviations (Figure 4.4). The dynamics of the predicted temperature of the muscles is shown at the Figure 4.5.

Placing the animal on a treadmill (speed 0 m/min) resulted in a small but significant decrease of core heat production. As the running speed increased the decrease in core heat production became more significant. This decrease was not able to fully compensate for the production of heat in muscles. At the highest running speed, the increase in muscle heat generation was approximately 0.4 ^{o}C/min, while P_0 dropped by only 0.1 ^{o}C/min. The difference between P_m values for 0 and 18 m/min was appr. 0.2^{o}C/min. This resulted in significant increases in overall heat accumulation at the ambient temperature of 32^{o}C (Figure 4.2 B). At room temperature the heat produced by muscles was half-compensated by the reduced core heat generation. This led to an increase in heat accumulation to be not significant (Figure 4.2 B).

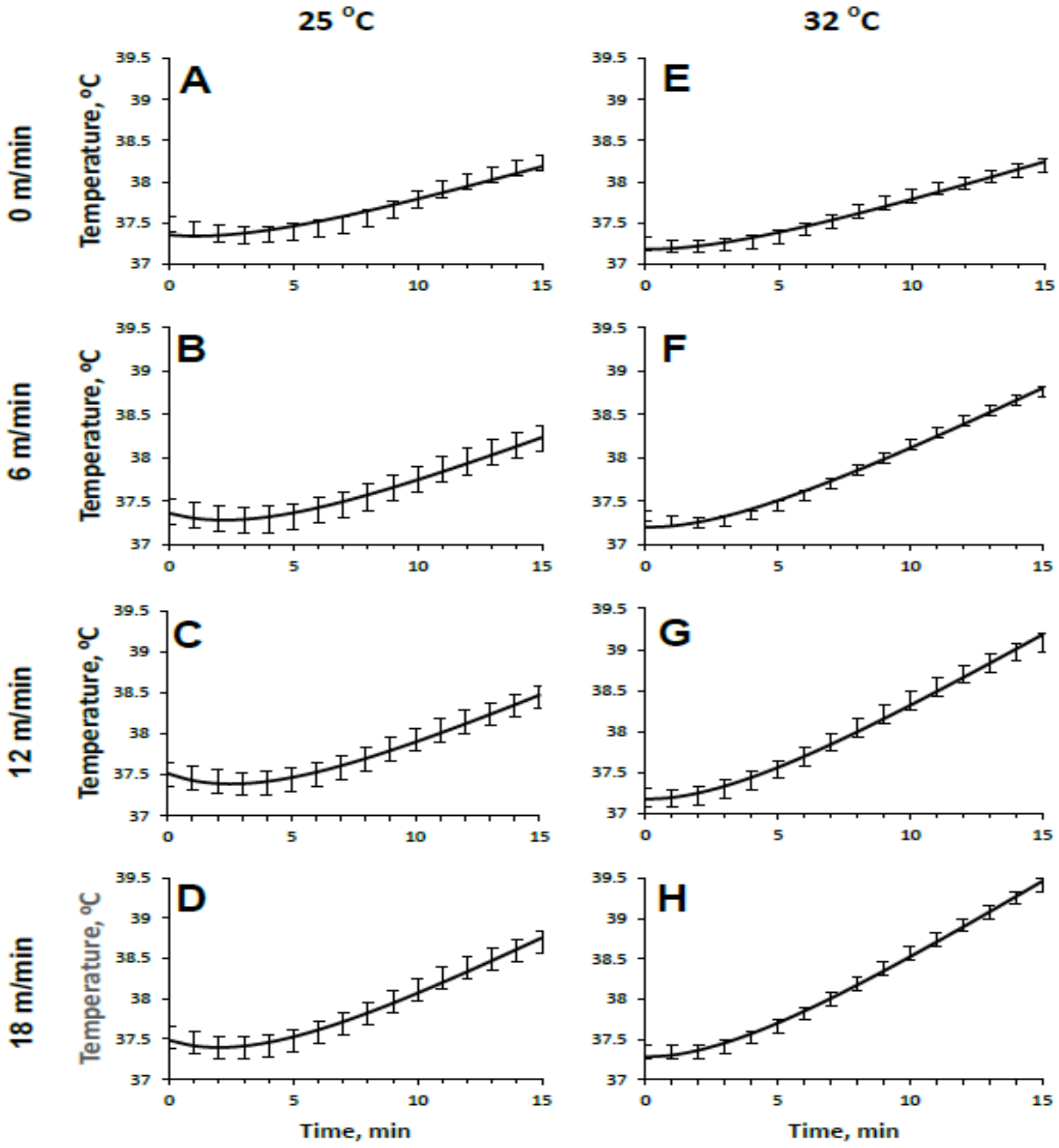

Figure 4.4 Comparison of the experimental data (error bars) and the core temperature curves as generated by the model (solid lines) using the parameter estimates represented in Fig. 3D,E. The error bars show the mean ± one standard deviation of the core body temperature over a group of rats. Rows of graphs correspond to different speeds of running (**A,E:** 0 m/min, **B,F:** 6 m/min, **C,G:** 12 m/min and **D,H:** 18 m/min as marked on the left). Columns of graphs correspond to different ambient temperatures (25^{o}C, first column; 32^{o}C, second column).

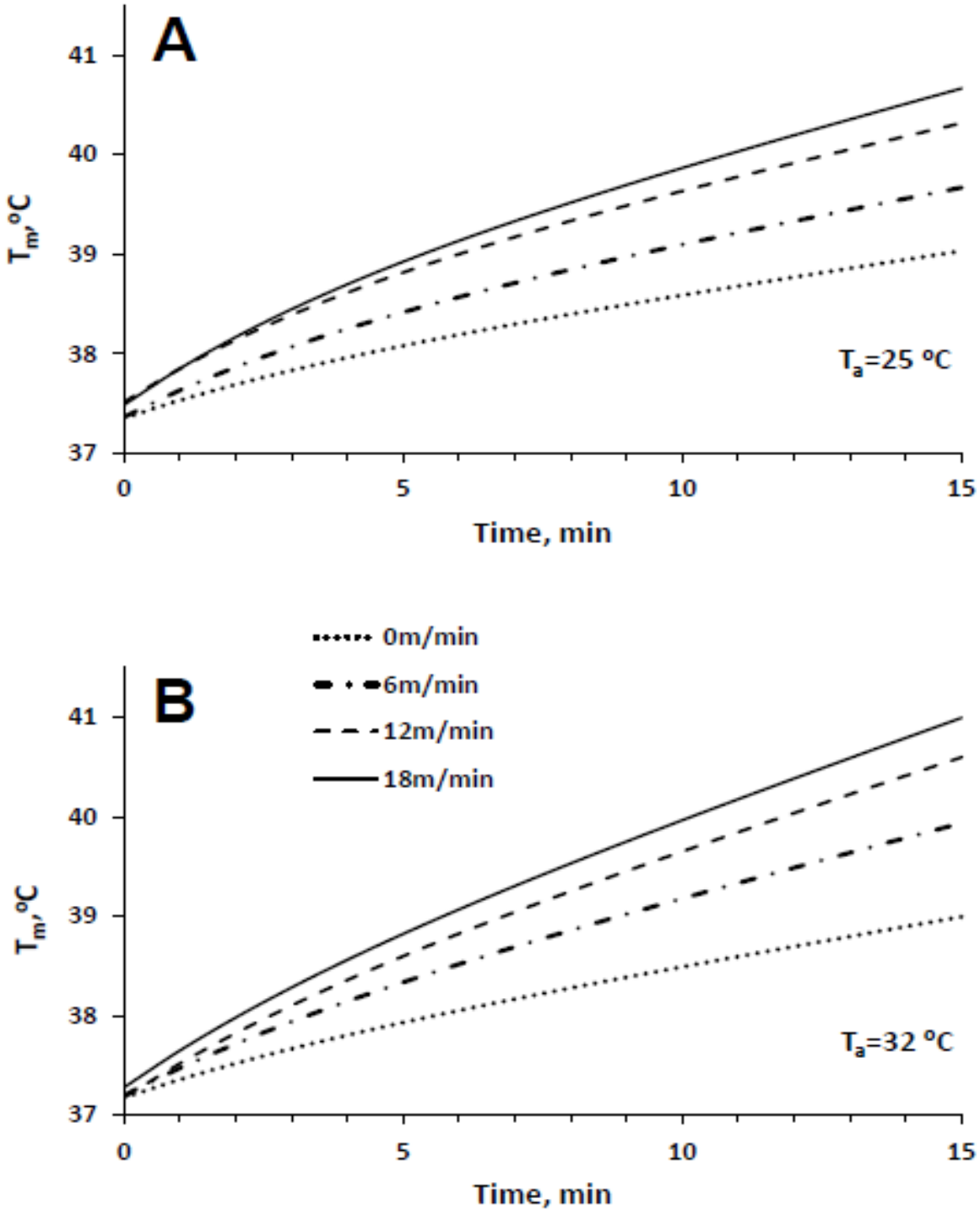

Figure 4.5 Muscle temperatures as predicted by the model. (**A**) at $T_a = 25\ ℃$ (**B**) at $T_a = 32\ ℃$.

4.5 Discussion

4.5.1 Overview

Treadmill exercise results in the steady production of heat in animals [79]. Our objective was to mathematically model core body temperature changes as a result of exercise as a first step in building a model to predict the expected core body temperature at any given point in time given a specific running speed and ambient temperature. We also attempted to model physiologic and metabolic responses, which are difficult to directly measure in exercising animals: muscle temperature, and both muscle and core heat generation.

4.5.2 Relationship between various parameters characterizing heat production

Temperature changes in the body occur because metabolic processes generate heat. Increases in temperature occur when heat production is greater than dissipation into the environment, and decreases occur when it is less. In our model, heat production is separated into exercise-related, which occurs in muscles (P_m), and exercise-independent, which we assume to occur in the core. The heat production in the core was combined with the heat dissipation from the core indicating overall net heat change in the core and it was quantified as P_0.

Heat generation and dissipation is commonly expressed as power (P, energy divided by time) and is measured in units of energy per unit of time (e.g. Watt=Joule/sec). Heat accumulation is directly connected with changes in body temperature through heat capacity as dT/dt=P/Heat Capacity [80]. Both heat production during running and heat capacity are proportional to the body weight, therefore changes of body temperature are independent of body weight and are reflecting heat production per unit of weight. In this manuscript the heat production/ accumulation is always expressed in ^{o}C/min which can be translated to the power by multiplying by the heat capacity of the body.

As it will be discussed below, we accepted heat dissipation approximately constant throughout these experiments, because the body temperature is not changed strongly enough to activate thermoregulatory responses. Therefore, P_0 provides an estimate of the changes in heat production mediated by the core, and a sum ($P_0 + P_m$) can be considered an estimate of a change in total heat production in the organism.

At room temperature rats can run at the maximal speed used in this study, 18 m/min, for extended periods of time. We have noticed that rats will run for more than an hour at room temperature (unpublished observation). This means that at this speed, heat is generated by oxidative processes without significant accumulation of metabolic byproducts such as lactic acid. In this case the generated heat is proportional to oxygen consumption, because the differences related to metabolic substrate comprise less than 7% per unit of oxygen: if the substrate is carbohydrates, the energy generated from one liter of O_2 is 21.13 kJ, and it is 19.69 kJ if the substrate is fat [81]. Considering this, in the following discussion we will draw connections between studies that used various end-points – body temperature, heat production or oxygen consumption.

Via modeling, we have quantified several key phenomena. While some of those phenomena may appear counterintuitive, we found multiple evidences supporting our observations.

4.5.3 Delay in body temperature increase

When animals began running, their body temperature did not increase immediately. Instead there was a several minute long delay prior to the temperature elevation. Even more, there was a decrease in the temperature observed at the beginning of the run at room temperature. A graph of abdominal temperature versus running time revealed a delay in the temperature change at the beginning of the run in the study by Fuller *et al.* [82]. Hasegawa *et al* [83] also observed a similar delay: when a rat was transferred from a home cage to an idle treadmill, there were at least two data points, shown in 5 min time increments, before the slope of the temperature curve became positive (see Fig. 2 in [83]). Upon activation of a treadmill, there was an immediate temperature increase, however, there was a 10 min delay prior to reaching the maximum slope [83]. In a separate study from the same group a similar delay was shown (see Fig. 2 in [84]).

The mechanism of this delay at the beginning of run is explained by our model. As soon as exercise begins, contracting muscles begin to produce heat, yet this heat is not transmitted to the core immediately. Until muscles become physically warmer than the core, there is no net transfer of the heat to the core, and no changes in the core body temperature occur. The rate of heat transfer from the muscles to the core is proportional to the difference in temperatures between the core and the muscles and the heat transfer coefficient η which defines the inertia of this process. Therefore, the delay in the core temperature increase is concerned with the time needed

for sufficient heat accumulation in muscles to activate the heat transfer from muscles to the core. When a larger time scale (1 h or longer) is considered, this delay would be hardly noticeable; however, on a time scale of 15 min, this delay is an important part of the system's dynamics.

4.5.4 A decrease in temperature in the beginning of the run at room temperature

A slight decrease in body temperature in the beginning of each run was clearly present at room temperature; this was absent at high ambient temperature. We speculate that the mechanism of this "hypothermia" may be a compensatory adjustment of heat production in the body core, which is not yet compensated by heat transfer from the muscles. It takes some time for the produced heat to increase temperature of the muscles, and only after that additional heat can be transferred to the core. During this time, the heat produced in the core by the decrease of heat accumulation is less than the amount of heat dissipated to the environment. This results in a transient decrease of the body temperature. That decrease is significantly smaller or nonexistent in hot environments due to low baseline heat production and a smaller difference between the temperatures of the environment and the core. An anticipatory decrease of heat accumulation in the core occurs at all speeds including 0. So the very fact of the transfer of an animal to the treadmill evokes preparation for the exercise.

4.5.5 Relative independence of body temperature changes on exercise intensity at room temperature

This phenomenon is best demonstrated by linear increase in body temperature in graded exercise studies. An experimental protocol of Balthazar *et al.* [85] had initial speed of 10 m/min with 5% incline and increased the speed every 3 min by 1 m/min. In this protocol of graded exercise body temperature increases were virtually linear. Despite increasing speed (the maximal speed was 16 m/min) the increase of body temperature was so close to linear that the authors calculated the average slope over the whole run. The rate of change of the body temperature measured by Hasegawa *et al.* [86] was also independent of the work load with speeds between 10 and 26 m/min (see Fig. 1 in [86]).

In experiments presented in this manuscript, during the linear part of the temperature increase the slope of heat accumulation in rats running at 18 m/min is significantly higher than in rats on the idle belt of the treadmill in hot environment but not at room temperature (Figure 4.2 B). This slope is dependent on both P_0 and P_m with $(P_0 + P_m/2)$ providing a good estimate. At high

ambient temperatures $P_0 = 0$ and cannot be decreased with increasing speed. Accordingly, the slope increases as P_m increases (Figure 4.3 D). As a result, the slope is higher in running rats compared with idle rats (Figure 4.2 B). In contrast, at room temperature, P_0 decreases with the increasing speed (Fig. 3E), while P_m has the same dependence on the speed as in the hot environment. This means that at room temperature an increase of the temperature slope with an increase in treadmill speed is partially offset by decreasing heat accumulation in the core (Figure 4.2). As a result, due to variability present in all biological systems, the increase in the slope does not reach statistical significance (Figure 4.2 B).

At the first glance, this independence contradicts not only common sense, but also experimental data demonstrating that at higher speeds body temperatures of rats are higher (see, for example, [87]). To interpret this contradiction, it is important to consider a time frame of the experiments: Tanaka *et al.* [87] explicitly stated that they measured the rectal temperature at the steady state (after 30 min of running). As shown in the referenced manuscript, in the beginning of the run the cutaneous dissipation of heat is not effective, and body temperature increases due to increased heat production. As soon as body temperature reaches cutaneous vasodilation threshold, the steady state is established. In other words, the steady state is defined by a thermoregulatory threshold of cutaneous vasodilation, which is increasing with the running speed. Correlation between thermoregulatory threshold and running speed is the reason of higher body temperature at higher speeds. We argue below that in the time frame of our experiments the thermoregulatory heat dissipation is not activated.

Alternatively, in studies showing initial phases of temperature increases in rats running at various speeds, the slopes of temperature are impressively similar (Figs. 2 and 6 in [88]). Even more, in the study of Kunstetter *et al.* [88] despite initial phases are similar, the temperature dynamics in different groups separates dramatically when thermoregulatory heat loss responses are activated after the (brain) temperature exceeds heat dissipation threshold.

4.5.6 Transfer to a treadmill accounts for a large part of temperature change during exercise

When animals were placed on a treadmill and stayed at least 30 min, Hasegawa et al. [83] found that their body temperature rose by 1 ^{o}C and remained elevated without any trend to return to baseline. After stabilization of the increased temperature, running at 10 m/min raised the temperature by an additional 0.5 ^{o}C in 15 min when it again reached a plateau. So placing the

animal on the idle treadmill accounted for approximately 2/3 of total increase of the body temperature. From equations [2, 3] it follows that the additional overall heat accumulation ($P_0 + P_m$ in our study) is proportional to the change in equilibrium temperature after sufficient time. The sum ($P_0 + P_m$) when staying on the idle belt was about 0.17 ^{o}C/min (see Figure 4.3D,E), while at a treadmill speed of 12 m/min (closest to the speed used in [83]) it is approximately 0.25 ^{o}C/min, so a transfer to the belt accounts for approximately the same 2/3 of the increase in the rate of heat accumulation in the whole body during running at 12 m/min.

Further increases in speed do not dramatically increase heat production. Brooks & White [89] reported that oxygen consumption was 50 ml/kg/min when running at 15 m/min speed on a treadmill with 1% incline, and increased only to approximately 65 ml/kg/min at 45 m/min with the same incline.

4.5.7 Suppression of thermoregulatory metabolism by exercise

In our study we showed that rats exposed to exercise exhibited a decrease in their core heat production. Similar effects of thermoregulation suppression were described in the study by Guimaraes et al. [90]. When rats were exposed to 12^{o}C, their core body temperature went up (a well-known phenomenon from other studies [91]). However, when the animals were forced to run at the same temperature, their body temperature was lower than at rest. Running at progressively colder temperatures resulted in lower body temperatures at equilibrium, which were achieved after 15-30 min of exercise. Similar observations were presented in [92]. Assuming that running produces the same amount of heat regardless of the ambient temperature, one can conclude that in colder environment the exercise suppresses the thermoregulatory heat production more in absolute values. In fact, Makinen et al. [93] observed that exercise did not increase oxygen consumption in rats exposed to 0^{o}C, which means that intense thermoregulatory heat production was substituted by thermogenesis induced by exercise.

4.5.8 Two compartments are necessary to explain complex temperature dynamics

In a model with a single compartment, the increase of heat generation would result in an immediate growth of the body temperature. In contrast, we observed a clear delay between the beginning of an exercise and the temperature rise. Therefore, a single compartmental model is not able to accurately describe changes in body temperature during running.

It appears that a two-compartment model reproduces experimental data with sufficient level of precision. For simplicity sake we named the additional heat produced from exercise as the heat produced by muscles, P_m. It is important to note that this variable can include heat produced by other organs as well (e.g., the heart or brain), and disregards any heat produced by the muscles at rest. In fact, an immediate increase of brain temperature during exercise [92, 94] is a feature of "muscle temperature" in our model, and indicates that additional heat production in the brain during the exercise contributes to the "muscle" compartment of our model. The rate of the initial temperature change in the second compartment (the core) is defined by the difference between overall heat production in the core and dissipation to the environment, P_0. In the later times, temperature change in the core will be also modified by heat transfer from warmer "muscles". Note again that the use of P_0 is a simplification to refer to any heat produced by the body that is not directly related to additional heat resulting from exercise. It also allows us to disregard different forms of heat dissipation from the body by combining them in a single term.

4.5.9 Prior restrictions on model parameters

Parameter confidence regions on the (P_0, P_m) plane appeared to be ellipses strongly extended in a certain direction (see Figure 4.3 A) providing an indication that the model is underdetermined. As a result, the model parameter estimates had large standard errors and, hence, did not differ statistically significantly between various speeds and ambient temperatures. As described in the methods, our findings became much more conclusive when additional restrictions were applied. Two reasonable hypotheses were formulated and proved to not contradict to the initial estimates of the parameters of the model. First, we hypothesized that in hot environment there was no room to decrease heat generation in the core, supported by the fact that 95% P_0 confidence regions for each speed in $T_a = 32°C$ included 0 (Figure 4.3A). Therefore, we assumed that the amount of heat generated in the core body was at its minimum level and it could not be further reduced to compensate the additional heat coming from the muscles. This hypothesis is firmly footed in the concept of a thermoneutral zone (TNZ). $T_a = 32°C$ is just exceeding the estimate of the upper border of the TNZ for rats [6]. This means that at $T_a = 32°C$, the rat does not generate heat to keep its core temperature steady. Instead the only heat that the rat generates is in the process of sustaining normal bodily functions.

Next, we hypothesized that heat generation in the muscles, P_m, at given running speed is independent of the ambient temperature. Figure 4.3 C represents the P_m estimates for 0, 6, 12, and 18 m/min speed of treadmills at both values of T_a. There is no statistically significant difference between values for matching speeds, which is compatible with the above idea.

Using these two restrictions provided more precise estimates of the model parameters (compare Figure 4.3 B and C with Figure 4.3 D and E). This allowed us to conclude that the heat generated by the muscles increases with the speed, but this increase saturates as speed is increased. As soon as we used the P_m estimates obtained by fixing $P_0 = 0$ for the models with the high ambient temperature ($T_a = 32\ °C$) as priors for the model with the ambient temperature $T_a = 25°C$, we were able to calculate changes in the core heat production at $T_a = 25°C$ with much better accuracy (Figure 4.3 E). Again the compensatory decrease in the core heat generation appeared statistically significant even when the animal was placed on the idle treadmill, and saturated at the speed of 12 m/min.

4.5.10 Role of heat dissipation

There are two ways in which the net heat accumulation P_0 can be decreased by exercise. It can be due to suppression of thermogenesis, which is used to keep body temperature constant in relatively cold environment, or it can occur through increased heat dissipation. The major mechanism responsible for controlling heat dissipation in mammals is cutaneous blood flow. Cordeiro et al. [95] recorded the body temperature of rats running at 18 m/min at 5% incline simultaneously with the tail temperature — a marker of heat dissipation. The tail temperature reached its maximum at approximately 20 minutes, and this moment corresponded to the beginning of plateau phase of body temperature at approximately 38.5^{o}C. The experimental set up for our study with the highest speed was the same except we did not impose the incline. Running time in our experiment was 15 min, and we did not observe plateauing of the body temperature. Hasegawa et al.[86] also confirmed that at body temperatures below 38^{o}C, the tail is not dissipating heat effectively. Cutaneous heat loss threshold temperature in running rats is at or above 38.5^{o}C in other studies as well [96, 97]. Tanaka et al [87] also demonstrated that the threshold for cutaneous vasodilation increases with increasing speeds and exceeded 39^{o}C when running required above 70% of maximal VO_2 consumption, which approximately corresponds to the maximal running speed in our experiments [98]. This let us consider that at least for most of

the experimental time we did not reach conditions for significant cutaneous vasodilation resulting in noticeable additional heat loss. As a result, the changes in P_0 account for alterations in the thermoregulatory heat generation.

4.6 Biological implications

4.6.1 Outline

In this study we quantitatively describe a particular thermoregulatory mechanism concerned with partial compensation of heat overproduction during exercise. This mechanism is based on the reduction of regulatory thermogenesis. We hypothesize that the impairments of this mechanism may lead to faster overheating and hence may underlie heat injury/stroke in some cases.

For example, heat illness is typically observed in individuals exercising in hot environment. However, there are multiple occasions when it affects competitors in events in moderate climate, when majority of participants appears to be not prone to this medical condition. Surprisingly, the correlation with running speed is often significant but fails to reliably explain more than a fraction of the variability in body temperatures [99, 100]. In modeling terms it means that high body temperature is not a direct consequence of extreme amounts of heat due to the intensity of running. Less effective suppression of baseline thermoregulatory heat production could be one of mechanisms which results in overheating in some athletes.

4.6.2 Are changes in metabolism specific to exercise?

One could interpret the increase in body temperature at the idle belt as a stress response, which remains despite rat familiarization to running on a treadmill. However, one can also notice that this increase is a part of a pattern: the core heat production drops while the heat production in muscles increases. The same phenomenon was observed in rats that were actually running. This allows formulating a hypothesis that muscular metabolic engagement and a compensatory decrease in the core heat production are not a response to exercise per se, but an anticipatory response to the need to run. In some situations this demand may never actualize (when the speed is 0).

Can we distinguish between anticipation of exercise and stress? The very definition of general adaptation syndrome by Selye as “a generalized effort of the organism to adapt itself to new

conditions" [101], suggests that reactions to exercise could be considered as responses to stress. Noteworthy, stress is typically associated with locomotion, and helps to prime the organism for fight-or-flight [102].

4.6.3 Temperature of muscles as a critical physiological end-point

It is difficult to measure muscle temperature in humans and animals while they are exercising without negatively affecting their ability to run. In those experiments where researchers placed temperature probes adjacent to muscles of exercising animals [77], similar values to what we predict (Figure 4.5) were observed (39^{o}C adjacent to muscles after 15 min at 9 m/min in [77] vs 39.5^{o}C in the muscle after same time at 12 m/min in our model at room temperature).

Our modeling shows that the temperature in muscles when running with the fastest speed, 18 m/min, reaches 41^{o}C and approach the levels ($41\text{-}42^{o}$C) at which the muscle tissue can be damaged [103]. Avoiding this damage is important for selection of appropriate training regimens, especially in highly competitive athletes. Modeling may serve as an effective tool to determine if specific exercise regimens and conditions can result in thermal injury.

4.6.4 Energy production as a marker of substrate utilization

Heat production is a measure of substrate utilization during exercise, and as such is directly linked to weight loss induced by exercise. Therefore, knowing heat production during exercise is important from public health viewpoint. The finding that energy expenditure is relatively independent of the exercise load could have quite far-reaching considerations for fitness practitioners. In our experimental conditions, most important factor associated with calorie expenditure was that exercise was occurring; the intensity of the exercise appears to have had a minor influence.

4.7 Conclusions

Our study serves as a step towards a comprehensive mathematical model of the thermoregulation during exercise. Inclusion of both thermogenesis and heat dissipation together with corresponding control mechanisms are needed to predict adverse temperature in exercising individuals. In this paper we have studied in rodents an "Activity for free" phenomenon [74], which is a significant thermoregulatory mechanism activated by exercise. The phenomenon is

relatively obvious biologically – when additional heat is produced by exercise, the generation of heat aimed at maintaining body temperature can be reduced. The energy which was used for maintaining body temperature is now used for locomotion (thus the name “Activity for free”). However, for the first time we had characterized this phenomenon quantitatively. At room temperature, rats are able to save from a quarter to a half of energy used for running. This compensatory suppression of metabolism is quickly saturating with the load. At running speeds as low as 12 m/min with zero incline the drop of metabolic activity in the core is already maximal. We predict that in colder conditions, which induce significant levels of metabolic support for homeothermy, this compensation could be more substantial.

CHAPTER 5. AMPHETAMINE ENHANCES ENDURANCE BY INCREASING HEAT DISSIPATION

5.1 Introduction

In many conditions exhaustion may serve as an important safety mechanism keeping the organism from irreversible damage caused by intense exercise [104]. It was previously shown that low to moderate doses of amphetamine increase the time until exhaustion in exercising rats [105, 106]. Although amphetamine usage is prohibited during competitions, it may be used in some situations to improve performance by delaying exhaustion [107]. However, the mechanism by which amphetamine increases the time to exhaustion is unknown.

High body temperature is one of the strongest exhaustion signals [108]. During exercise, the temperature of the muscles as well as the core body temperature is elevated as a consequence of increased heat production in the muscles. To limit the temperature growth, regulatory heat dissipation mechanisms, e.g. vasodilatation and evaporative cooling through saliva spreading in rodents or sweating in humans, are engaged to help remove heat during physical exercise [109, 110]. The balance between heat production and heat dissipation is crucial for keeping the temperature of different compartments of the body in a safe range.

Amphetamine is known to affect the thermoregulatory system [111] by altering both heat production and heat dissipation. It has been previously shown that amphetamine increases the temperature at which exhaustion occurs at a high ambient temperature, producing a risk of developing exertional heat stroke [98]. Production of large amounts of heat by the muscles during exercise results in muscle tissue temperature being higher than core temperature. Muscle tissue itself can be damaged if its temperature becomes too high [103]. Damage to the myocytes releases the content of the cells into the circulation. Misbalance of electrolytes can lead to cardiac arrhythmias, while a release of myoglobin may cause renal failure [112]. Unfortunately, thermal or biochemical damage to the myocytes is not usually detected until post exercise. Therefore, any alterations in the thermoregulatory system that lead to higher muscle temperatures can be extremely dangerous.

In this study we aimed to find how amphetamine affects the mechanisms of exhaustion in exercising rats. To do so, we collected experimental data on heat production and the core temperature in rats running on a treadmill, and calculated the unobserved parameters, such as

muscle temperature and heat dissipation, using our previously published mathematical model [4].This approach helped us to identify a novel and counterintuitive mechanism underlying ergogenic effect of amphetamine, as well as provided new arguments on potential danger of using psychostimulants to improve performance during exercise.

5.2 Methods and Data Preparation

5.2.1 Experimental design

On the day of experiment rats were brought to the experimental room and allowed to adapt to the experimental condition. Telemetric recording of body temperature was initiated. After at least 30 minutes of baseline recording, the animal was administered with amphetamine or saline intraperitoneally according to the protocol. Immediately after the injection, animals were placed on a belt of the treadmill, and gas analysis was initiated. After 12 minutes, the treadmill was activated with the intensity of exercise increased every 3 minutes according to the experimental protocol (Figure 5.1).

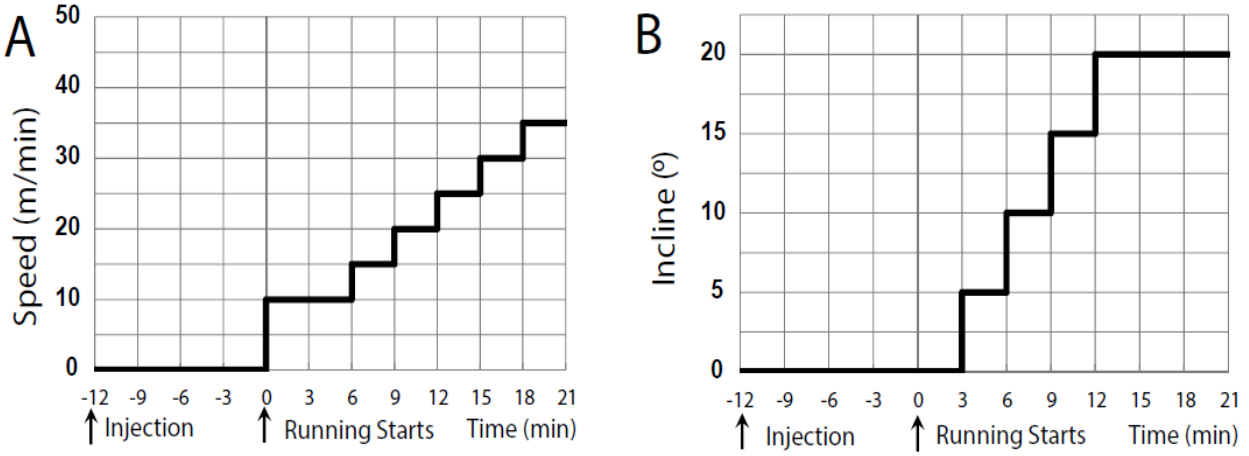

Figure 5.1 The experimental protocol: (A) Speed and (B) incline of the treadmill. Rats were injected with amphetamine or saline 12 min before the treadmill belt was activated.

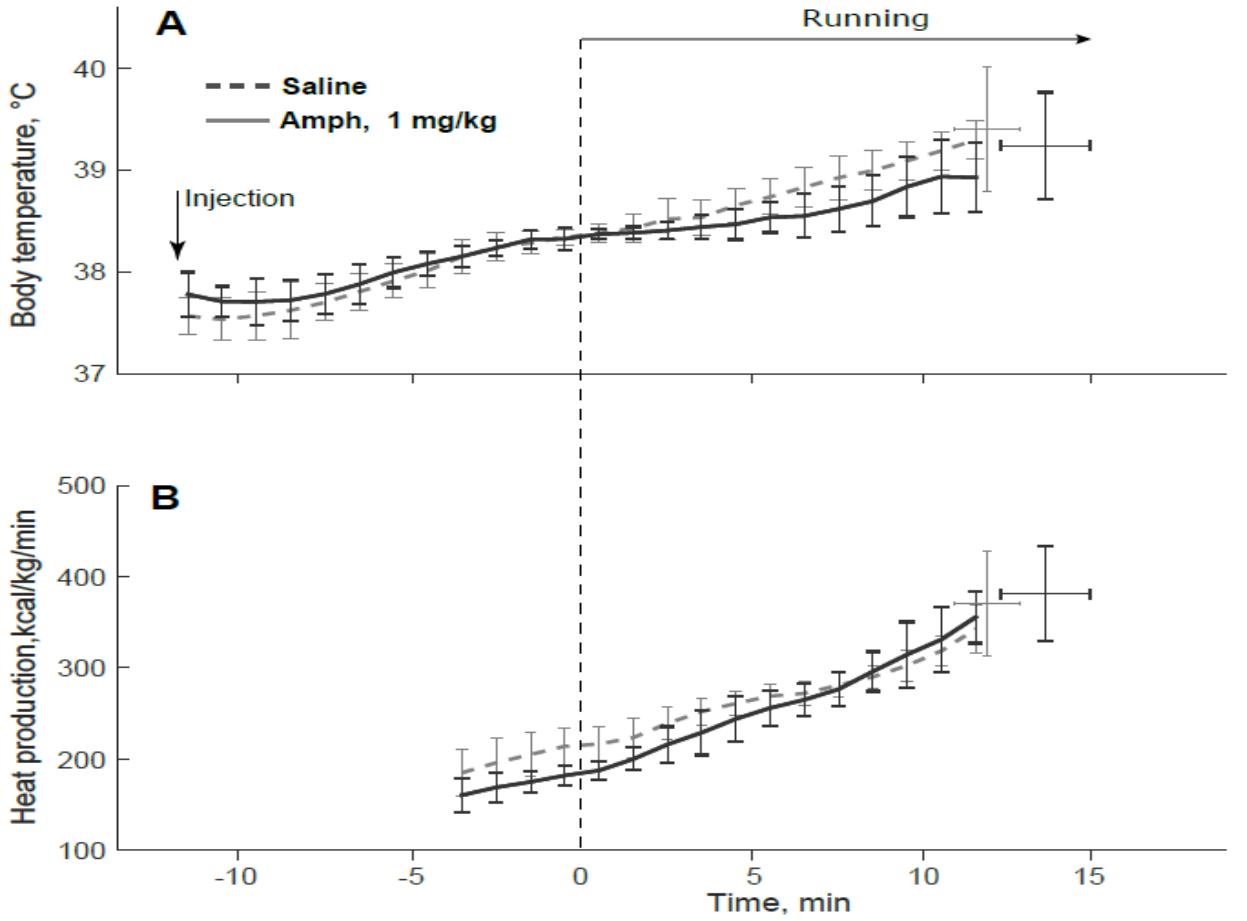

Figure 5.2 Changes in the core body temperature and heat production in rats running on a treadmill after 1 mg/kg of amphetamine. A. The body temperature after saline injection (dashed line), or amphetamine injection (solid line). Error bars represent standard deviations over a group of rats. B. Heat production calculated from O_2 consumption and CO_2 production.

5.2.2 Data analysis and statistical procedures

We calculated the average and the standard deviations of the core body temperatures and VO_2 for all groups. Considering that the dose of 1 mg/kg of amphetamine did not affect body temperature with statistical significance, for modeling purposes we only used data for the control group (injected with saline) and amphetamine group which received 2 mg/kg of amphetamine. In order to obtain consistent datasets, we discarded data points starting when at least one of the rats in each group dropped out. Thus, the experimental data from t = -12 min to t = 13 min for saline (n=6), and from $t = -12$ min to t = 15 min for amphetamine (n=6) was used for estimating model parameters. So, we used $\{T_k(t)\}_{t=-12}^{N}$ as the set of data points for k^{th} group (where k = saline or Amph) and N=13 or 15 for saline and Amph, respectively. The initial VO_2 level was

measured after the calibration time of the instrument. The level was steady before the running started. Accordingly, we considered O_2 consumption constant from -12 min to 0 min for each group and equal to the mean value of VO_2 at t = 0 min. The experimental data used for the model calibration are shown in Figure 5.3.

Between-group comparison of heat dissipation and heat production was performed using z-test. Statistical significance was defined as a p-value <0.05. Values are presented as mean ± SE.

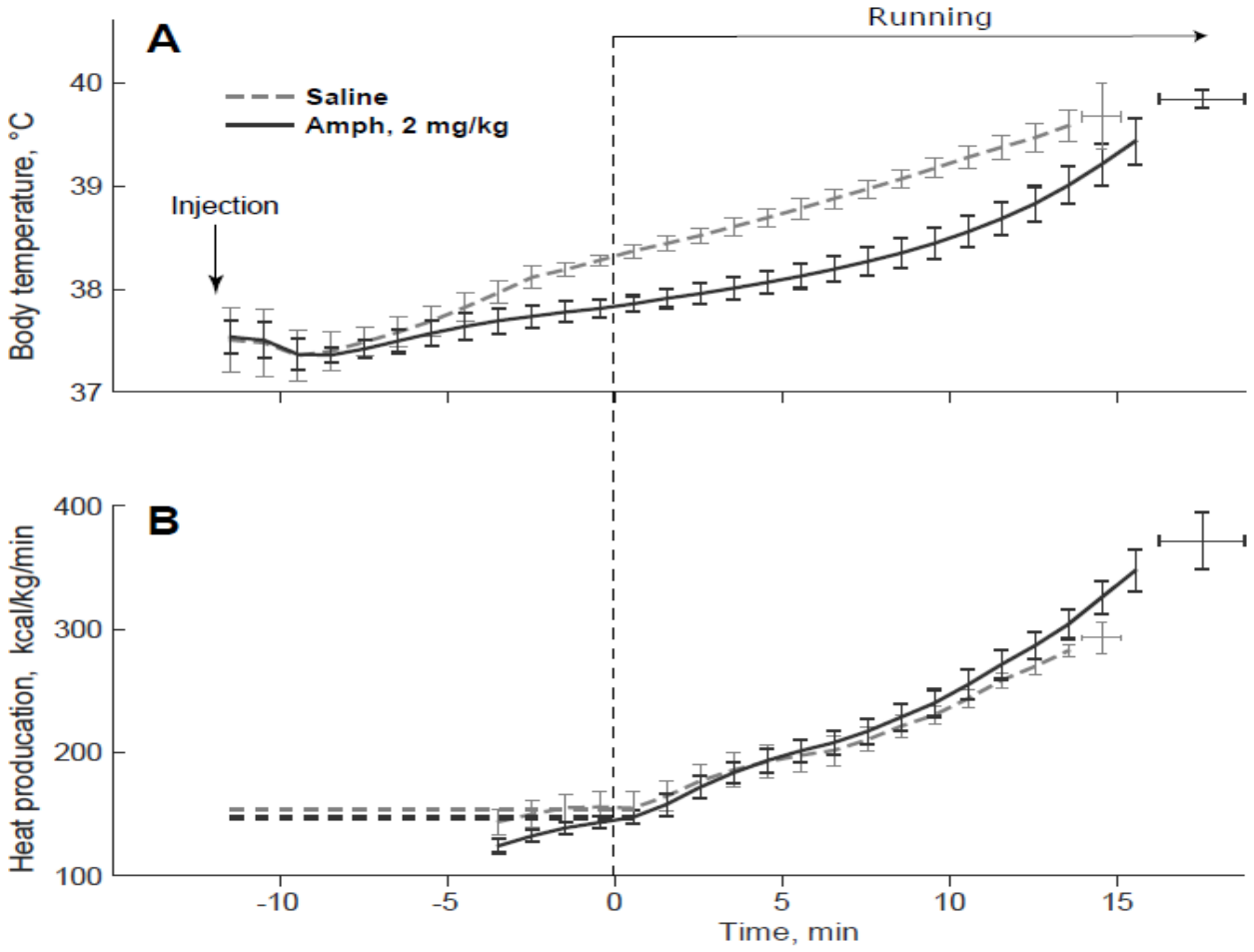

Figure 5.3 Changes in the core body temperature and heat production in rats running on a treadmill after 2 mg/kg of amphetamine. A. The body temperature after saline injection (dashed line), or amphetamine injection (solid line). Error bars represent standard deviations over a group of rats. B. Heat production calculated from O_2 consumption and CO_2 production. For modeling purposes, the heat production was assumed to be constant before the start of run (horizontal dashed lines).

5.3 Model Construction

5.3.1 General Model

In order to quantify heat generation and heat loss in all groups, we adapted a mathematical model describing the temperature changes in two compartments, representing the core and the muscles [4]. In the model, the heat production parameter in the core, P_c, is defined as total heat generated in the core body per time unit divided by the heat capacity of the core. Similarly, the heat production in the muscles, P_m, is extra heat generated in the muscles by physical activity per time unit divided by heat capacity of the muscles. Both parameters have units of $°C/min$. The muscles exchange heat with the core proportionally to the heat transfer coefficient η and the difference between temperatures of two compartments $(T_c - T_m)$. The value of η was fixed at 0.125 min^{-1} based on [4]. Heat exchange between the core and environment is proportional to another heat transfer coefficient η_a and the difference of temperatures between the core and environment, $(T_c - T_a)$. Therefore, changes in the core and the muscle temperatures are described by a system of two first-order differential equations:

$$\begin{aligned} \frac{dT_c}{dt} &= P_c - \eta(T_c - T_m) - \eta_a(T_c - T_a) \\ \frac{dT_m}{dt} &= P_m - \eta(T_m - T_c) \end{aligned} \qquad (5.1)$$

As noted, the heat production and the heat dissipation parameters in this model have units of $°C/min$. However, they can be easily converted into units of power (*Joules/min*) by multiplying by the heat capacity (in *Joules/*$°C$) of the corresponding compartment [79].

In accordance with experimental data in [77] we assumed that at the beginning of the experiment (prior to the run) the temperature of the muscles was equal to the temperature of the core. Specifically, T_c and T_m are the same at $t = -12$ min when each rat was just placed on a treadmill after an injection: the initial conditions are $T_m(-12) = T_c(-12) = T_0$. Initial temperature for each group was calculated as the averaged core body temperature from $t = -15$ min to $t = -12$ min.

Almost all the energy generated in the body is due to oxidation. Total energy production in the body is proportional to the amount of consumed oxygen, VO_2 (liter per kg). Some portion of the energy is spent for the mechanical work (*MW*, cal/kg/min), and the rest is transformed to the heat.

Accordingly, after denoting the coefficient of proportionality between total energy production and oxygen consumption by α, for the total heat production we have:

$$m_m P_m + m_c P_c = (m_m + m_c)(\alpha \cdot VO_2(t) - MW) \quad (5.2)$$

Here m_m and m_c are heat capacities of the muscles and the core, respectively, and $m_m + m_c$ is a total heat capacity of a rat. Taking into account that the skeletal muscle mass of a rat constitutes approximately 45-50% of its body weight [75] with the mass of a skeleton constituting only about 3%, we set $m_m = m_c$ in the model. Accordingly, the above equation reduces to the form of:

$$P_m + P_c = 2(\alpha \cdot VO_2(t) - MW) \quad (5.3)$$

The coefficient α can be calculated as calorific value (*CV*) divided by the specific heat of the body. The latter for a rat is approximately 0.8 kcal/(kg·ºC) [79]. CV is calculated as:

$$CV = 3.815 + 1.232RER \text{ (kcal/liter)} \quad (5.4)$$

where *RER* stands for the respiratory exchange ratio, which is the ratio of the carbon dioxide production (VCO_2) to the oxygen consumption (VO_2) [81].

The mechanical work consists in climbing the treadmill at the given *speed* (m/min) and *incline* (°) (see Figure 5.1) and can be estimated as $MW = g \cdot speed \cdot \tan(incline)/4.184$ in cal/kg/min, where g=9.8 m/s^2 is gravitational acceleration.

5.3.2 Model Parameters Estimation

Since VO_2 and VCO_2 were measured, once we determine P_c, then P_m can be calculated using (5.3). Accordingly, model (5.1) has two undetermined independent parameters, P_c and η_a. We used Bayesian approach to find statistical distributions for these parameters. Specifically, for each group *k*, measured core temperature values $\{T_k(t)\}_{t=-12}^{N}$ were considered independent normal random variables with the mean values $T_c(\eta_a, P_c, t)$ (solution of (5.1)), and standard deviations $\sigma_k(t)$ calculated from experimental data. Based on this assumption, the likelihood (conditional joint probability density function) was calculated:

$$L(\{T^k(t)\}_{t=-12}^{N}|\eta_a, P_c) \sim \exp\left\{-\frac{1}{2}\sum_{t=0}^{N}\frac{\left(T_k(t) - T_c(\eta_a, P_c, t)\right)^2}{\sigma_k^2(t)}\right\} \quad (5.5)$$

where $k =$ Saline or Amph, and $N = 13$ or 15 for Saline and Amph, respectively. The likelihood (5.5) was sampled using Markov Chain Monte Carlo approach by Metropolis-Hastings algorithm [1, 51-53, 67, 78].

5.4 Results

5.4.1 Experimental Data

Baseline core body temperature of all rats was uniform in the range of $37.5 \pm 0.3\ °C$. As soon as rats were placed on a treadmill, their body temperature dropped slightly (Figure 5.2 and Figure 5.3, from -12 min to -10 min,). The presence of a "hypothermic" phase is related to the decrease in core heat production in physiologic "anticipation" of/during exercise, which was described by us earlier [4]. Eventually, the body temperatures of rats in all groups started rising.

Low dose of amphetamine (1 mg/kg, i.p.) significantly affected neither body temperature, nor oxygen consumption at any time point (Figure 5.2). Similarly, there was no effect of this dose on the body temperature at the time of exhaustion. In contrast, higher dose of amphetamine (2 mg/kg) had significant effects on both temperature dynamics and exhaustion time. The amphetamine injected group had lower core body temperature than the saline group throughout the experiment (Figure 5.3 A). Amphetamine also significantly changed the dynamics of temperature: in rats treated with saline the temperature increased at a steady rate, while temperature increase in the amphetamine group was significantly slower in the beginning of the run (Figure 5.3 A). Compared to controls, amphetamine extended the time to exhaustion: 17.3 ± 0.6 min vs 14.8 ± 0.8 ($p < 0.05$). Interestingly, the temperature at exhaustion was not significantly different between the groups (40.0 ± 0.2 after amphetamine vs 39.9 ± 0.2 after saline, $p > 0.05$).

The effect of amphetamine on body temperature during running had no correlation with VO_2 consumption. For all matching workloads there was no significant difference in VO_2 consumption between rats which received amphetamine or saline (Figure 5.3B). However, longer

runs and, hence, higher workloads after amphetamine were accompanied by a higher maximal VO_2 at the end of run (VO_{2max}).

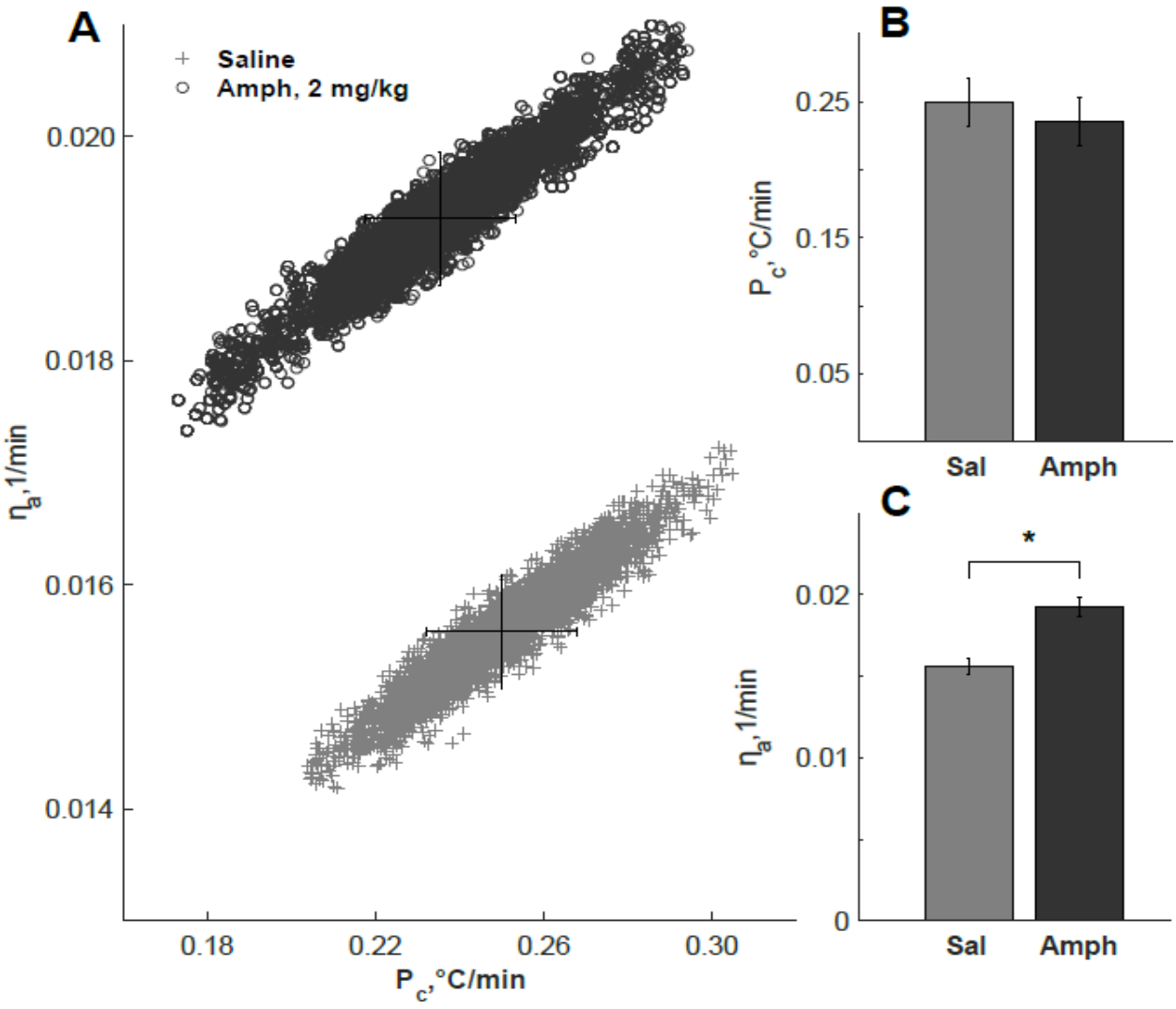

Figure 5.4 Model parameter estimates: A. Statistical ensembles of parameters P_c (heat production in the core) and η_a (heat exchange between the core and the environment) for saline (crosses) and amphetamine (open circles) generated by Markov Chain Monte-Carlo sampling (see text for details). Mean values and standard errors of P_c (B) and η_a (C) for saline and amphetamine groups. * - statistically significant difference ($p<0.05$).

5.4.2 Amphetamine increases heat dissipation

Slower core body temperature increase in the Amph group can be explained either by an increase in heat dissipation, i.e. an increase in η_a, or by a decrease in heat accumulation at the core body, i.e. a decrease in P_c (see (5.1)). We estimated these parameters, P_c and η_a, by fitting the mathematical model (5.1), (5.3) to the experimental data shown in Figure 5.3A. Figure 5.4A contains ensembles of parameters (P_c, η_a) distributed according to the corresponding posterior probability density functions (likelihoods, see Methods). These ensembles were generated by Markov Chain Monte-Carlo method as described in Methods. Statistical analysis of these samples showed that the heat production in the core body (P_c) was not significantly different between the groups: 0.25 ± 0.02 ^{o}C/min after saline vs 0.24 ± 0.02 ^{o}C/min after amphetamine (Figure 5.4B). In contrast, the heat dissipation coefficient for the Amph group (0.0194 ± 0.0005 min^{-1}) was significantly higher ($p<0.005$) than heat dissipation in the saline group (0.0156 ± 0.0005 min^{-1}) (Figure 5.4C). For each group, we fitted the core body temperature dynamics based on the total heat production in the body (from VO_2), as well as we sampled values of heat production in the core, P_c, and heat dissipation, η_a. As shown in Figure 5.5A, at most probable values of P_c and η_a (best fit), the model reproduced the core temperature dynamics after both saline and amphetamine within one standard deviation.

5.4.3 Muscle temperature reaches higher levels in amphetamine treated rats

Using Eq. (5.3), we calculated the heat production by muscles P_m, and then estimated the temperature of the muscles by plugging sampled values of parameters (P_c, η_a), shown on the Fig. 4, to Eq. (5.3). Throughout the run, the muscle temperature in the saline group was slightly higher than in the Amph group. However, the difference in muscle temperature between the two groups was dramatically smaller that the difference of core body temperatures. Due to the fact that after amphetamine, rats were able to run almost 3 minutes longer than control rats, the muscle temperature at the end of the run in the Amph group reached values that were significantly higher than in the saline group. The highest muscle temperatures at the end of run after saline and amphetamine were estimated as 41.2 ± 0.1 ^{o}C and 41.9 ± 0.2 ^{o}C, respectively (Figure 5.5B).

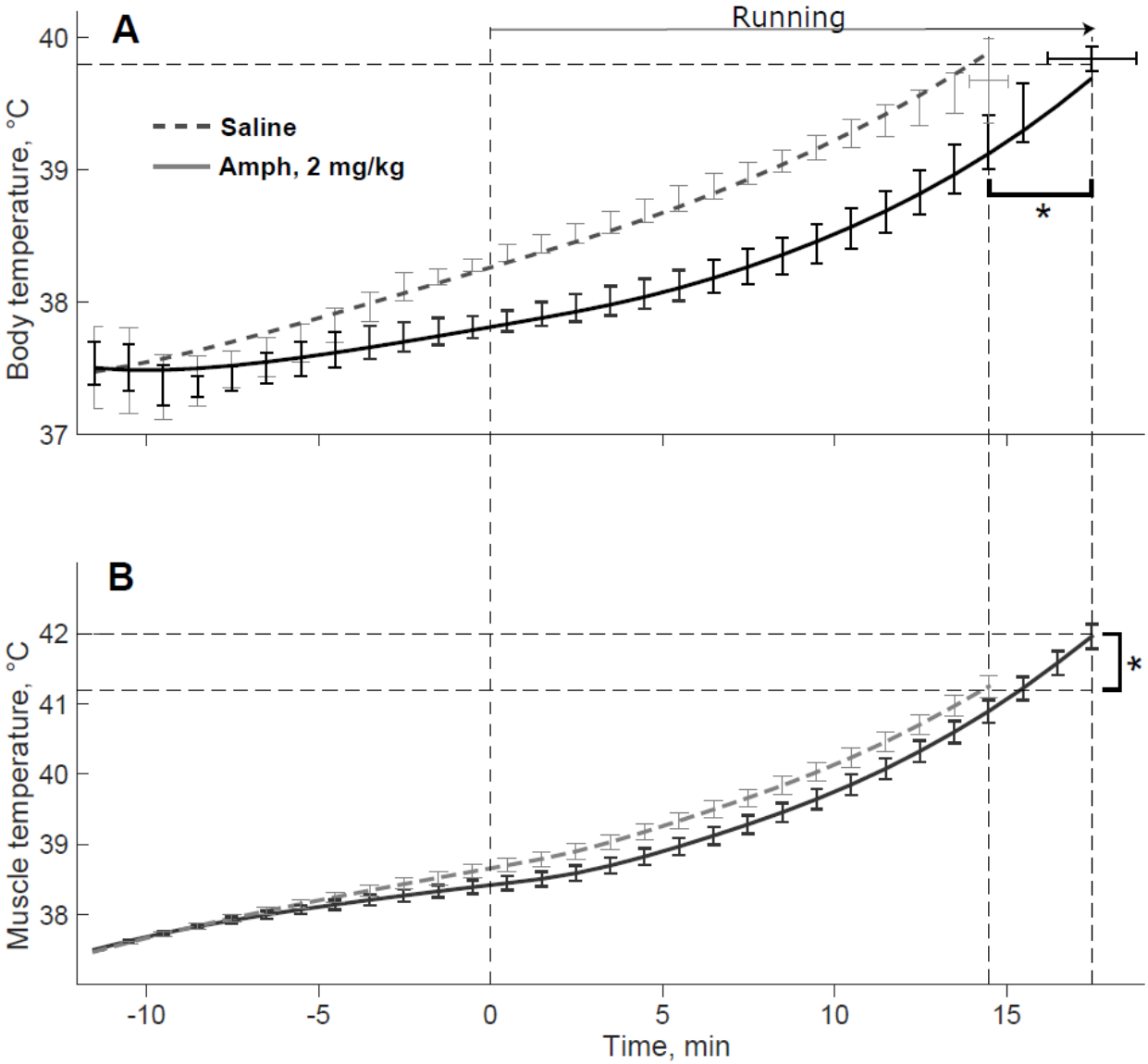

Figure 5.5 Comparison of experimental data and model performance, and calculated temperature of the muscles: A. Calculated core body temperature of rats injected with saline (dashed line) or amphetamine (solid line) together with the experimental data (shown by error bars representing the mean +/- standard deviation). Dashed vertical lines show the beginning of running (t=0) and the average time of exhaustion in two groups. B. Calculated muscle temperature dynamics for the two groups. Error bars represent standard errors. * - statistically significant difference ($p<0.05$).

5.5 Discussions

5.5.1 Overview

Amphetamine at low to moderate doses enhances physical performance of humans and animals [105, 106, 114]. We observed that relatively low dose of amphetamine (2 mg/kg) increases time to exhaustion in rats exercising with high intensity (high speed treadmill running) at room temperature. This dose of amphetamine is similar to those that animals self-administer [115, 116] and comparable to a typical dose that humans use (~50mg). Our observations are in line with previous studies showing enhanced endurance in rodents treated with amphetamine [106, 117, 118]. In this study we provide a novel potential mechanistic interpretation of this phenomenon; we show that amphetamine increases heat dissipation which helps the core body temperature to delay reaching the threshold for exhaustion.

Considering that well-controlled body temperature is one of the determinants of endurance, the goal of the present study was to evaluate the effect of amphetamine on the thermoregulatory system in rats running on a treadmill. We applied mathematical modeling to explain the amphetamine-induced changes of the body temperature dynamics in running rats. This approach allowed us to calculate parameters that are difficult to measure experimentally, i.e. heat dissipation coefficient, heat production in the core and the muscles, and muscle temperature.

Proper functioning of thermoregulatory system plays an important role in ones' ability to maintain particular levels of physical activity. Excessively high body temperature can cause (or underlie) exhaustion and limit exercise duration. Walters at el. [119] and Fuller at el. [120] provided evidence of the existence of a limiting body temperature; they showed that at a point of exhaustion from voluntary running on a treadmill, the abdominal and the hypothalamic temperatures reached certain thresholds. Moreover, the limiting temperatures were independent of ambient (T_a) and initial (T_0) temperatures. In agreement with these experimental observations, the core body temperatures of rats at the end of running due to exhaustion were not statistically different between Amph and saline groups in our study (Figure 5.3A). However, at any time point during the run the core body temperature of rats treated with amphetamine remained significantly lower than of control rats. This strongly suggests that Amphetamine delayed temperature rise to the critical value at which exhaustion occurred and, as the result, significantly increased the time to exhaustion.

Based on VO_2 and VCO_2 measurements we calculated the total heat production in both groups. We found no significant difference in heat production during running between the groups, meaning that changes in temperature dynamics are caused either by redistribution of heat production in the body, or by an increase in heat dissipation. To discriminate between these two possibilities, we used a mathematical model (5.1), (5.3) describing temperature changes in the core and muscle compartments during run. For this purpose we adapted the model from [4]. Previously, for simplicity, heat dissipation to the environment and heat production in the core were combined in a single term: overall net heat production in the core. We augmented that model by incorporating heat production in the core and heat dissipation to the environment explicitly. This improvement allowed us to use experimental data to estimate heat dissipation coefficient (η_a) and heat production parameter (P_c), and then to infer which parameter is affected by amphetamine. We found that amphetamine significantly enhances heat dissipation and has no effect on heat production.

While the rise of T_c was slowed down by increased heat dissipation, the cooler core was not able to significantly delay the rise of T_m. Therefore, at any selected time the muscle temperature was not significantly different between Amph and Saline group. However, due to increased running time in Amph group, the muscle temperature in this group was significantly higher at the end of running (Figure 5.5). This difference of almost 1ºC brings the temperature of muscles to the level that could result in physical damage of muscle tissue from hyperthermia.

Based on the above, we can hypothesize that exertional exhaustion may be mediated by failure of thermoregulatory mechanisms to keep the core body temperature below the threshold. The same mechanism indirectly allows keeping the temperature of contracting muscles within safe range. Administration of psychostimulants does not change the threshold for the core temperature at room temperature. However, it tricks the thermoregulatory system by an “unauthorized” increase of heat dissipation and, thus, increasing the gap between the temperatures of the core and the muscles, which may be potentially dangerous for the latter.

5.5.2 Model assumptions

We considered the heat dissipation coefficient η_a constant throughout the exercise. This assumption is based on the following logic. Major changes of heat dissipation in running rats occur when thermoregulatory mechanisms dilate cutaneous vessels. Tail temperature is a well-accepted marker of thermoregulatory heat dissipation. [87] measured the body temperature and the tail temperature in rats running with various speeds at room temperature. The threshold temperature for heat dissipation (body temperature at which heat dissipation starts increasing) quickly rises with the increasing work intensity and at the highest workloads it reaches a maximum value of $39.3\,°C$. Therefore, in the beginning of our experimental protocol, the body temperature was too low for cutaneous vasodilation to occur. Later on, the body temperature increased, but so did the workload. As a result, according to [87], the heat loss threshold would not be hit before the core body temperature reached levels of approximately $39\,°C$. In our experiments, the highest T_c values at the end of the analyzed period were $39.6\,°C$ for Saline group and $39.4\,°C$ for Amph group. Therefore, it was reasonable to consider that the heat dissipation did not change within the interval used for model calibration.

Also, when cutaneous vasodilation finally kicks in, body temperature in running animals stops rising and in most cases plateaus [87]. In our recordings we did not observe any instances of temperature plateauing before animals stopped running, which also confirms that the threshold of thermoregulatory changes in heat dissipation was not reached. This allowed us to assume that the heat dissipation coefficient was constant throughout the exercise.

5.5.3 Amphetamine increases VO2max by slowing the temperature rise

Our data show that amphetamine *per se* does not significantly affect oxygen consumption (VO_2) at the same exercise intensity. VO_2max in the amphetamine group is increased because rats injected with amphetamine can run for longer times thus undergoing a higher physical load according to the protocol. The important implication of our study is that due to higher heat dissipation, it takes longer for the temperature of amphetamine-treated rats to reach the threshold for exhaustion. This is why they continue to run at higher speeds/inclines, and, thus, exhibit higher VO_2max at the end of the run. Accordingly, higher VO_2max in the amphetamine group is indirectly caused by higher heat dissipation.

5.5.4 Amphetamine increases heat dissipation, but does not suppress thermogenesis

Our modeling results show that a relatively low dose of amphetamine (2 mg/kg) increases heat dissipation, which in turn slows down the core body temperature rise. This finding was made possible by simultaneous measurements of the core body temperature and energy expenditure. Core body temperature was significantly lower in the amphetamine group, while energy expenditure was no different between the groups, meaning that total thermogenesis was not affected by amphetamine. Using mathematical modeling we were able to answer the question whether amphetamine redistributes heat generation between body compartments, or it affects heat removal from the body. We found that amphetamine increases heat dissipation from the core, while its effect on heat production is significant neither in the core nor in the muscles. As a direct experimental validation of our result, whole body calorimetry could be used.

Spreading of saliva, which is one of heat dissipation control mechanism in rats, is difficult to employ while running. Water evaporation from the respiratory tract, which is increased during the exercise [87] due to increased ventilation and higher body temperature is dictated by energy demand rather than thermoregulation. Therefore, rats control their heat exchange with the environment during exercise predominantly by dilating or constricting cutaneous blood vessels. Due to absence of fur and large surface area, the tail is the major thermoregulatory organ in rats.

More than forty years ago, [111] measured the tail temperature of rats after treatment with various doses of amphetamine. They reported an amphetamine-induced dose-dependent decrease in tail temperature, suggesting that amphetamine induces cutaneous vasoconstriction and, thus, decrease in heat dissipation. Considering that hyperthermia induced by amphetamine or its derivatives is one of the major complications and may be life-threatening [121, 122], an increase in heat dissipation coefficient found in this study is counterintuitive. Nevertheless, using a simple mathematical model, we directly linked heat production (based on oxygen consumption) and body temperature increase (characterizing the retained heat), which allowed for reliable estimation of the heat produced and dissipated. Our estimates unequivocally show a significant increase in heat dissipation coefficient after amphetamine administration and no evidence of altered heat production.

One of possible explanations of the seeming discrepancy is that profound hyperthermia is associated with higher doses (5 mg/kg and above), while we studied relatively low doses (1-2 mg/kg). Our findings may have implications on the mechanistic interpretation of previous

experimental results concerned with effects of amphetamine and its derivatives on temperature dynamics. Recently Molkov et al. published experimental and modeling data on extremely complex dose-dependence of temperature effects of methamphetamine [1]. The interpretation was that in doses exceeding 1 mg/kg methamphetamine activated an inhibitory component, which reversed effects of excitatory influence of lower doses on heat production. Therefore, the aforementioned intricate dose-dependence is a result of delicate balance between activation of excitatory and inhibitory pathways controlling heat generation [123], while both components are mediated by orexinergic neurotransmission [124]. In that study, based on existing literature data, we explicitly assumed that at room temperature amphetamines do not increase heat dissipation; an assumption that may require reassessment in light of the findings presented in this study.

We are not aware of any specific mechanisms that can explain the increase of heat dissipation by amphetamine during running. However, we estimated the change of the heat dissipation coefficient to be less than 30%. It is dramatically smaller than more than 10-fold range of metabolic activity. Assuming that thermoregulatory variations in heat dissipation are comparable in magnitude, and that those variations are in significant part mediated by cutaneous vasodilation, the inhibitory effect of amphetamine on cutaneous vasoconstriction may be modulatory. For example, there is a possibility that activation of alpha2-adrenoreceptors in ventromedial raphe by amphetamine could be a culprit [125], which is similar to what Molkov et al. suggested as a possible mechanisms of inhibitory component in the thermoregulatory effects of methamphetamine [1].

Tail temperature seems to be a good indicator of the changes in heat dissipation mediated by cutaneous vasodilation. However, there are serious limitations on what tail temperature measurements can reveal. Tail flow modulation supports changes of heat dissipation in a multifold range (100-fold increase of flow), so the change of heat dissipation within 30%, found in our study, will not be statistically significantly reflected in the tail temperature. In addition, other than vasomotor mechanisms should be considered, e.g. an increase in respiratory evaporation or a change of insulating properties of fur.

Possible mechanistic interpretations do matter for translational importance of our observations, as some physiological mechanisms in rodents could be missing in humans and vice versa.

5.5.5 Implications for exercise at different ambient temperatures

An interesting testable prediction provided by our study is that the effect of amphetamine may depend on ambient temperature. Since the heat exchange with the environment is proportional to the temperature gradient (the difference between the body temperature and the ambient temperature), the same change in the heat conductance (heat transfer coefficient in our model) would lead to greater variations in total heat loss in colder environments. Accordingly, we expect that at higher (lower) ambient temperatures the effect of amphetamine on endurance is weaker (stronger) given that the increase in heat conductance is the same.

5.6 Conclusion

Using core body temperature dynamics and mathematical modeling, we estimated parameters that are hard to measure experimentally, i.e. the distribution of heat production in the core and muscles and the heat dissipation coefficient. We found that in rats, amphetamine (2 mg/kg) slows down the temperature rise during treadmill exercise at room temperature by increasing heat dissipation. We suggest that this psychostimulant increases the time to exhaustion in rats, at least in part, by delaying the moment when the core body temperature exceeds the threshold defining exhaustion. The calculated muscle temperature at the end of run in rats after amphetamine was almost one degree higher than after saline which may be health-threatening. We conclude that while amphetamine improves endurance and extends the time at which exhaustion occurs, its use can result in health-threatening complications.

CHAPTER 6. CONCLUSION

In this thesis, we used a new mathematical modeling approach to learn insightful information about thermoregulation system and how Methamphetamine and Exercise impact its mechanism. These findings and learnings can be split into two main categories: Mathematical Modeling Developments and New Biological Insights.

6.1 Mathematical Modeling Developments

In this thesis, we used a new mathematical modeling approach that was first introduced in [1] as the main and base framework. By expanding this model to some case study, we were able to explore some of the underlying components of thermoregulation which are impacted by Meth or Exercise. Moreover, we measured some of their properties and correlations. For this purpose, we used a combination of Neural Network and Bayesian approach which allowed us to calculate the statistical significances in changes of these components. Also, we developed reduced models and explained uncertainties in our models and discussed their impacts on each component of the models. For each model, we tried to make meaningful biological interpretations for when our models is perturbed under these uncertainties. Finally, for some hypothetical studies, we were able to calculate the changes in our model's parameters which then allow us to make prediction for the future of the system. These predictions were helpful to explain some of the extreme reactions of the system that have been reported or can be proven experimentally.

6.2 New Biological Insights

In Orexin study, we discovered that both Meth and stress activate the excitatory component and evoke temperature response. Also, we explained that the neural circuitry of thermoregulation system in our model have meth sensitive components which are mediated by orexin receptors and hence can be suppressed by SB. Insufficient inhibitory drive can cause fatal hyperthermia after relatively low doses of Meth.

In Circadian Study, we were the first to measure and compare the body temperature responses in rats to injections of Meth during daytime and at night where the temperature changes were much weaker than daytime. Using our model, we inferred that during night the baseline activity of the

excitatory components are elevated and thus the additional response to the Meth injection is weaker during night than similar dose during daytime. We also found that once Meth is washed out of the blood, temperature stabilized at lower level that initial temperature.

Our Exercise study demonstrated that both thermogenesis and heat dissipation together with corresponding control mechanisms are critical to quantify the changes in body temperature during exercise. We were the first to characterize “Activity for free” phenomenon. Also, we predicted that, in colder condition than room temperature, the compensatory suppression of metabolism is much greater than half of metabolism. Finally, we discussed that some unusual compensatory adjustment in thermoregulation system might be the cause for heat injuries during exercise.

Last but not least, we combined Exercise and Amphetamine to perturb the thermoregulation system. We were able to measure the dynamics of heat production and dissipation in the core and muscles. We discovered that during exercise at room temperature, injection of Amphetamine (2 mg/kg) can increase the heat dissipation which results in reduction of the temperature rise. This mechanism increases the exhaustion threshold in rats and allows them rats to run longer. However, when Amphetamine is injected, the muscle temperature is almost one degree higher at the end of running compare to when only Saline is injected. This can result in serious muscle injuries and other health threatening conditions.

BIBLIOGRAPHY

1. Molkov, Y.I., M.V. Zaretskaia, and D.V. Zaretsky, *Meth math: modeling temperature responses to methamphetamine.* Am J Physiol Regul Integr Comp Physiol, 2014. **306**(8): p. R552-66.
2. Behrouzvaziri, A., et al., *Orexinergic Neurotransmission in Temperature Responses to Methamphetamine and Stress: Mathematical Modeling as a Data Assimilation Approach.* PLoS One, 2015(in press).
3. Behrouzvaziri, A., et al., *Circadian variability of body temperature responses to methamphetamine.* Am J Physiol Regul Integr Comp Physiol, 2017: p. ajpregu 00170 2017.
4. Yoo, Y., et al., *Exercise Activates Compensatory Thermoregulatory Reaction in Rats: A Modeling Study.* J Appl Physiol (1985), 2015: p. jap 00392 2015.
5. Morozova, E., et al., *Amphetamine enhances endurance by increasing heat dissipation.* Physiol Rep, 2016. **4**(17).
6. Romanovsky, A.A., A.I. Ivanov, and Y.P. Shimansky, *Selected contribution: ambient temperature for experiments in rats: a new method for determining the zone of thermal neutrality.* J Appl Physiol (1985), 2002. **92**(6): p. 2667-79.
7. Phelps, G., H.A. Speaker, and K.E. Sabol, *Relationship between methamphetamine-induced behavioral activation and hyperthermia.* Brain Research, 2010. **1357**: p. 41-52.
8. Dimicco, J.A. and D.V. Zaretsky, *The dorsomedial hypothalamus: a new player in thermoregulation.* Am J Physiol Regul Integr Comp Physiol, 2007. **292**(1): p. R47-63.
9. Zaretskaia, M.V., et al., *Chemical stimulation of the dorsomedial hypothalamus evokes non-shivering thermogenesis in anesthetized rats.* Brain Res, 2002. **928**(1-2): p. 113-25.
10. Rusyniak, D.E., et al., *Microinjection of muscimol into the dorsomedial hypothalamus suppresses MDMA-evoked sympathetic and behavioral responses.* Brain Res, 2008. **1226**: p. 116-23.
11. Hunt, J.L., et al., *Dorsomedial hypothalamus mediates autonomic, neuroendocrine, and locomotor responses evoked from the medial preoptic area.* Am J Physiol Regul Integr Comp Physiol, 2010. **298**(1): p. R130-40.
12. Rusyniak, D.E., et al., *3,4-Methylenedioxymethamphetamine- and 8-hydroxy-2-di-n-propylamino-tetralin-induced hypothermia: role and location of 5-hydroxytryptamine 1A receptors.* J Pharmacol Exp Ther, 2007. **323**(2): p. 477-87.
13. White, S., et al., *Gestation time-dependent pharmacokinetics of intravenous (+)-methamphetamine in rats.* Drug Metab Dispos, 2011. **39**(9): p. 1718-26.
14. Fujimoto, Y., et al., *The pharmacokinetic properties of methamphetamine in rats with previous repeated exposure to methamphetamine: the differences between Long-Evans and Wistar rats.* Exp Anim, 2007. **56**(2): p. 119-29.
15. Milesi-Halle, A., et al., *Sex- and dose-dependency in the pharmacokinetics and pharmacodynamics of (+)-methamphetamine and its metabolite (+)-amphetamine in rats.* Toxicol Appl Pharmacol, 2005. **209**(3): p. 203-13.
16. Ootsuka, Y., E. Nalivaiko, and W.W. Blessing, *Spinal 5-HT2A receptors regulate cutaneous sympathetic vasomotor outflow in rabbits and rats; relevance for cutaneous vasoconstriction elicited by MDMA (3,4-methylenedioxymethamphetamine, "Ecstasy") and its reversal by clozapine.* Brain Res, 2004. **1014**(1-2): p. 34-44.

17. Myles, B.J., et al., *The effects of methamphetamine on core body temperature in the rat--part 1: chronic treatment and ambient temperature.* Psychopharmacology (Berl), 2008. **198**(3): p. 301-11.
18. Rusyniak, D.E., et al., *The orexin-1 receptor antagonist SB-334867 decreases sympathetic responses to a moderate dose of methamphetamine and stress.* Physiology and Behavior, 2012. **107**(5): p. 743-750.
19. Sabol, K.E., et al., *Methamphetamine and core temperature in the rat: Ambient temperature, dose, and the effect of a D2 receptor blocker.* Psychopharmacology (Berl), 2013.
20. Broadley, K.J., *The vascular effects of trace amines and amphetamines.* Pharmacol Ther, 2010. **125**(3): p. 363-75.
21. Broadley, K.J., et al., *Functional evaluation of the receptors mediating vasoconstriction of rat aorta by trace amines and amphetamines.* Eur J Pharmacol, 2013. **715**(1-3): p. 370-80.
22. UNODC. *Annual Report 2008*. 2008; Available from: www.**unodc**.org/documents/about-**unodc**/AR08_WEB.pdf.
23. Jordan, S.C. and F. Hampson, *Amphetamine poisoning associated with hyperpyrexia.* British Medical Journal, 1960. **2**(5202): p. 844.
24. Kojima, T., et al., *A fatal methamphetamine poisoning associated with hyperpyrexia.* Forensic Science International, 1984. **24**(1): p. 87-93.
25. Kalant, H. and O.J. Kalant, *Death in amphetamine users: causes and rates.* Canadian Medical Association Journal, 1975. **112**(3): p. 299-304.
26. Ginsberg, M.D., M. Hertzman, and W.W. Schmidt-Nowara, *Amphetamine intoxication with coagulopathy, hyperthermia, and reversible renal failure. A syndrome resembling heatstroke.* Annals of Internal Medicine, 1970. **73**(1): p. 81-5.
27. Westover, A.N., P.A. Nakonezny, and R.W. Haley, *Acute myocardial infarction in young adults who abuse amphetamines.* Drug and Alcohol Dependence, 2008. **96**(1-2): p. 49-56.
28. O'Connor, A.D., D.E. Rusyniak, and A. Bruno, *Cerebrovascular and cardiovascular complications of alcohol and sympathomimetic drug abuse.* Medical Clinics of North America, 2005. **89**(6): p. 1343-58.
29. Kendrick, W.C., A.R. Hull, and J.P. Knochel, *Rhabdomyolysis and shock after intravenous amphetamine administration.* Ann Intern Med, 1977. **86**(4): p. 381-7.
30. Verschraagen, M., et al., *Post-mortem cases involving amphetamine-based drugs in The Netherlands. Comparison with driving under the influence cases.* Forensic Sci Int, 2007. **170**(2-3): p. 163-70.
31. De Letter, E.A., et al., *Amphetamines as potential inducers of fatalities: a review in the district of Ghent from 1976-2004.* Med Sci Law, 2006. **46**(1): p. 37-65.
32. Wellman, P.J., *Influence of amphetamine on brown adipose thermogenesis.* Research Communications in Chemical Pathology and Pharmacology, 1983. **41**(1): p. 173-6.
33. Blessing, W.W., A. Zilm, and Y. Ootsuka, *Clozapine reverses increased brown adipose tissue thermogenesis induced by 3,4-methylenedioxymethamphetamine and by cold exposure in conscious rats.* Neuroscience, 2006. **141**(4): p. 2067-73.
34. Sprague, J.E., et al., *UCP3 and thyroid hormone involvement in methamphetamine-induced hyperthermia.* Biochemical Pharmacology, 2004. **68**(7): p. 1339-43.

35. Pedersen, N.P. and W.W. Blessing, *Cutaneous vasoconstriction contributes to hyperthermia induced by 3,4-methylenedioxymethamphetamine (ecstasy) in conscious rabbits.* J Neurosci, 2001. **21**(21): p. 8648-54.
36. Blessing, W.W., et al., *Clozapine reverses hyperthermia and sympathetically mediated cutaneous vasoconstriction induced by 3,4-methylenedioxymethamphetamine (ecstasy) in rabbits and rats.* J Neurosci, 2003. **23**(15): p. 6385-91.
37. Kerman, I.A., H. Akil, and S.J. Watson, *Rostral elements of sympatho-motor circuitry: a virally mediated transsynaptic tracing study.* J Neurosci, 2006. **26**(13): p. 3423-33.
38. Kerman, I.A., et al., *Distinct populations of presympathetic-premotor neurons express orexin or melanin-concentrating hormone in the rat lateral hypothalamus.* Journal of Comparative Neurology, 2007. **505**(5): p. 586-601.
39. Estabrooke, I.V., et al., *Fos Expression in Orexin Neurons Varies with Behavioral State.* Journal of Neuroscience, 2001. **21**(5): p. 1656-1662.
40. Fadel, J., M. Bubser, and A.Y. Deutch, *Differential Activation of Orexin Neurons by Antipsychotic Drugs Associated with Weight Gain.* Journal of Neuroscience, 2002. **22**(15): p. 6742-6746.
41. Samson, W.K., et al., *Cardiovascular regulatory actions of the hypocretins in brain.* Brain Research, 1999. **831**(1-2): p. 248-53.
42. Shirasaka, T., et al., *Neuronal effects of orexins: relevant to sympathetic and cardiovascular functions.* Regulatory Peptides, 2002. **104**(1-3): p. 91-5.
43. Monda, M., et al., *Sympathetic and hyperthermic reactions by orexin A: Role of cerebral catecholaminergic neurons.* Regulatory Peptides, 2007. **139**(1-3): p. 39-44.
44. Yoshimichi, G., et al., *Orexin-A regulates body temperature in coordination with arousal status.* Experimental Biology and Medicine, 2001. **226**(5): p. 468-476.
45. Tupone, D., et al., *An orexinergic projection from perifornical hypothalamus to raphe pallidus increases rat brown adipose tissue thermogenesis.* J Neurosci, 2011. **31**(44): p. 15944-55.
46. Johnson, P.L., et al., *A key role for orexin in panic anxiety.* Nature Medicine. **16**(1): p. 111-5.
47. Samson, W.K., et al., *Hypocretin/orexin type 1 receptor in brain: role in cardiovascular control and the neuroendocrine response to immobilization stress.* American Journal of Physiology, 2007. **292**(1): p. R382-R387.
48. Rusyniak, D.E., et al., *The orexin-1 receptor antagonist SB-334867 decreases sympathetic responses to a moderate dose of methamphetamine and stress.* Physiol Behav, 2012.
49. Cruickshank, C.C. and K.R. Dyer, *A review of the clinical pharmacology of methamphetamine.* Addiction, 2009. **104**(7): p. 1085-1099.
50. DiMicco, J.A., et al., *Stress-induced cardiac stimulation and fever: common hypothalamic origins and brainstem mechanisms.* Auton Neurosci, 2006. **126-127**: p. 106-19.
51. Loskutov, E.M., et al., *Markov chain Monte Carlo method in Bayesian reconstruction of dynamical systems from noisy chaotic time series.* Phys Rev E Stat Nonlin Soft Matter Phys, 2008. **77**(6 Pt 2): p. 066214.
52. Mukhin, D.N., et al., *Modified Bayesian approach for the reconstruction of dynamical systems from time series.* Phys Rev E Stat Nonlin Soft Matter Phys, 2006. **73**(3 Pt 2): p. 036211.

53. Molkov, Y.I., et al., *Prognosis of qualitative system behavior by noisy, nonstationary, chaotic time series.* Phys Rev E Stat Nonlin Soft Matter Phys, 2011. **84**(3 Pt 2): p. 036215.
54. Feigin, A., et al., *Prognosis of qualitative behavior of a dynamic system by the observed chaotic time series.* Radiophysics and quantum electronics, 2001. **44**(5-6): p. 348-367.
55. Molkov, Y.I. and D.V. Zaretsky, *Balanced excitation and inhibition in temperature responses to meth.* Temperature, 2014: p. 00-00.
56. Kukkonen, J.P. and C.S. Leonard, *Orexin/hypocretin receptor signalling cascades.* Br J Pharmacol, 2014. **171**(2): p. 314-31.
57. Peyron, C., et al., *Neurons containing hypocretin (orexin) project to multiple neuronal systems.* J Neurosci, 1998. **18**(23): p. 9996-10015.
58. Khoo, S.Y. and R.M. Brown, *Orexin/hypocretin based pharmacotherapies for the treatment of addiction: DORA or SORA?* CNS Drugs, 2014. **28**(8): p. 713-30.
59. Baimel, C., et al., *Orexin/hypocretin role in reward: implications for opioid and other addictions.* Br J Pharmacol, 2014.
60. Sakurai, T., *Orexin deficiency and narcolepsy.* Curr Opin Neurobiol, 2013. **23**(5): p. 760-6.
61. Nishino, S. and M. Okuro, *Emerging treatments for narcolepsy and its related disorders.* Expert Opin Emerg Drugs, 2010. **15**(1): p. 139-58.
62. Molkov, Y.I. and D.V. Zaretsky, *Balanced excitation and inhibition in temperature responses to meth.* Temperature, 2014. **1**(3): p. 154-156.
63. Mohawk, J.A. and M. Menaker, *A new (and different) circadian pacemaker.* Cell Cycle, 2009. **8**(18): p. 2861-2.
64. Mohawk, J.A., M.L. Baer, and M. Menaker, *The methamphetamine-sensitive circadian oscillator does not employ canonical clock genes.* Proc Natl Acad Sci U S A, 2009. **106**(9): p. 3519-24.
65. Jeffreys, H., *Scientific Inference*. 3rd ed. ed. 1973: Cambridge University Press.
66. Molkov, Y.I., et al., *Using the minimum description length principle for global reconstruction of dynamic systems from noisy time series.* Phys Rev E Stat Nonlin Soft Matter Phys, 2009. **80**(4 Pt 2): p. 046207.
67. Molkov, Y.I., et al., *Random dynamical models from time series.* Phys Rev E Stat Nonlin Soft Matter Phys, 2012. **85**(3-2): p. 036216.
68. Press, W.H., *Numerical recipes : the art of scientific computing*. 3rd ed. 2007, Cambridge ; New York: Cambridge University Press.
69. Ladabaum, U., et al., *Obesity, abdominal obesity, physical activity, and caloric intake in US adults: 1988 to 2010.* Am J Med, 2014. **127**(8): p. 717-727.e12.
70. Boden, B.P., et al., *Fatalities in high school and college football players.* Am J Sports Med, 2013. **41**(5): p. 1108-16.
71. *Heat-related deaths after an extreme heat event--four states, 2012, and United States, 1999-2009.* MMWR Morb Mortal Wkly Rep, 2013. **62**(22): p. 433-6.
72. Running_USA. *2014 Annual Marathon Report*. 2014 March 23, 2014 [cited 2015 April 20]; Available from: http://www.runningusa.org/marathon-report-2014.
73. Goforth, C.W. and J.B. Kazman, *Exertional heat stroke in navy and marine personnel: a hot topic.* Crit Care Nurse, 2015. **35**(1): p. 52-9.

74. Humphries, M.M. and V. Careau, *Heat for nothing or activity for free? Evidence and implications of activity-thermoregulatory heat substitution.* Integr Comp Biol, 2011. **51**(3): p. 419-31.
75. Franco, F.S., et al., *The effects of a high dosage of creatine and caffeine supplementation on the lean body mass composition of rats submitted to vertical jumping training.* J Int Soc Sports Nutr, 2011. **8**: p. 3.
76. DeMoss, D.L. and G.L. Wright, *Sex and strain differences in whole skeletal development in the rat.* Calcif Tissue Int, 1998. **62**(2): p. 153-7.
77. Gavini, C.K., et al., *Leanness and heightened nonresting energy expenditure: role of skeletal muscle activity thermogenesis.* Am J Physiol Endocrinol Metab, 2014. **306**(6): p. E635-47.
78. Robert V. Hogg, J.W.M., Allen T. Craig, *Introduction to Mathematical Statistics*. 6 ed., Upper Saddle River, NJ 07458: Pearson Prentice Hall.
79. Gordon, C.J., *Thermal biology of the laboratory rat.* Physiol Behav, 1990. **47**: p. 963-91.
80. Gordon, C.J., in *Temperature regulation in laboratory rodents.* 1993, Cambridge University Press. p. 8-11.
81. Lusk, G., *The elements of the science of nutrition. 4th ed.* 1928, Philadelphia: W.B.Saunders Company.
82. Fuller, A., R.N. Carter, and D. Mitchell, *Brain and abdominal temperatures at fatigue in rats exercising in the heat.* J Appl Physiol (1985), 1998. **84**(3): p. 877-83.
83. Hasegawa, H., et al., *Effects of ambient light on body temperature regulation in resting and exercising rats.* Neurosci Lett, 2000. **288**(1): p. 17-20.
84. Hasegawa, H., et al., *Alteration in dopamine metabolism in the thermoregulatory center of exercising rats.* Neurosci Lett, 2000. **289**(3): p. 161-4.
85. Balthazar, C.H., et al., *Performance-enhancing and thermoregulatory effects of intracerebroventricular dopamine in running rats.* Pharmacol Biochem Behav, 2009. **93**(4): p. 465-9.
86. Hasegawa, H., et al., *Continuous monitoring of hypothalamic neurotransmitters and thermoregulatory responses in exercising rats.* J Neurosci Methods, 2011. **202**(2): p. 119-23.
87. Tanaka, H., M. Yanase, and T. Nakayama, *Body temperature regulation in rats during exercise of various intensities at different ambient temperatures.* Jpn J Physiol, 1988. **38**(2): p. 167-77.
88. Kunstetter, A.C., et al., *Association between the increase in brain temperature and physical performance at different exercise intensities and protocols in a temperate environment.* Braz J Med Biol Res, 2014. **47**(8): p. 679-88.
89. Brooks, G.A. and T.P. White, *Determination of metabolic and heart rate responses of rats to treadmill exercise.* J Appl Physiol Respir Environ Exerc Physiol, 1978. **45**(6): p. 1009-15.
90. Guimaraes, J.B., et al., *Fatigue is mediated by cholinoceptors within the ventromedial hypothalamus independent of changes in core temperature.* Scand J Med Sci Sports, 2013. **23**(1): p. 46-56.
91. Ishiwata, T., et al., *Changes of body temperature and thermoregulatory responses of freely moving rats during GABAergic pharmacological stimulation to the preoptic area and anterior hypothalamus in several ambient temperatures.* Brain Res, 2005. **1048**(1-2): p. 32-40.

92. Fonseca, C.G., et al., *Hypothalamic temperature of rats subjected to treadmill running in a cold environment.* PLoS One, 2014. **9**(11): p. e111501.
93. Makinen, T., et al., *Energy cost and thermoregulation of unrestrained rats during exercise in the cold.* Comp Biochem Physiol A Physiol, 1996. **114**(1): p. 57-63.
94. Damasceno, W.C., et al., *The dynamics of physical exercise-induced increases in thalamic and abdominal temperatures are modified by central cholinergic stimulation.* Neurosci Lett, 2015. **590**: p. 193-8.
95. Cordeiro, L.M., et al., *Inhibition of tryptophan hydroxylase abolishes fatigue induced by central tryptophan in exercising rats.* Scand J Med Sci Sports, 2014. **24**(1): p. 80-8.
96. Leite, L.H., et al., *Central angiotensin AT1-receptor blockade affects thermoregulation and running performance in rats.* Am J Physiol Regul Integr Comp Physiol, 2006. **291**(3): p. R603-7.
97. Wanner, S.P., et al., *Increased brain l-arginine availability facilitates cutaneous heat loss induced by running exercise.* Clin Exp Pharmacol Physiol, 2015. **42**(6): p. 609-16.
98. Zaretsky, D.V., et al., *The ergogenic effect of amphetamine.* Temperature, 2014. **1**: p. 242-247.
99. Cheuvront, S.N. and E.M. Haymes, *Thermoregulation and marathon running: biological and environmental influences.* Sports Med, 2001. **31**(10): p. 743-62.
100. Maughan, R.J., *Thermoregulation in marathon competition at low ambient temperature.* Int J Sports Med, 1985. **6**(1): p. 15-9.
101. Selye, H., *A syndrome produced by diverse nocuous agents.* Nature, 1936. **138**(3479): p. 32.
102. Cannon, W.B., *Bodily Changes in Pain, Hunger, Fear and Rage: An Account of Recent Researches into the Function of Emotional Excitement.* 1915, New York, London: Appleton.
103. Kregel, K.C., *Heat shock proteins: modifying factors in physiological stress responses and acquired thermotolerance.* J Appl Physiol (1985), 2002. **92**(5): p. 2177-86.
104. Noakes, T.D., *Fatigue is a Brain-Derived Emotion that Regulates the Exercise Behavior to Ensure the Protection of Whole Body Homeostasis.* Front Physiol, 2012. **3**: p. 82.
105. Wyndham, C.H., et al., *Physiological effects of the amphetamines during exercise.* S Afr Med J, 1971. **45**(10): p. 247-52.
106. Gerald, M.C., *Effects of (+)-amphetamine on the treadmill endurance performance of rats.* Neuropharmacology, 1978. **17**(9): p. 703-4.
107. WADA, *Anti-doping testing figures report.* 2012.
108. Walters, T.J., et al., *Exercise in the heat is limited by a critical internal temperature.* J Appl Physiol (1985), 2000. **89**(2): p. 799-806.
109. Young, A.A. and N.J. Dawson, *Evidence for on–off control of heat dissipation from the tail of the rat.* Canadian Journal of Physiology and Pharmacology, 1982. **60**(3): p. 392-398.
110. Horowitz, M., D. Argov, and R. Mizrahi, *Interrelationships between heat acclimation and salivary cooling mechanism in conscious rats.* Comp Biochem Physiol A Comp Physiol, 1983. **74**(4): p. 945-9.
111. Borbely, A.A., I.R. Baumann, and P.G. Waser, *Amphetamine and thermoregulation: studies in the unrestrained and curarized rat.* Naunyn Schmiedebergs Arch Pharmacol, 1974. **281**(4): p. 327-40.

112. Lima, R.S., et al., *Acute kidney injury due to rhabdomyolysis.* Saudi J Kidney Dis Transpl, 2008. **19**(5): p. 721-9.
113. Lambert, M.I. and T.D. Noakes, *Dissociation of changes in VO2 max, muscle QO2, and performance with training in rats.* J Appl Physiol (1985), 1989. **66**(4): p. 1620-5.
114. Weiss, B. and V.G. Laties, *Enhancement of human performance by caffeine and the amphetamines.* Pharmacol Rev, 1962. **14**: p. 1-36.
115. Pickens, R. and W.C. Harris, *Self-administration of d-amphetamine by rats.* Psychopharmacologia, 1968. **12**(2): p. 158-63.
116. Schenk, S., et al., *MDMA self-administration in rats: acquisition, progressive ratio responding and serotonin transporter binding.* Eur J Neurosci, 2007. **26**(11): p. 3229-36.
117. Molinengo, L. and M. Orsetti, *Drug action on the "grasping" reflex and on swimming endurance; an attempt to characterize experimentally antidepressant drugs.* Neuropharmacology, 1976. **15**(4): p. 257-60.
118. Bhagat, B. and N. Wheeler, *Effect of amphetamine on the swimming endurance of rats.* Neuropharmacology, 1973. **12**(7): p. 711-3.
119. Walters, T.J., et al., *Exercise in the heat is limited by a critical internal temperature.* Journal of Applied Physiology, 2000. **89**(2): p. 799-806.
120. Fuller, A., R.N. Carter, and D. Mitchell, *Brain and abdominal temperatures at fatigue in rats exercising in the heat.* Journal of Applied Physiology, 1998. **84**(3): p. 877-883.
121. Fitzgerald, K.T. and A.C. Bronstein, *Adderall(R) (amphetamine-dextroamphetamine) toxicity.* Top Companion Anim Med, 2013. **28**(1): p. 2-7.
122. Kiyatkin, E.A., et al., *Critical role of peripheral vasoconstriction in fatal brain hyperthermia induced by MDMA (Ecstasy) under conditions that mimic human drug use.* J Neurosci, 2014. **34**(23): p. 7754-62.
123. Molkov, Y.I. and D.V. Zaretsky, *Balanced Excitation and Inhibition in Temperature Responses to Meth.* Temperature, 2014. **1**: p. 154-156.
124. Behrouzvaziri, A., et al., *Orexinergic neurotransmission in temperature responses to methamphetamine and stress: mathematical modeling as a data assimilation approach.* PLoS One, 2015. **10**(5): p. e0126719.
125. Madden, C.J., et al., *alpha2 Adrenergic receptor-mediated inhibition of thermogenesis.* J Neurosci, 2013. **33**(5): p. 2017-28.